THE COMPARATIVE EMBRYOLOGY OF THE EUMECOPTERA (INSECTA, MECOPTERA)

By

NOBUO SUZUKI

1982

Submitted in partial fulfillment of the requirements for the degree of Doctor of Science, in Doctoral Program in Biological Sciences, University of Tsukuba.

CONTENTS

INTRODUCTION 1
MATERIALS AND METHODS 4
OBSERVATIONS 7
I. Oviposition and organization of newly laid eggs . . 7
II. Egg period 13
III. Early embryonic development 14
IV. External feature of embryos during middle and late development 20
V. Change of egg size and hatching 35
VI. Formation of inner layer and embryonic envelopes 38
VII. Organogenesis 43
1. Ectodermal derivatives 43
i) Invaginations 43
a) Endoskeletons, salivary and anal glands 43
b) Corpora allata and prothoracic glands 49
c) Tracheae 52
ii) Oenocytes and trichogen cells 56
iii) Nervous system 59
a) Ventral nerve cord 59
b) Brain 62
c) Stomatogastric nervous system 64
iv) Sense organ - larval eyes 67
2. Mesodermal derivatives 71
i) Segmentation of inner layer, formation of coelomic sacs, and differentiation of splanchnic and somatic mesoderm 71
ii) Circulatory system 75
a) Aorta 75
b) Heart, pericardial cells, dorsal diaphragm and blood cells 76
iii) Suboesophageal bodies 79
iv) Gonads 81
v) Differentiation of muscles and fat bodies . . . 84

vi) Musculatures of thoracic and abdominal segments of first instar larva 85
3. Alimentary canal formation 86
i) Stomodaeum or foregut 86
ii) Proctodaeum or hindgut, and malpighian tubules 87
iii) Midgut 89
4. The other structures and phenomena 93
i) Fate of embryonic envelopes 93
ii) Formation of abdominal legs 96
iii) Formation of anal legs and telson 99
iv) Serosal cuticle 100
v) Embryonic diapause 101
GENERAL DISCUSSION AND CONCLUSION 103
I. Alimentary canal formation 103
1. Stomodaeum and proctodaeum 103
2. Midgut 104
II. Homology in larval abdominal legs and thoracic legs 106
III. Interpretation on the metamerism in terminal region of the abdomen 110
IV. Phylogenetic consideration on mecopteran families from embryological aspects 113
1. Ooplasm 115
2. Inner layer formation 116
3. Type of germ band 117
4. Germ band or rudiment formation 117
5. Genealogical tree of the Mecoptera based on the embryological characters 118
SUMMARY 121
ACKNOWLEDGEMENTS 127
LITERATURE CITED 129
FIGURES 147

INTRODUCTION

The Mecoptera is known first from the Lower Permian and this fossil record, Platychorista vinosa and Protomerope permiana, is the oldest among the holometabolan insects. The typical mecopteran insects have two pairs of similar wings, the subcostal vein not extending to the wing apex, only one sector branching from the radius, an unbranched anterior cubital vein, and no scales. Based on the fossil records and comparative morphology of the wing-venation (Tillyard, 1935; Hennig, 1981), the Mecoptera is considered to belong to one of the most primitive groups in the holometabolan insects.

The Mecoptera, Siphonaptera, Diptera, Trichoptera and Lepidoptera have been regarded as forming a Panorpoid complex of orders. Of course, this is centered on the Mecoptera, and from the early Panorpoid stock there probably arose on the hand the Diptera and Siphonaptera, and on the other hand the Trichoptera and Lepidoptera.

As for the holometabolan embryology, that of coleopteran, dipteran and lepidopteran insects has been studied in detail. However the embryology of the Mecoptera is poorly known in spite of the significance of the phylogenetic position in holometabolan orders.

To this day, there are five papers concerning the embryology of the Mecoptera except for the unpublished study in Panorpa communis by Wolf (1961). Two of them

are on the early embryology of Panorpa pryeri (Ando, 1960), and P. japonica, Panorpodes paradoxa, Bittacus mastrillii and B. marginatus (Ando, 1973). The remaining three are on the embryogenesis of the larval abdominal legs (Ando and Haga, 1974) in P. pryeri and B. mastrillii, and of the larval compound eye (Ando and Suzuki, 1977) and of the alimentary canal (Suzuki and Ando, 1981) in P. pryeri.

It is thought that the embryology of the Mecoptera probably suggests the basic pattern of the embryology of Panorpoid orders and holometabolans, since the Mecoptera is considered to occupy a primitive position in the holometabolan phylogeny. However the entire embryonic development of the Mecoptera is never known as mentioned before.

Furthermore, on the relationship of families of the Mecoptera, there are some arguments. For example, Tillyard (1935) divided the Mecoptera into two suborders, i.e., the Protomecoptera, which has many cross veins on the wings and includes the Notiothaumidae and Meropeidae, and the Eumecoptera, which is considered to be more evolved than the Protomecoptera by him and includes the Nannochoristidae, Bittacidae, Boreidae and Panorpidae. Hinton (1958) advocated that the Boreidae should be separated from the Mecoptera, and established as the new order Neomecoptera based on the comparative anatomy of the larvae of Panorpoid orders. Recently, however, from the comparative morphology of exoskeleton of the genitalia, Mickoleit

(1978) and Willmann (1981) suggested that the Nannochoristidae and Bittacidae are thought to be the most primitive in the mecopteran families, and they have some doubts about the view of Tillyard (1935) and Hinton (1958).

For these above mentioned reasons, the author investigated the comparative embryology of the four families of the Eumecoptera; Panorpidae, Panorpodidae, Boreidae and Bittacidae. In this paper the author described 1) the embryonic development of these insects in detail, and 2) examined and discussed the phylogenetic relation of these families from the comparative embryological views obtained in the present study.

The author attempted to discuss some major subjects in the last chapter, "GENERAL DISCUSSION AND CONCLUSION", and to discuss the others in each item of "OBSERVATIONS".

In the text, except for the case when the scientific name of a certain insect appears at first, for a convenience, the generic name is made abbreviated and brief, or the specific epithet is omitted.

MATERIALS AND METHODS

Specimens used in the present study include four families, four genera and nine species of the Mecoptera, that is, Panorpa pryeri, P. japonica, P. nipponensis, P. helena of the Panorpidae; Panorpodes paradoxa of the Panorpodidae; Bittacus laevipes, B. mastrillii, B. marginatus of the Bittacidae; and Boreus westwoodi of the Boreidae. The author used mainly Panorpa pryeri as to the Panorpidae, and Bittacus laevipes as to the Bittacidae, because the author could observe only little differences of the embryogenesis between the species of the Panorpidae, and also between the species of the Bittacidae.

Pregnant females of P. pryeri were collected at Sugadaira, Sanada in Nagano Prefecture in June to July during 1980 to 1981. Each insect was reared in a small plastic cage with soil or quartz sands, and fed on killed dipteran or lepidopteran insects. In this condition the females laid their eggs. Newly laid eggs were transferred to another plastic case with a humid palster bottom and kept at 21°C.

Matured insects of Pd. paradoxa were captured at Sugadaira and Kakuma of Sanada, and Yamanokami of Suzaka, and Usuda of Saku in Nagano Prefecture in June to July during 1976 to 1982. Many pairs of the insects were reared in a mesh walled cage with humid tissue papers, and fed on the pollen and nectars of some flowers (Chrysanthemum leucan-

themum, Euonymus sieboldiana, Cornus controversa, etc.). Newly laid eggs on or in the tissue papers were kept in the similar condition to P. pryeri.

Mated females of B. laevipes were collected at Kakuma in August to September during 1978 to 1981. Each female was reared in a small plastic cage with a humid filter paper. The ovipodited and dropped eggs on the filter paper were carried to a plastic case with a humid plaster bottom, and kept at room temperature.

Pregnant females of Bo. westwoodi were obtained at Tübingen of West Germany in December of 1979, and reared with mosses in a laboratory, and eggs were collected from among the mosses. All of these procedures and fixation of eggs were done by Drs. G. Mickoleit and E. Mickoleit. Larvae and eggs of this species also were collected and fixed by Dr. H. Ando at Freiburg and Tübingen in early April of 1975.

Eggs and larvae were fixed in alcoholic Bouin's fluid warmed to 40°C (80°C or room temperature in some cases) for 30 min. Some newly laid eggs of B. laevipes were fixed in 2.5% glutaraldehyde in 0.05M cacodylate buffer at pH 7.2 for 12 hr and postfixed in Carnoy's fluid for 30 min at room temperature. After fixation, materials were preserved in 70% ethyl alcohol.

In the case of observations of external feature of embryos, the chorion, serosa and serosal cuticle were re-

moved by forceps, then the bared eggs were stained with Mayer's hematoxylin, and observed in distilled water. In order to the observation of the thoracic and abdominal musculatures of the first instar larva of P. pryeri, the fixed larvae were removed the head and posterior half of the abdomen, and were stained with eosin, and observed in telepineole after dehydration.

For sectioning the eggs and larvae, the materials were embedded paraffin, paraffix or paraplast, after dehydration through an ethyl, normal or tertiary butyl alcohol series. They were cut into 6 to 10μm-thick and stained with Delafield' hematoxylin and eosin, and borax carmin in some cases.

Drawings were made with the aid of Abbe's camera lucida.

Materials for the scanning electron microscope were prepared as follows. Fixed materials by the methods above mentioned were rinsed in distilled water added a little detergent. After the dehydration through an ethyl or tertiary butyl alcohol-isoamyl acetate series, they were dried by the critical point drying method and coated with gold. In the case of B. laevipes eggs, granules coated the surface of the egg were removed in 5 to 10% sodium hypochrorite solution. Observations were examined under the scanning electron microscope, JSM T-200 of JEOL.

OBSERVATIONS

I. Oviposition and organization of newly laid eggs

Panorpa pryeri

Twelve females reared in 1981 laid eggs thirteen times, and the number of laid eggs at a time was 18 to ca. 100 (average, 50.7) and only one female oviposited at twice (39 and 70 eggs). It seems, however, that a female oviposits several times in nature.

A cluster of laid eggs is held together by the sticky substance that covers the surface of the each egg.

The newly laid egg is oval in shape, though the anterior half is slightly sharp, and their size is ca. 1000 by ca. 600μm (Fig. 1). The outer chorion is covered with a honeycombed network (Figs. 1, 2), and on the some corners of these minute polygons there appears a brushy process which is concerned with an aeropyle (Fig. 2).

The honeycombed pattern of the chorion on and near the anterior pole is different from other regions (Fig. 3) and the author could not find the micropyle at this region even by the observations using SEM and the light microscope. There is a very thin vitelline membrane below the chorion. The color of the newly laid egg is creamy white and turns dark gray by half a day. The periplasm is 4 to 5μm-thick (Fig. 18) and ca. 10μm-thick near the both poles of the egg, and occupies ca. 5% of the egg volume. The maturation of the female pronucleus is observ-

ed in the cytoplasmic island that lies a little anterior from the center of the egg length (Fig. 18). The cytoplasmic reticulum or reticuloplasm is found between the yolk spherules and vacuoles (Figs. 18, 19). The disk-shaped polar granule (40 to 50μm in diameter) is found in the periplasm on the posterior pole (Fig. 19). The spermatozoon is observed near the anterior pole of the egg (Fig. 25). Yolk spherules are homogeneously stained with eosin, and their diameter varies from 5 to 15μm. Small yolk spherules mainly distribute in the peripheral zone. The total volume of the eosinophilic yolk spherules occupies ca. 80% of the egg volume*.

Panorpodes paradoxa

During 1979 to 1981, the author obtained ca. 100 egg batches contained ca. 50 to 60 eggs in each batch. The batch is held together with the sticky substance as in P. pryeri.

The shape of the newly laid egg is oval and its size is 750 to 800 by ca. 500μm (Fig. 4). The chorion bears the honeycombed pattern that becomes weak near the both po-

---

* The percentage of the area of eosinophilic yolk spherules in sections was estimated as the rate of the total volume of eosinophilic yolk spherules against the egg volume. The percentage was nearly equal at any regions of the egg in the same species.

les, and the author failed to find micropyles from these regions (Fig. 5).

The chorion is very thin and creamy white just after oviposition, and turns dark by several hours. A relatively large quantity of the periplasm (5 to 6μm-thick and ca. 6% of the egg volume) and cytoplasmic reticulum are found in the egg (Fig. 20). Yolk spherules are stained homogeneously with eosin, and their diameter is ca. 10μm, and the total volume of the eosinophilic yolk spherules occupies ca. 60% of the egg volume. There are many vacuoles considered to be traces of dissolved lipid yolk spherules (Fig. 20). Maturating female pronucleus situates in the cytoplasmic island of the periplasm (Fig. 21) near the middle part of the egg. The author could not find the polar granule in this species.

Bittacus laevipes

The author got eggs from 62 females during 1978 to 1981, and a female oviposits ca. 26 eggs (ca. 10 eggs per day). The oviposition almost always started at 4 to 5 o'clock p.m. and continued for a few hours. The hanging females oviposit eggs, and an egg exists at the tip of the abdomen and drops out as soon as the following egg is laid.

The shape of the newly laid egg is almost spherical, ca. 700μm in diameter (Fig. 6). On the surface of the

chorion there are numerous granular substances, but after removing them the surface of chorion appears a polygonal pattern (Fig. 7).

Two to five micropyles (Fig. 8) are observed on the both poles of the egg. The chorion is very tough and thick (ca. 25μm), and the endochorion of 2 to 3μm thickness is stained faintly with eosin (Fig. 22). The egg color is yellow just after oviposition, and turns dark brown by several hours. The periplasm is very thin (2 to 3μm) and lightly stained with hematoxylin (Fig. 22), and occupies ca. 2% of the egg volume. Little cytoplasmic reticulum is observed.

Yolk spherules are homogeneously stained with eosin, and their diameter is ca. 20μm though there are smaller spherules in periphery. The rate of the total volume of eosinophilic yolk spherules against the egg volume is less than 70%. No polar granule is found in this species.

Boreus westwoodi

The shape of matured ovarian eggs and newly laid eggs is oval and the size is 450 to 500 by 250 to 300μm (Fig. 9).

On the surface of the chorion there appears a honeycombed network, and the network becomes faintly near the both poles of the egg as in that of Pd. paradoxa. On the both poles two micropyles are found (Fig. 10). The

chorion is ca. 2μm-thick and thickens near the both poles (Fig. 23). The chorion is transparent even if the embryogenesis proceeds.

The periplasm (2 to 3μm-thick and 3 to 4% of the egg volume) and cytoplasmic ruticulum are poor (Fig. 24) though richer than those of B. laevipes. The maturating female pronucleus in the cytoplasmic island of the periplasm locates at the region of a third of the egg length from the anterior pole. The yolk spherules are stained homogeneously with eosin and their size in maximum is about 20μm in diameter. The total volume of eosinophilic yolk spherules occupies ca. 60% of the egg volume. The author could not find the polar granule in this species.

Discussion on this item

It seems that eggs are laid in the crevice of soil in Panorpa spp. (Miyake, 1912; Yie, 1951; Ando, 1960, 1973; Byers, 1963), Panorpodes (Ando, 1973), and among the moss in Boreus spp. (Withycombe, 1922; Cooper, 1974). It seems also general that the oviposition of Bittacus is practiced while hanging as in Bittacus nipponicus (Ishii, 1937), B. laevipes, B. mastrillii, B. marginatus, though B. stigmaterus (Setty, 1931) deposits the eggs, alighting on the ground.

The shape of the newly laid eggs is oval in Panorpa (Miyake, 1912; Yie, 1951; Ando, 1962, 1973; Byers, 1963),

Panorpodes (Ando, 1973), and Boreus spp. (Withycombe, 1922; Cooper, 1974). In Bittacus, however, the shape varies from cuboidal (B. stigmaterus, Setty, 1931; B. nipponicus, Ishii, 1937) to spherical (B. apicalis, Hinton, 1981; B. mastrillii, B. marginatus, Ando, 1973; B. laevipes). Ando (1973) observed that the shape of the oocyte in ovariole of B. mastrillii during chorion formation is spheroidal.

As for the micropyles, Ando (1973) described the micropyles on the posterior pole of the egg in B. mastrillii, and Hinton (1981) on the anterior pole in B. pilicornis. It is possible that they failed to find the micropyles on the other pole, because the micropyles were observed on the both poles in B. laevipes.

Eosinophilic yolk spherules of P. pryeri and B. laevipes may correspond to the protein yolk of P. communis (Ramamurty, 1964a). Ando (1973) mentioned that the very thin periplasm of B. mastrillii is observed discontinuously. In B. laevipes, however, the periplasm is observed continuously, though it is thin as in B. mastrillii.

The polar granules were observed in the eggs of P. pryeri, P. japonica (Ando, 1973) and P. communis (Ramamurty, 1964b), so that the existence of the polar granules is considered to be the common nature in the egg of Panorpa.

II. Egg period

The egg period of the species investigated in the present study is shown in Table 1 comparing with those of other species reported by several authors.

Table 1. Egg period of Panorpidae, Panorpodidae, Bittacidae and Boreidae

Panorpidae	
Panorpa pryeri	ca. 150 hr (21°C)
Panorpa pryeri	150-160 hr (ca. 21°C) (Ando, 1960)
Panorpa nipponensis	ca. 140 hr (25°C)
Panorpa japonica	ca. 160 hr (21°C), ca. 150 hr (25°C)
Panorpa klugi (=japonica)	6-8 days (Miyake, 1912)
Panorpa japonica	168-180 hr (18-24°C) (Ando, 1973)
Panorpa helena	ca. 8 days
Panorpa bicornuta	ca. 7 days (22°C) (Ando, 1973)
Panorpa communis	144 hr (21°C) (Wolf, 1961)
Panorpa communis	5-9 days (Steiner, 1930)
Panorpa nuptialis	8 days (Byers, 1963; Gassner, 1963)
Panorpa folsa	9-13 days
Panorpa akasakai	15-16 days
Panorpa taiwanensis	15-16 days (Yie, 1951)
Panorpa shibatai	15-16 days
Panorpa pectinata	15-16 days

Table 1. (continued)

Panorpa longiramina	14 days	(Yie, 1951)
Panorpa ochraceocauda	7 days	
Neopanorpa makii	7 days	
Neopanorpa ophthalmica	6 days	
Neopanorpa formosana	6-8 days	
Neopanorpa sauteri	5-14 days	

Panorpodidae

Panorpodes paradoxa	28-40 (mean, 32.6) days (21°C)
Panorpodes paradoxa	ca. 26 days (20-24°C) (Ando, 1973)

Bittacidae

Bittacus laevipes	250-300 (mean, 270) days
Bittacus mastrillii	ca. 245 days (Ando, 1973)
Bittacus marginatus	ca. 240 days (Ando, 1973)
Bittacus nipponicus	ca. 290 days (Ishii, 1937)
Bittacus stigmaterus	216-256 (mean, 226) days (Setty, 1931)
Bittacus punctiger	20-37 days (Setty, 1940)
Bittacus pilicornis	29-78 days (Setty, 1940)

Boreidae

Boreus hyemalis	9-10 days (8.8°C) (Withycombe, 1922)
Boreus hyemalis	21 days (21°C) (Strübing, 1950)
Boreus notoperates	24 days (20°C) (Copper, 1974)

Discussion on this item

There are not so many reports on the life history and egg period of mecopteran insects, and the life histories of panorpid ones are examined most circumstantially. The egg period of the Panorpidae seems to vary from one to two weeks, and that of the Panorpodidae, that is, Pd. paradoxa, is three to six weeks.

The egg period of several species of the Bittacidae is more than 200 days and they pass the winter in the egg stage, though B. punctiger and B. pilicornis overwinter in the larval stage (Setty, 1940). Setty (1931) observed the exceptional short egg period that is 58 days in B. stigmaterus, and this fact suggests that the egg hibernation is not fixed perfectly in this species.

The elongation of the egg period in Bo. hyemalis is known accompanied with the rise of the incubation temperature (Withycombe, 1922; Strübing, 1950). This phenomenon seems to be concerned with the nature that the oviposition of the species occurs in winter, and the low temperature may be favorable for the embryonic development in the species.

III. Early embryonic development

In this section the author will describe the embryonic development from just oviposition to completion of the cellular blastoderm as Stage 1.

Panorpa pryeri

The early embryonic development of P. pryeri was studied in detail by Ando (1960), and the result in the present study agreed with his result.

Stage 1. 0-28 hr

Just after oviposition, the metaphase of the first maturation division is found in the cytoplasmic island, and the second maturation division occurs at 1 hr after oviposition (Fig. 18). The spermatozoon is observed near the anterior pole of the egg (Fig. 25), and soon transforms into the male pronucleus at there. The female pronucleus moves to the male pronucleus and the fertilization occurs.

The second cleavage occurs at 4 hr, and the seventh cleavage occurs at 8 hr after oviposition. The polar granule which located at the posterior pole of the egg disappears by the ninth cleavage (ca. 10 hr after oviposition). At 12 hr after oviposition, cleavage cells reach into the periplasm and the syncytial blastoderm is formed (Fig. 26), though they reach to both poles a little later. The penetrating cleavage cells or syncytial blastoderm cells divide mitotically again.

At about 20 hr after oviposition, the formation of cell membrane of syncytial blastoderm cells begins, and the periplasm which does not participate in the blastoderm formation becomes the inner periplasm by the completion

of blastoderm cells (Fig. 27). The cleavage cells which did not participate in the blastoderm formation remain in the yolk and become primary yolk cells*. The aggrigate composed of some dozens of primary yolk cells is situated at the center of the egg, and the nuclei of them degenerate later.

The cellular blastoderm is formed at 22 hr after oviposition. The blastoderm cells are ca. 20μm in width and the diameter of their nuclei and yolk cells is ca. 10 to 15μm.

Panorpodes paradoxa

Stage 1. 0-32 hr

Just after oviposition, the female nucleus shows the metaphase of the first maturation division in the cytoplasmic island. After fertilization, the first cleavage occurs (Fig. 28) near the egg center. At 12 hr after oviposition, the sixth cleavage commences and the cleavage cells are located at zone of 150 to 200μm inward from the egg surface.

At 1 day after oviposition, the cleavage cells reach the egg periphery, and yolk spherules are often found in the syncytial blastoderm (Fig. 29). The nuclei of

---

* In the present paper, the term "yolk cell" has been adopted instead of "yolk nucleus".

the syncytial blastoderm cells are soon partitioned by the formation of the cell membrane, and the cellular blastoderm is completed. The yolk spherules are seen in the blastoderm cells, and the inner periplasm exists as in P. pryeri (Fig. 30).

Bittacus laevipes

Stage 1. 0-3 days

Just after deposition, the female nucleus indicates the metaphase of the first maturation division (Fig. 22), the second maturation division follows 3 hr later. The author could not observe the fertilization.

At 1 day after oviposition, the fifth cleavage occurs and the cleavage cells get to the egg periphery at 2 days after oviposition. The syncytial blastoderm cells divide mitotically. At this time, some nuclei divide tangentially against the egg surface, and they seem to be concerned with the formation of secondary yolk cells (Fig. 31).

At 3 days after oviposition, syncytial blastoderm cells divide again, and the cellular blastoderm is completed (Fig. 32).

Boreus westwoodi

In Bo. westwoodi, the author could not know how old the fixed eggs are, and could not study the late embryonic development.

Stage 1.

The maturation of the female pronucleus and the fertilization were not able to be observed. When the fifth to the sixth cleavage occurs, the cleavage cells are located at the zone where is ca. 100μm inward from the egg surface.

As development proceeds cleavage cells reach into the egg periphery (Fig. 33) and inclease in number (Fig. 34). Then the cell membrane appears and the cellular blastoderm is completed (Fig. 35).

Discussion on this item

In P. pryeri, Pd. paradoxa and B. laevipes, the female nucleus of the newly laid egg indicated the metaphase of the first maturation division as in P. communis (Wolf, 1961), and this fact is known in many insects, e.g., in odonatan Calopteryx atrata (Ando, 1962), blattarian Blatta germanica (Wheeler, 1889), megalopteran Sialis mitsuhashii (Suzuki, Shimizu and Ando, 1981), trichopteran Stenopsyche griseipennis (Miyakawa, 1973), hymenopteran Athalia proxima (Farooqi, 1963). The inner periplasm found in P. pryeri and Pd. paradoxa is also known in some holometabolans, i. e., Stenopsyche (Miyakawa, 1973), Athalia (Farooqi, 1963), dipteran Dacus tryoni (Anderson, 1962). As Ando (1960) described, the existence of the inner periplasm is probably related to the thickness of the periplasm.

The intake of yolk spherules into the blastoderm cells, appeared in Pd. paradoxa, is not so general, though the similar phenomena occur in coleopteran Epilachna vigintioctomaculata (Miya and Abe, 1966) and lepidopteran Endoclita signifer and E. excrecens (Ando and Tanaka, 1980).

Generally speaking, the early embryonic development of P. pryeri, Pd. paradoxa, B. laevipes and Bo. westwoodi seems to be similar to those of other many insects.

IV. External feature of embryos during middle and late development

Panorpa pryeri

Stage 2. 28-47 hr

At 28 hr after oviposition, the embryonic and extraembryonic areas differentiate in the uniform blastoderm. The cells of the embryonic area (= ventral plate) are ca. 12μm in height and their nuclei are ca. 10μm in diameter (Fig. 36). These of the extraembryonic area are 20 to 25μm in height, and their nuclei of ca. 15μm in diameter are placed at the distal side of the cells. Extraembryonic cells have many vacuoles (Fig. 37). Although the embryonic and extraembryonic areas differentiate in the blastoderm, in this stage the nuclei are located at the same intervals as those in the blastoderm stage. At 32 hr after oviposition, the mitotical figures are observed

almost only in the embryonic area.

At 36 hr after oviposition, in the embryonic area the cells roud to some extent and become 18 to 20μm in height, and their nuclei become smaller (ca. 8μm in diameter), though there are found only little changes in the extraembryonic area. Almost all of the mitotical figures are also found in the embryonic area.

At 45 hr after oviposition, the amniotic folds appear at the anterior and posterior margins of the embryonic area (Fig. 38). At this time, the cells of the extraembryonic area are ca. 30μm in height and their nuclei are 15 to 20μm in diameter, and many nuclei are situated at the inner or proximal sides of the cells. The cells of the embryonic area scarcely alter morphologically except for the increase in their number.

At 46 hr after oviposition, the amniotic fold appears in the whole margin of the embryonic area diminishing in size. On the median line of the embryonic area the primitive groove occurs from the caudal end of the line (Fig. 39).

Stage 3. 47-51 hr

At 47 hr after oviposition, a pear-shaped germ band is formed, and the large part of its ventral side is covered with the amnion (Figs. 40, 41). It takes only ca. 2 hr from the appearance of the amniotic fold to the

completion of the pear-shaped germ band.

At 49 hr after oviposition, the amniotic fold spreads further, and the protocorm of the germ band elongates backward along the egg surface and its caudal end takes a level indicated the arrow of Fig. 42.

Stage 4. 51-60 hr

The amnion covers the ventral surface of the embryo perfectly, and there appears a notch in the center of the anterior margin of the protocephalon (Fig. 43) at 51 hr after oviposition. The yolk cleavage begins.

At 52 hr after oviposition, a low protuberance, which is the rudimental labrum, becomes recognized at the anteromedial part of the protocephalon. The germ band more elongates and reaches three quarters of the egg circumference (Fig. 44).

At 54 hr after oviposition, the labrum anlage begins to be a pair. A pair of rudimental antennae appears, and each segment of the intercalary, mandible, maxilla and labium differentiates (Fig. 45).

At 57 hr after oviposition, the length of the germ band becomes longer than that of 52 hr, and a shallow invagination or developing stomodaeum is found in the center of the protocephalon. Three thoracic segments become distinguishable in thie stage (Fig. 46).

Stage 5. 60-80 hr

At 60 hr after oviposition, the germ band attains the length of five sixths of the egg circumference (Fig 48). The abdominal rudiment segments to ten metameres and small paired thoracic appendages arise (Fig. 47).

At 70 hr after oviposition, cephalic lobes of the embryo take a position on the anterior pole of the egg and the gnathal segments begin to gather (Fig. 49).

Stage 6. 80-100 hr

At 80 hr after oviposition, the anteriorward shift of the gnathal segments proceeds further, and the rudimental maxilla divides into the coxopodite and telopodite (Fig. 50). Paired tracheal invaginations appear from the second thoracic segment to the eighth abdominal segment at the anterolateral parts of the each segments.

At 90 hr after oviposition, the future galea and lacinia are formed from the inner side of the coxopodite of the maxilla (Fig. 51). The thoracic appendages divide into three segments, and small paired processes appear on the first eight abdominal segments (Fig. 51). They are arranged in a row with the anlagen of the thoracic appendages and slightly increase in size during embryonic development. On the lateral margin of the first nine abdominal segments rudimantal paired dorsal processes are formed (Fig. 52), and a pair of the future larval compound

eyes becomes to make an appearance on the lateral side of the embryonic head.

Stage 7. 100-110 hr

At 100 hr after oviposition, the head of the embryo approaches to the completion morphologically (Fig. 53). Each thoracic appendage consists of four segments as in the first instar larva. The spiracles on the second and third thoracic segments disappear, and a pair of new spiracles appears at the posterolateral parts of the bases of the first thoracic appendages (Fig. 53).

Paired processes, i.e., rudiments of so-called abdominal legs develop on the ganglia of the first eight abdominal segments (Fig. 54). The dorsal processes of the first nine abdominal segments elongate, and a tip of the process of the tenth abdominal segment is observed beyond anal legs (Fig. 53).

Stage 8. 110-120 hr

At 110 hr after oviposition, the embryo more elongates and its caudal end almost touches its head (Fig. 55). From this time the yolk becomes to be consumed rapidly, and at 116 hr after oviposition the embryo revolves in the manner which twists sideways the posterior half of its abdomen around the rest of the embryo (Fig. 56). The dorsal closure of the embryo is completed without the

first to the fifth abdominal segment.

Stage 9. 120-150 hr

At 120 hr after oviposition, the embryo finishes the revolution (Fig. 57), and the dorsal closure is also finished at the dorsal side of the anterior half of the abdomen.

At 130 hr after oviposition, the embryo almost gets an appearance of the first instar larva, and an egg tooth is formed on the top of the cranium (Fig. 58).

Stage 10. first instar larva

The first instar larva hatches at ca. 150 hr after oviposition. Its body length is ca. 3mm. Characters of the first instar larva of P. pryeri are as follows; a pair of compound eyes which consist of ca. thirty ommatidia in each, paired abdominal legs located on the first eight abdominal segments, paired dorsal processes on the first nine abdominal segments and a dorsal process on the tenth abdominal segment (Fig. 11).

Panorpodes paradoxa

Stage 2. 32 hr - 4 days

At 32 hr after oviposition, the blastoderm becomes to thicken (Fig. 59) especially near the posterior pole and this thick region is the embryonic area (= germ

disk). In the area there are some cells which were divided inwards from the blastoderm cells (Fig. 60) and they seem to be future germ cells.

At 40 hr after oviposition, cells of the embryonic area become higher and of the extraembryonic area lower or thinner (Fig. 61). At this time, an aggregation composed of about a dozen of primary yolk cells is often found in the center of the egg. As development proceeds the embryonic area commences to sink into the yolk (Fig. 62).

At 2 days after oviposition, the invaginating embryonic area develops a sac-shaped germ rudiment (Figs. 63, 64). Nuclei of the extraembryonic area or serosa are stained deeper than those of the germ rudiment with hematoxylin (Fig. 64).

At 3 days after oviposition, the germ rudiment is almost released from the egg periphery (Fig. 65). It contains the developing amnion and the embryo which soon begins to form the inner layer or mesoderm. The yolk cleavage is observed.

Stage 3. 4-14 days

At 4 days after oviposition, the germ rudiment is completely immersed in the yolk. At 7 days the germ rudiment or embryo takes a position of the center of the egg (Fig. 66).

As development proceeds the embryo elongates and approaches to the egg periphery again, and at 10 days after oviposition the embryo touches the egg periphery with its protocephalon (Fig. 67).

Stage 4. 14-19 days

At 12 days after oviposition, the embryo comes out on the yolk except for the posterior half of the protocorm, but the segmentation of the embryo can not be seen in this stage (Fig. 68).

At 16-17 days after oviposition, the embryo exposes its figure on the yolk except for the fourth and following abdominal segments (Figs. 69, 70). A shallow pit or future stomodaeum arises in the center of head lobes.

Stage 5. 19-21 days

At 19 days after oviposition, anlagen of gnathal and thoracic appendages make their appearance (Figs. 71, 72). The embryo comes out with the posterior abdominal half on the yolk, and this developing abdomen consists of ten segments.

At 21 days after oviposition, the gnathal segments of the embryo commence to move forward, and paired spiracles are observed from the second thoracic to the eighth abdominal segment (Fig. 73).

Stage 6. 23-25 days

At 23 days after oviposition, the gnathal segments become more compact than in the prior stage. The spiracles of the second and third thoracic segments disappear and a pair of new spiracles appears on the first thoracic segment (Fig. 74). Paired swellings arise on the ventral surface of the first eight abdominal segments (Fig. 75), and they are arranged in a row with the developing thoracic appendages. The swellings do not develop further.

At 25 days after oviposition, the head and caudal end of the embryo almost touch each other (Fig. 76) and it is just before revolution.

Stage 7. 25-31 days

At 25 to 27 days after oviposition, the revolution occurs and the manner of the revolution is shown diagrammatically in Figs. 77, 78, 79. The dorsal closure finishes shortly after the revolution.

Stage 8. 31-33 days

At 31 days after oviposition, the embryo almost gets an appearance of the first instar larva (Fig. 80) and gets an egg tooth on the top of the head, and stays in the egg for one or two days. As the hatching is coming to, mandibular tips become fulvous.

Stage 9. First instar larva

At ca. 33 days after oviposition, the first instar larva hatches. Its body length is ca. 2mm (Fig. 12) and has no eyes. On the medioventral line of the first eight abdominal segments has a median minute process in each one (Fig. 13), and those of the first and second thoracic segments are especially mimute. The newly hatched larva bears relatively long setae, but has no dorsal processes existing in P. pryeri.

Bittacus laevipes

Stage 2. 3-4 days

At 3 days after oviposition or shortly after the blastoderm completion, a part of the blastoderm becomes thick and forms a circular germ disk that is ca. 200μm in diameter (Fig. 81).

Stage 3. 4-20 days

At 4 days after oviposition, the germ disk widens (Fig. 82), and the germ disk or germ band becomes pear-shape at 5 days (Fig. 83).

As development proceeds the narrow germ band elongates, and at 9 days after oviposition it has a body length of a fourth of the egg circumference (Fig. 84).

Stage 4. 20-50 days

At 20 days after oviposition, head lobes of the embryo become distinguishable (Fig. 85), but the segmentation of the embryo is not discernible.

At 25 days, segments from the intercalary to the tenth abdominal are observed though indistinctly, and a shallow pit or rudimental stomodaeum appears in the center of the head lobes (Fig. 86). A pair of labral rudiments is formed.

At 35 days after oviposition, the labral rudiments increase in size and antennal anlagen occur (Fig. 87). The rudimental stomodaeum invaginates deeper. The embryo elongates to the length of a half of the egg circumference.

At 45 days, the paired labral rudiments begin to fuse, and anlagen of the mandible, maxilla and labium develop in this stage (Figs. 88, 89).

Stage 5. 50-65 days

At 50 days after oviposition, the embyro elongates and its length corresponds to three quarters of the egg circumference. At the same time, anlagen of thoracic appendages are discernible (Fig. 90).

At 55 days, the labral rudiments almost fuse and the opening of the developing stomodaeum is hiden by them (Fig. 91). The anlagen of the thoracic appendages elongate.

Stage 6. 65-248 days

At 65 days after oviposition, the distal parts of both rudimental mandibles turn medioventral, and each pair of the developing thoracic appendages meets with their apexes on the medioventral line of the embryo (Fig. 92). The embryo gets into diapause at this stage.

Stage 7. 248-262 days

Although almost all embryos get into diapause at about 65 days after oviposition, the time of the termination of diapause is difference between embryos to some extent. The day from the termination of diapause to hatching, however, is approximately regualr, so that the author set the day of the termination of diapause to the 248th day from oviposition for the convenience of following descriptions.

From 248 days to 260 days after oviposition, the developing gnathal appendages shift their positions as shown in Figs. 93, 94, 95, 96. The maxillary rudiment differnetiates into two parts, i.e., the lateral one is the developing maxillary palp and the medial one is further divided into the future galea and lacinia, and the labral rudiment diminishes in size and shifts medioventrally (Fig. 95).

At ca. 250 days after oviposition, paired spiracles

appear from the second thoracic to the eighth abdominal segment, and on the ventral side of the abdomen there appear two pairs of small processes in each of the first eight abdominal segments. The outer processes are arranged in a row with the rudimental thoracic appendages (Fig. 94), and the inner processes become so-called abdominal legs of the first instar larva in future.

At 260 days after oviposition, a pair of new spiracles appears on the first thoracic segment (Fig. 96), but those of the second and third thoracic segments disappear. Dorsal processes elongate and paired larval eyes are discernible (Fig. 96).

Stage 8. 262-268 days

At 262 days after oviposition, the yolk diminishes in size (Fig. 97), and the embryo revolutes at ca. 263 days after oviposition (Fig. 98). After revolution, the embryo finishes the dorsal closure. The embryo puts its caudal end on any side of the head (Fig. 99) and puts it on the opposite side at about a day later (Fig. 100).

Stage 9. 268-270 days

At 268 days after oviposition, the embryo almost completes morphologically (Fig. 101). On the cranium an egg tooth and a small process are found. The process is made of a thickening of the ectoderm (Fig. 102), and

the author was not able to find innervations from the brain to the thickening.

At half a day later, tips of the egg tooth and mandibles become fulvous, and the antennae and dorsal processes bear fulvous at one or more days later.

Stage 10. First instar larva

The first instar larva hatches at ca. 270 days after oviposition, and is ca. 3.5mm in length (Fig. 14). Paired larval eyes consist of seven ommatidia (Fig. 15). Paired abdominal legs are observed on the first eight abdominal segments. Long paired dorsal processes are situated on the abdominal segments, though that of the tenth segment is single. There are many clavate setae on the body wall.

Boreus westwoodi

Stage 2.

After the completion of the thin cellular blastoderm, the elliptic embryonic area or ventral plate which is composed of vacuolated cells differentiates (Fig. 103). The cells of its area are much thicker than those of the extraembryonic one, and the lateral plates, and the middle plate which later becomes the inner layer are distinguishable in the anterior part of the embryonic area (Fig.

104).

Stage 3.

As development proceeds, a pear-shaped embryo appears (Fig. 105) and the ventral side of the embryo is covered with the thick amnion (Fig. 106). The embryo elongates and a notch appears in the center of the anterior margin of the protocephalon (Fig. 107).

Stage 4.

A shallow invagination which is the future stomodaeum first becomes evident in the center of the protocephalon, and the gnathal and thoracic segments are observed (Fig. 108). The caudal end of the embryo is located on the posterior pole of the egg.

Stage 5.

The embryo elongates and its abdomen consists of ten segments (Fig. 110). The width of the last three abdominal segments is narrower than that of prior segments. At the same time, paired labral and antennal rudiments appear in the protocephalon (Fig. 109), and paired anlagen of gnathal and thoracic appendages are also discernible.

As development proceeds, the gnathal segments shift forward and then the labial anlagen move medioventrally (Fig. 111). The developing thoracic appendages are com-

posed of three segments, and paired small swellings are arranged in a row with the thoracic appendages on the first eight abdominal segments (Fig. 112).

Larva

The larva is fat scarabaeiform or weevil larva-like (Fig. 16), and the first thoracic legs are smaller than the other thoracic legs. Although the larva has relatively long setae, there are no dorsal processes which occur in P. pryeri and B. laevipes.

The middle and late embryonic development of P. pryeri, Pd. paradoxa, B. laevipes and Bo. westwoodi is summarized in Table 2 on the following page.

V. Change of egg size and hatching

Panorpa pryeri, Panorpodes paradoxa and Bittacus laevipes

As for measurement of eggs, fixed eggs were always employed.

The change of the egg size from oviposition to just before hatching is shown in Fig. 113, and outlines of the newly laid and full-grown eggs are drawn diagrammatically in Fig. 114. The volume of the full-grown egg increased ca. 2.5 times large as that of the newly laid one in P. pryeri, ca. 2.1 times in Pd. paradoxa, and ca. 3.4 times in B. laevipes.

Table 2. Middle and late development of Panorpa pryeri, Panorpodes paradoxa, Bittacus laevipes and Boreus westwoodi

Stage				State of development
P.	Pd.	B.	Bo.	
(1) 3 hr	(1)	(1) 10 hr	(1)	Pronuclei fuse.
22 hr	28 hr	3 days		Blastoderm completes.
(2) 28 hr	(2) 32 hr	(2) 3.5 days	(2)	Embryonic area appears.
46 hr	3 days	(3) 4 days	(3)	Inner layer differentiates.
(3) 51 hr	(3) 4 days	9 days		Embryo is covered with amnion.
52 hr	10 days	(4)	(4)	Labium appears.
(4) 54 hr	(4) 15 days			Gnathal segments appear.
57 hr	17 days			Thoracic segments appear.
(5) 60 hr	(5) 19 days	25 days	(5)	Ten abdominal segments appear.
70 hr	21 days	(5) 55 days		Gnathal segments move forward.
(6) 80 hr		(6) 65 days	-	Spiracles appear from t2 to a8.
100 hr	(6) 23 days	(7) 260 days	-	Spiracles appear on t1.
(7) 116 hr	(7) 26 days	(8) 263 days	-	Embryo revolutes.
(8) 120 hr	27 days	264 days	-	Dorsal closure completes.
130 hr	(8) 31 days	(9) 268 days	-	Egg tooth appears.
(9) 150 hr	(9) 33 days	(10) 270 days	-	Larva hatches.

The parenthesized number indicates the number of stage.

P., P. pryeri; Pd., Pd. paradoxa; B., B. laevipes; Bo., Bo. westwoodi; t1, 2, first and second thoracic segments; a8, eighth abdominal segment.

The time of the hatching was roughly same in a same egg cluster in P. pryeri and Pd. paradoxa, though the time varies in a same cluster, and in some cases the difference of the time becomes about a month in B. laevipes. The larva cut the chorion with the egg tooth and came out of the egg in P. pryeri. The newly hatched larvae often eat the choria and also chopped insects in P. pryeri and B. laevipes. However the newly hatched larvae of Pd. paradoxa never eat the choria and chopped insects, so that they seem to be not carnivorous.

Discussion on this item

There are not so many reports on the change of egg size during the embryogenesis of mecopteran insects. Yie (1951) studied in detail the change of egg size in P. folsa. According to him, the egg volume just before hatching gets ca. 2.2 times large as that of the newly laid egg.

The present data concerned with the rate of the volume of the full-grown egg against the newly laid one approximately agreed with the data obtained in other mecopteran insects, for example, ca. 2.6 times in P. nuptialis (Byers, 1963), ca. 4 times in B. stigmaterus (Setty, 1931) and ca. 3.5 times in Bo. notoperates (Cooper, 1974).

Gassner (1963) observed that the larva of P. nuptialis cut the chorion and came out from the egg as

observed in P. pryeri. The first instar larva of Bo. notoperates has no egg tooth and cut the chorion with the mandible according to Cooper (1974).

The fact that the newly hatched larvae of Panorpa eat the chorion is already known (Yie, 1951; Byers, 1963). As for Bittacus, however, this fact was confirmed for the first time in B. laevipes.

VI. Formation of inner layer and embryonic envelopes

Panorpa pryeri

Middle in Stage 2, the future middle plate and lateral ones differentiate in the embryonic area, and the future amnion becomes discernible in the anterior part of the embryonic area (Fig. 115). Late in Stage 2, the amniotic folds appear in the posterior and anterior margins of the embryonic area. At the same time, cells of the embryonic area thicken a little near the posterior pole of the egg (Fig. 116).

As development proceeds, the primitive groove arises from near the posterior pole of the egg, and reaches to the posterior part of the protocephalon at Stage 3 (Fig. 40). The amnion covers the large part of ventral surface of the embryo. The manner of formation of the amniotic fold is shown diagrammatically in Fig. 117. The extraembryonic area becomes the serosa.

At the beginning of Stage 3, the amnion almost

covers the embryo. At the same time, several cells of the middle plate begin to invaginate at the preoral region (Fig. 118).

Middle in Stage 3, the middle plate becomes multi-cell layers at the preoral region (Fig. 119). At the post-oral region, however, the inner layer formation already commences in the manner of the invagination of the tubular middle plate (Fig. 120). Soon this tubular middle plate begins to break.

Late in Stage 3, the ventral side of the embryo is compoletely covered with the amnion, and the primitive groove reaches to the anterior margin of the proto-cephalon. At the preoral region, the multi-cell layered middle plate invaginates as tubular-form (Fig. 121). The primitive groove near the caudal end of the embryo begins to close. At the end of Stage 3, the primitive groove almost disappears at a whole region of the embryo.

Panorpodes paradoxa

Middle in Stage 2, the germ rudiment begins to invaginate into the yolk mass, and nuclei of the developing serosa are heavily stained with hematoxylin as mentioned before (Fig. 64).

Late in Stage 2, there occur the primitive groove and inner layer on median line of the sac-like germ rudiment (Fig. 122). The serosa becomes thin (ca. 15μm),

though the amnion keeps the original thickness.

Middle in Stage 3, the serosa becomes thinner (ca. 10μm), and the yolk spherules existing in cells of the embryonic and extraembryonic areas disappear.

Late in Stage 3, the serosal cells become much thinner (ca. 5μm) and their nuclei become flat (Fig. 123). At the end of Stage 3, the developing amnion becomes membraneous (Fig. 124), and the inner layer at the protocephalon spreads sideways, but the inner layer near the caudal end still keeps a tubular form.

Bittacus laevipes

In Stage 3, it is observed that cells on the median line of the embryo proliferate inward (Fig. 125), and these cells become to be the inner layer or mesoderm.

As development proceeds, the inner layer cells increase in number, and are found along the median line of the embryo from the anterior end to the posterior one at the middle of Stage 3 (Fig. 126).

By the same time, the amnion covers the ventral surface of the embryo.

Boreus westwoodi

In Stage 3, the middle plate which differentiated in Stage 2 becomes a tubular form and invaginates on the median line of the embryo (Fig. 106).

At the same time, the ventral surface of the embryo is covered with the vacuolated amnion. As development proceeds, the tubular form of the middle plate breaks down at the anterior part of the embryo (Fig. 127), but persists in the posterior part of the embryo.

In Stage 4, the tubular form of the middle plate finally disappears at the posterior part of the developing embryo.

Discussion on this item

Johannsen and Butt (1941) classified the inner layer formation of the pterygotes into following three types. The first type is that the inner layer is formed by a sinking middle plate which will be converted into a sunken tube by the approach and fusion of the lateral plates. The second type is that the inner layer is formed by a sinking middle plate which is cut off from the lateral plates. The third type is that the inner layer is formed by the inward proliferation of the cells along the median line of the embryo without the differentiation of the middle plate.

The first type is observed in many holometabolan insects, for example, Megaloptera, Sialis mitsuhashii (Suzuki, Shimizu and Ando, 1981), Neuroptera, Chrysopa perla (Bock, 1939), Trichoptera, Stenopsyche (Miyakawa,

1974a), Coleoptera, Tenebrio molitor (Ullmann, 1964), Diptera, Dacus (Anderson, 1962), etc., and in some hemimetabolan Hemiptera, i.e., Pyrilla perpusilla (Sander, 1956) and Gerris paludum insuralis (Mori, 1969).

The second type is observed in Isoptera, Kalotermes flavicollis (Striebel, 1960), Hemiptera, Oncopeltus fasciatus (Butt, 1949) and Hymenoptera, Apis mellifica (Nelson, 1915).

The third type is reported in some hemimetabolan insects, i.e., Odonata (Ando, 1962), Blatta (Wheeler, 1889) and Orthoptera, Locusta migratoria migratorioides (Roonwal, 1936), and some Symphyta of the Hymenoptera, Pteronidea ribessii (Shafiq, 1954). It is generally thought that the third type is more primitive than two former types.

In the some Lepidoptera, Peiris rapae (Eastham, 1927), Heliothis zea (Presser and Rutschky, 1957) and Chilo suppressalis (Okada, 1960), the type of the inner layer formation differs at the parts of the embryo, so that several embryologists doubt the phylogenetic significance as to the manner of the inner layer formation. However it is also possible to regard the fact that the differences in the inner layer formation occur as a significant character for those lepidopteran species.

In P. pryeri, Pd. paradoxa and Bo. westwoodi, the inner layer is formed by the first type same as in P.

communis (Wolf, 1961) and other many holometabolans. On the other hand, in B. laevipes it is formed only by the third type. Considering the little existence of the inner layer formation by the third type in the Holometabola, it seems that B. laevipes is more primitive than P. pryeri, Pd. paradoxa and Bo. westwoodi in the inner layer formation.

In the psocopteran Liposcelis divergens (Goss, 1953) and lepidopteran Pieris (Eastham, 1927) and Diacrisia virginica (Johhansen, 1929), the developing amnion grows by mitosis and covers the ventral surface of the embryo. In P. pryeri and Pd. paradoxa, however, little mitoses in the developing amnion were observed.

VII. Organogenesis

1. Ectodermal derivatives

i) Invaginations

a) Endoskeletons, salivary and anal glands

Panorpa pryeri

Six pairs of ectodermal invaginations were observed in the cephalognathal region in this species (Fig. 128). Namely, there appear the anterior and posterior tentoria, extensor and flexor mandibular apodemes, maxillary apodemes and salivary gland. Moreover the labral apodeme and anal gland appear singly on the median line of the embryo.

Late in Stage 5, the paired invaginations of anterior tentoria appear at the posterior parts of the intercalary

segment or anterolateral parts of bases of the mandibular appendages, and paired invaginations of salivary glands arise at the posteromedial parts of bases of the labial appendages (Fig. 129).

Middle in Stage 6, the paired invaginations of flexor mandibular apodemes arise at the posterolateral parts of bases of the mandibular appendages, and the paired invaginations of posterior tentoria appear at the anterolateral parts of bases of the labial appendages (Figs. 130, 131). At the same time, tips of the invaginations of the salivary glands become sac-shaped at the second thoracic segment.

In Stage 7, maxillary apodemes begin to invaginate at the posteromedial part of bases of maxillary appendages. The distal ends of the both posterior tentoria fuse with each other and form a central body, and then distal ends of the both anterior tentoria fuse with the central body (Fig. 132). The developing flexor mandibular apodemes become L-shaped in the transverse section of the middle portion. The rudiments of extensor mandibular apodemes arise at the anterior parts of the madibular bases. The openings of the rudimental salivary glands fuse with each other forming a common duct. From there, the forked ducts extend to the third thoracic segment, and the sac-shaped distal ends occupy the first and second abdominal segments.

At the same time, a shallow invagination which is the rudiment of the median labral apodeme is formed at the dorsocentral point of the clypeolabral suture, and the other shallow invagination which also makes its appearance between the ninth and tenth abdominal segments on the medioventral line.

Middle in Stage 7, the median labral apodeme becomes deeper (Fig. 133), and from its distal end muscles extend posteriorly.

Middle in Stage 8, the developing anal gland becomes deeper and its surrounding mesodermal cells begin to differentiate into muscles and fat bodies, but the depth of the median labral apodeme is same as in the prior stage.

Fig. 134 shows the endoskeletons of the first instar larva diagrammatically. Only the tentoria directly continue with the cuticle of the cranium (Fig. 135). The maxillary apodemes indirectly connect with the labium through the membraneous zone or conjunctiva. The mandibular apodemes only connect with the conjunctiva located between the mandible and cranium (Fig. 136).

The anal gland of the first instar larva is often surrounded with fat bodies (Fig. 137).

Panorpodes paradoxa and Bittacus laevipes

In Pd. paradoxa and B. laevipes, six pairs of ectodermal invaginations with two other single ones at the similar

regions of embryos are found as in P. pryeri.

In Pd. paradoxa, ectodermal invaginations arise at the end of Stage 4 without a labral apodeme and anal gland which are formed in Stage 6. The lumen of the gland of the first instar larva is filled with the cytoplasm of the gland cells.

In B. laevipes, ectodermal invaginations begin to appear at the end of Stage 5 without a labral apodeme and anal gland which arise at the end of Stage 7. The anal gland of the first instar larva has a lumen as in P. pryeri.

In Bo. westwoodi, the anal gland was not found in the larva.

Discussion on this item

At the cephalognathal region, four pairs of the ectodermal invaginations appear in many insects, viz., Odonata, Epiophlebia superstes (Ando, 1962), Trichoptera, Stenopsyche (Miyakawa, 1974b), Lepidoptera, Pieris (Eastham, 1930), Hymenoptera, Apis (Nelson, 1915), etc. The paired anterior tentoria invaginate from the posterior part of the intercalary segment or the anterior margin of the mandibular segment. The mandibular apodemes appear at the posterior part of the mandibular segment. In the Coleoptera, Lytta viridana (Rempel and Church, 1971), Tenebrio (Ullmann, 1967), Diptera, Chilo (Okada, 1960) and P.

pryeri, two pairs of mandibular apodemes, i.e., flexor and extensor mandibular ones appear.

The paired posterior tentoria arise at the posterior part of the maxillary segment or the anterior part of the labial segment, but they appear at the anterior part of the maxillary segment in Locusta (Roonwal, 1937).

Eastham (1930) considered that the arrangement of cephalic apodemes follows a metameric sequence, and this view is generally accepted. There are, however, some disputes concerned with the association of some apodemes, especially the anterior tentorium, with particular segments.

Eastham (1930) and Ullmann (1967) maintained that the anterior tentoria are derived from the antennal segment, because they observed that the invaginations of anterior tentoria appeared at the posterior part of the antennal base. Okada (1960), and Rempel and Chruch (1971) associated this tentoria with the intercalary segment, and the author agrees with them in P. pryeri, Pd. paradoxa and B. laevipes, because the anterior tentorial invaginations never arise at the base of the antennae.

Rempel and Church (1971) found the paired labral apodemes in Lytta and suggested the possibility of the appendicular nature of the labrum. The labral apodeme of P. pryeri, Pd. paradoxa and B. laevipes, however, develops singly from its appearance, so that this apodeme

seems not to be the true one being a mark of the metamerism.

The central body of the tentorium is derived from the posterior tentorial invaginations in the odonatan Tanypteryx pryeri (Ando, 1962), Locusta (Roonwal, 1937), Tenebrio (Ullmann, 1967) and Lytta (Rempel and Church, 1971), or from the anterior tentorial invaginations in the coleopteran Calandra oryzae (Tiegs and Murray, 1938). The formation of the central body is the same as in the former group in P. pryeri, Pd. paradoxa and B. laevipes.

Rempel and Church (1971) associate the extensor mandibular apodeme with the antennal segment in Lytta. The author could not determine the association of the extensor apodeme, because the invagination of the apodeme appears between the anterior part of the mandibular base and the posterior part of the antennal base. Considering, however, that only one pair of the ectodermal invaginations is allowed to be basically associated with one segment in the cephalognathal region (Eastham, 1930; Matsuda, 1965; Ullmann, 1967), the extensor mandibular apodemes should be associated with the antennal segment, because the flexor apodeme is associated with the mandibular segment, and the anterior tentorium is associated with the intercalary segment in P. pryeri, Pd. paradoxa and B. laevipes.

The existence of the anal gland is unknown in insects without in P. pryeri, Pd. paradoxa and B. laevipes. The anal glands of some coleopteran insects appear in the

epidermis of the rectum (Snodgrass, 1935) and are a different organ from that of the mecopteran insects. The anal glands of P. pryeri, Pd. paradoxa and B. laevipes seem to have a spinal nature, because it arises as a single invagination and has little glandular features at least in the first instar stage.

b) Corpora allata and prothoracic glands

Bittacus laevipes

In Stage 7, there appears a pair of cell masses in the ectoderm just in front of the invaginating anterior tentoria (Fig. 138). The mass consists of about a dozen cells which their cytoplasm is stained faintly with eosin, and this mass is the rudimental corpus allatum.

At the end of Stage 7, the anlage of the corpus allatum moves inward keeping a connection with the body wall and is situated between the anterior tentorium, flexor mandibular apodeme and suboesophageal ganglion (Fig. 139).

In Stage 8, the rudimental corpus allatum loses its connection with the body wall, and takes a position on the side of the stomodaeum at the posterior margin of the cranium of the embryo which is the same as that of the first instar larva (Fig. 140).

On the other hand, a shallow ectodermal invagination becomes visible at the anterior margin of the first thoracic segment on the medioventral line at the end of Stage

7. The invagination deepens and passes between the developing interganglionic connectives, and the distal part of the invagination grows bilaterally and the cytoplasm of the parts becomes to be stained faintly with eosin (Fig. 141). These distal parts are likely to be future prothoracic glands.

The author failed to observe the further development of these rudiments. The prothoracic glands are found on the connectives in front of the first thoracic ganglion in the first instar larva (Fig. 142).

Panorpa pryeri and Panorpodes paradoxa

In P. pryeri, a pair of cell masses appears at the posterior part of the intercalary segment or in front of the invaginations of the developing anterior tentoria (Fig. 129). The cell mass is composed of four to five cells which have nuclei poorly stained with hematoxylin, and this cell mass seems to be a future corpus allatum.

The author could not follow the further development of the corpora allata.

The corpora allata of the first instar larva of these species are located just behind of the corpora cardiaca (Fig. 169).

Discussion on this item

The origin of the corpora allata is generally con-

sidered as ectodermal (Nelson, 1915; Eastham, 1930; Roonwal, 1937; Ando, 1962; etc.), though Tiegs and Murray (1938) suggested that the corpora allata are derived from the antennal coelomic sac, i.e., mesodermal origin in Calandra.

The original segment of the corpora allata, however, seems to be not fixed, namely is associated with the intercalary segment in P. pryeri and B. laevipes; with the mandibular segment in dragonflies (Ando, 1962), Pieris (Eastham, 1930), Chilo (Okada, 1960); or with the maxillary segment in Apis (Nelson, 1915), Oncopeltus (Dorn, 1972), Lytta (Rempel, Heming and Church, 1977), Stenopsyche (Miyakawa, 1974b).

The developing corpora allata are surrounded with the cellular sheath derived from the antennal mesoderm in Locusta (Roonwal, 1937), but this phenomenon was never observed in P. pryeri, Pd. paradoxa and B. laevipes.

The corpora allata of P. pryeri and Pd. paradoxa finally become to be close together with the corpora cardiaca, and this fact is also observed in Chilo (Okada, 1960), Oncopeltus (Dorn, 1972) and Lytta (Rempel, Heming and Church, 1977).

The prothoracic glands are generally derived from a pair of invaginations formed at the posteroventral margin of the labial segment or the anteroventral margin of the first thoracic segment (Okada, 1960; Ando, 1962; Miyakawa,

1974b). The prothoracic glands of B. laevipes seem to be derived from a single invagination and have some doubts about its formation. Recently, however, Rempel, Heming and Church (1977) reported that the prothoracic glands of Lytta are derived from a single invagination at the labial-prothoracic intersegmental region on the medioventral line as in B. laevipes.

c) Tracheae

Panorpa pryeri

Late in Stage 5, paired tracheal invaginations become evident (Fig. 143) on the second thoracic segment to the eighth abdominal segment. They locate at the anterolateral parts of bases of the developing second thoracic appendages and comparable regions of each of following nine segments. These invaginations are shallow, however the spiracles disappear, and a pair of new spiracles is found than others and grow anteriorly. Middle in Stage 6, the tracheal rudiments in the mesothorax begin to fork (Fig. 144), while the other invaginations possess the original depth.

In Stage 7, the mesothoracic tracheal rudiments elongate into the gnathal segment, and then their openings or spiracles disappear, and a pair of new spiracles is found on the posterior part of the prothorax (Fig. 53). These new spiracles seem to be anterioly shifted spiracles of

the mesothorax, because the tracheal invaginations are never found on the pro- and mesothoracic segments at once, and the tracheal invaginations on the prothorax already have long branched tracheal trunks from their first appearance. The openings of the tracheal invaginations on the metathorax become to be vestigial. Each of tracheal invaginations connects with those of the anterior and posterior segments by Stage 8. Late in the stage, the proximal parts of the tracheal invaginations commence to form rudimental atriums. The openings of the tracheal invaginations on the metathorax finally close, though vestigial tracheal trunks contact with the inner side of the body wall (Fig. 145) and the connections are observed also in the first instar larva.

In Stage 9, the developing atriums become chitinous, and those of the first instar larva have chitinous compartments around the openings (Fig. 146).

Panorpodes paradoxa and Bittacus laevipes

The tracheal formation of Pd. paradoxa and B. laevipes is similar to that of P. pryeri.

In Pd. paradoxa, late in Stage 5, paired tracheal invaginations appear on the mesothoracic segment to the eighth abdominal segment, and in Stage 7 in B. laevipes. A pair of tracheal invaginations shifts from the mesothoracic segment to the prothoracic one in Stage 6 in Pd.

paradoxa and late in Stage 7 in B. laevipes, while the openings of the tracheal invaginations on the metathoracic segment disappear. The vestigial tracheal trunks of the metathoracic segment, however, are contacting with the inner side of the metathoracic body wall in the first instar larvae of Pd. paradoxa and B. laevipes as in P. pryeri.

Discussion on this item

The embryonic development of the tracheal system is investigated in detail by Ando (1962), and Rempel and Church (1972).

The paired tracheal invaginations at first arise on the mesothoracic segment to the seventh or eighth abdominal segment of the embryos in many insects, for example, in the Odonata (Ando, 1962), Locusta (Roonwal, 1937), Siphonaptera, Ctenocephalides felis (Kessel, 1939), Tenebrio (Ullmann, 1967), P. pryeri, Pd. paradoxa and B. laevipes.

In Locusta (Roonwal, 1937), the spiracles of the meso- and metathoracic segments migrate forward as development proceeds, and finally the former is located at the pro- and mesothoracic intersegmental zone, and the latter at the posterior margin of the mesothoracic pleuron.

In the holometabolan embryos, the migration of the mesothoracic spiracles to the prothoracic segment is known

in Ctenocephalides (Kessel, 1939), Lytta (Rempel and Church, 1972), P. pryeri, Pd. paradoxa and B. laevipes, so that the prothoracic spiracles of these species are apparently originated from the mesothoracic segments, and this fact supports Matsuda's view (1970) that in the Holometabola, "the anterior thoracic spiracle has shifted its position anteriorly from the primitive position on the mesothorax".

Snodgrass (1935) suggests that in the adult of apterygote Japygidae, Heterojapyx gallardi, the spiracles of the thorax do not correspond in their position to those of the abdomen, so that the thoracic spiracles are not serially homologous to the abdominal spiracles.

The thoracic spiracles, however, of P. pryeri, Pd. paradoxa and B. laevipes are apparently arranged in a row with the abdominal spiracles during the embryonic stage, therefore the author believes that the thoracic spiracles are serially homologous to the abdominal ones.

In the hymenopteran Apis (Nelson, 1915) and Athalia (Farooqi, 1963), a pair of tracheal invaginations arises in the maxillary segment in the embryonic stage, and in Apis, tracheal trunks in the head are derived from these invaginations. However in P. pryeri, Pd. paradoxa and B. laevipes those invaginations were never observed.

During the embryogenesis, the spiracles of the metathoracic segment disappear, and the only vestigial tra-

cheal trunks connect with the inner side of the body wall in the first instar larvae in P. pryeri, Pd. paradoxa and B. laevipes. The same fact is reported by Rempel and Church (1972) in Lytta.

In the mecopteran Nannochoristidae, Choristella philpotti (Pilgrim, 1972), there are nonfunctional and vestigial spiracles on the metathoracic segment in the larval stage, and this fact seems to suggest the primitive nature of this species from the result of the present study.

ii) Oenocytes and trichogen cells

Panorpa pryeri

In Stage 7, there are found paired cell masses in the ectoderm at just posteromedial positions of the spiracles of the first eight abdominal segments. These cell masses are stained poorly with hematoxylin and consist of four to five cells which are large in size (ca. 20μm) and have large nuclei (ca. 10μm in diameter) (Fig. 147). These cell masses are the rudimental oenocytes. On the other hand, there are also observed paired cell masses in the ectoderm at the medial parts of bases of the developing dorsal processes on the first nine abdominal segments. These cell masses consist of ten to twelve cells which have the similar characters as appeared in the rudimental oenocytes. Moreover there arise paired cell

masses in the ectoderm at the lateral parts of bases of the developing abdominal legs of the first eight segments. These cell masses contain five to six cells which have the similar characters as the rudimental oenocytes.

Late in Stage 9, all of these cell masses become to be stained much lighter with hematoxylin, and they are situated at almost original positions contacting with the inner side of the body wall in the first instar larva. During the embryogenesis, cell divisions of the oenocytes were never seen.

On the other hand, there are observed some cells which have larger nuclei (ca. 15μm in diameter) and cytoplasmic processes toward the body surface. They are the rudimental trichogen cells.

Panorpodes paradoxa and Bittacus laevipes

In Pd. paradoxa, the rudimental oenocytes appear as paired cell masses in the ectoderm at just posteromedial part of the spiracles of the first eight abdominal segments in Stage 5 (Fig. 149), and in Stage 7 in B. laevipes (Fig. 148). In Pd. paradoxa, this cell mass consists of seven to eight cells and the nuclei of the cells are 5 to 6μm in diameter and slightly larger than those of the surrounding ectodermal cells.

In B. laevipes, this cell mass contains about ten cells which are stained lightly with hematoxylin and have

large nuclei (ca. 7μm in diameter). At the same time, rudimental trichogen cells become apparent in the ectoderm of the body wall, and the oenocytes are still found in the first instar larvae in Pd. paradoxa and B. laevipes as in P. pryeri.

The oenocyte-like cell masses which are found at the both sides of the rudimental oceonocytes in P. pryeri are never found through the embryonic stage in Pd. paradoxa and B. laevipes.

Discussion on this item

The oenocytes appear in the ectoderm at the postero-medial parts of the spiracles on the first seven or eight abdominal segments in many insects, i.e., the orthopteran Locusta (Roonwal, 1937), neuropteran Chrysopa (Bock, 1939), lepidopteran Diacrisia (Johannsen, 1929), coleopteran Euryope terminalis (Paterson, 1932), dipteran Aedes aegypti (Raminani and Cupp, 1978), etc. In P. pryeri, Pd. paradoxa and B. laevipes, the manner of the oenocyte formation is the same as in the above mentioned species. The existence of the oenocyte-like cell masses found at the both sides of the oenocytes in P. pryeri may be unknown in other insect embryos.

In P. pryeri, Pd. paradoxa and B. laevipes, it seems that the oenocytes does not increase in number during the embryonic stage, but they increase in number in Euryope

(Paterson, 1932).

The rudimental trichogen cells newly appear at the stage when oenocytes are formed, and the nuclei of trichogen cells are larger than those of the oenocytes in P. pryeri, Pd. paradoxa and B. laevipes. These characters of the trichogen cells are also observed in Chrysopa (Bock, 1939) and Diacrisia (Johannsen, 1929).

iii) Nervous system

a) Ventral nerve cord

Panorpa pryeri

Late in Stage 4 or at the beginning of Stage 5, neuroblasts are discernible in the ectoderm of gnathal and following segments on both sides of the medioventral line of the embryo (Fig. 150). These cells are easily distinguished from the surrounding ectodermal cells, since they are stained lightly with hematoxylin, large in size (ca. 20μm) and have large nuclei (10 to 12μm in diameter). There are about ten neuroblasts on each side of the segment in the thoracic region. At the same time, there appears a shallow furrow along the medioventral line, and it is the rudimantal neural groove.

Late in Stage 5, the number of neuroblasts increases to fifteen to twenty on each side of the thoracic segment. In Stage 6, the neuroblasts repeat mitoses and pile up inward two rows of daughter cells which become the future

ganglion cells. The peripheral daughter cells become to be slightly flat and cover the developing ganglia (Fig. 151).

On the other hand, the neural groove deepens and the ectodermal cells of the medioventral line become to be situated between the developing ganglia. They are the rudimental median cord. As development proceeds, in the developing median cord, there occur three to four cells which are stained lightly with hematoxylin and have large nuclei (ca. 10μm in diameter)(Fig. 152). They are similar to the neuroblasts as to the above mentioned characters and are found in each of segments.

Middle in Stage 6, the paired developing ganglia begin to connect with each other by two commissures, though by only one commissure in the mandibular segment. The neuroblast-like cells of the median cord seem to participate in the formation of the glial elements (Fig. 153). At the same time, the peripheral daughter cells mentioned before begin to be membraneous, and seem to be the developing neurilemma.

Each ganglion in which the neuropiles do not yet differentiate is connected with adjacent ganglia by two connectives. The median cord almost loses its connection with the ventral epidermis. At the interganglionic regions, median cord cells do not participate in the ganglion formation and degenerate during the late embryogenesis.

Late in Stage 6, the ganglia of the mandibualr, maxillary and labial, and of the eighth to the tenth abdominal segments begin to gather. In Stage 7, these ganglionic concentrations further proceed, and the former forms a large suboesophageal ganglion at the posterior part of the head, and the latter forms a large synganglion at the eighth abdominal segment.

Panorpodes paradoxa, Bittacus laevipes and Boreus westwoodi

The formation of the ventral nerve cord in Pd. paradoxa and B. laevipes is basically the same as that of P. pryeri. In Pd. paradoxa and B. laevipes, at the end of Stage 4, neuroblasts are distinguishable in the ectoderm of the gnathal and following segments on both sides of the medioventral line (Fig. 154). In each of thoracic and abdominal segments, there are about a dozen neuroblasts on each side of the segment, and several large cells of the median cord seem to take part in the glial element formation in Pd. paradoxa and B. laevipes as in P. pryeri.

In Stage 6, the gnathal ganglia start gathering together, and the same tendency is observed in the eighth to the tenth abdominal ganglia of Pd. paradoxa and B. laevipes.

In Bo. westwoodi, neuroblasts are discernible in the gnathal and following segments at the end of Stage 4, and about ten neuroblasts are counted on each side of the

thoracic segments (Fig. 155).

b) Brain

Panorpa pryeri

Late in Stage 4, there arise three pairs of the protocephalic ectodermal bulges (Fig. 156) in which there are found some round cells, namely neuroblasts.

Middle in Stage 5, the neuroblasts increase in number and are stained lightly with hematoxylin (Fig. 157). These neuroblasts begin to form the tissues of lobus 1, 2 and 3 of the future protocerebrum. At the same time, paired neuroblast masses of which the future deutocerebrum are found in the ectoderm at both sides of the developing stomodaeum. On the other hand, a pair of neuroblast masses appears in the intercalary segment, and these masses develop to the future tritocerebrum. Fig. 158 shows diagrammatically the distributions of the ganglia and mesodermal cells of the cephalognathal region in this stage.

Middle in Stage 6, the neuroblasts of the lobus 1, 2 and 3 produce a large number of daughter cells by division and these lobi begin to be free from the protocephalic body wall. There is also a pair of small neuroblast masses at the median parts of the innermost lobi, namely lobi 3, and these masses seem to be lobi 3' (Fig. 159). The lobus 1, 2, 3 and 3' fuse with each other to form the

future protocerebrum, and at this time, this developing proto-, deuto- and tritocerebrum become to connect with neighbors. The optic plate differentiates in the protocephalic body wall connecting with the lobus 1 (Fig. 160).

In Stage 7, the paired lobi 3 are connected by the commissure, and the connective also appears between the proto- and deutocerebrum, and neuropiles are formed in the developing brain. The lobus 1 differentiates into the proximal and distal parts (Fig. 161), and the former is the future medulla, and the latter is the future lamina ganglionaris. The commissure of tritocerebrum located beneath the developing stomodaeum is formed (Fig. 132).

In Stage 9, the brain of the embryo reaches its completion. In the upper part of the lobus 2, there arise two to three round cells which have large nuclei (ca. 20μm in diameter). These nuclei are little stained with hematoxylin and contain a few particles stained with eosin. Regarding their position, they are probably considered as globuli cells of the corpora pedunculata. At the same time, the innervations are found from the deutocerebrum to the antennae, and also from the tritocerebrum to the frontal ganglion.

In the lobus 1, about a dozen cells which are stained slightly deeper with hematoxylin than surrounding cells are discernible at the distal margin of the medulla (Fig. 162). Their cytoplasm is stained darkly with eosin

in the first instar larva. Fig. 163 shows diagrammatically the brain of the first instar larva.

Panorpodes paradoxa, Bittacus laevipes and Boreus westwoodi

In B. laevipes, there are three pairs of the protocephalic bulges middle in Stage 4. Late in the stage, neuroblasts appear in the protocephalic ectoderm. The following embryonic development of the brain, including those of Pd. paradoxa, is basically the same as those of P. pryeri.

In Pd. paradoxa, neuroblasts appear in the protocephalic ectoderm late in Stage 4, and in Stage 5 in Bo. westwoodi.

c) Stomatogastric nervous system

Panorpa pryeri

Middle in Stage 5, three evaginations first become apparent along the mediodorsal line of the developing stomodaeum (Fig. 164). The future stomatogastric nervous system is derived from these three evaginations.

Middle in Stage 6, the evaginations elongate forward along the stomodaeal roof (Fig. 165). The rudiment of the frontal ganglion arises from the anterior evagination, those of the recurrent nerve and the hypocerebral ganglion are derived from the median and posterior evaginations respectively. As development proceeds, the tubular form

of the evaginations begins to break down.

In Stage 7, the developing frontal ganglion migrates forward, and the nerve fibers are formed within the frontal and hypocerebral ganglia, and recurrent nerve. The anlagen of the corpora cardiaca begin to differentiate from the anteroventral part of the developing hypocerebral ganglion which is situated near the bottom of the developing stomodaeum (Fig. 166).

Middle in Stage 7, the openings of the anterior two evaginations close, and then that of the posterior one also closes. Middle in Stage 8, the rudimental corpora cardiaca begin to shift laterally (Fig. 167).

In the first instar larva, the corpora cardiaca are located at the posterolateral parts of the hypocerebral ganglion (Fig. 168). There observes a pair of paracardiac nerves which run forward from the anterior ends of the corpora cardiaca. On the other hand, the corpora allata unite with the posterior ends of the corpora cardiaca (Fig. 169).

Panorpodes paradoxa and Bittacus laevipes

In Pd. paradoxa and B. laevipes the stomatogastric nervous system is formed from the three evaginations which arise at the stomdaeal roof in the beginning of Stage 5 (Fig. 170), and the formation of the system is fundamentally the same as that of P. pryeri.

Discussion on this item

The embryogenesis of the brain in P. pryeri, Pd. paradoxa and B. laevipes is similar to those observed in other insects (Roonwal, 1937; Kessel, 1939; Ando, 1962; Miyakawa, 1974b).

In Tenebrio (Ullmann, 1967), the neuroblasts do not appear in the lobus 1 or the optic lobe through the embryogenesis. The neuroblasts, however, apparently arise in the lobus 1 in P. pryeri, Pd. paradoxa and B. laevipes. Furthermore Ullmann (1967) states that the lobus 1 is derived from the ectodermal invagination, and the same manner of the lobus 1 formation is known in Lytta (Rempel, Heming and Church, 1977), though in P. pryeri, Pd. paradoxa and B. laevipes the lobus 1 is never derived from the ectodermal invagination as observed above mentioned species.

The stomatogastric nervous system originates from an evagination of the stomodaeal roof in Epiophlebia (Ando, 1962). Howerver in Chilo (Okada, 1960) and Aedes (Raminani and Cupp, 1978), no evaginations appear and the system is derived directly from the epipharyngeal roof. In P. pryeri, Pd. paradoxa and B. laevipes, the system originates from three evaginations of the stomodaeal roof as known in many other insects (Roonwal, 1937; Tiegs and Murray, 1938; Ullmann, 1967; Rempel and Church, 1969;

Miyakawa, 1974b).

As for the embryogenesis of the ventral nerve cord, there are two problems. The first is the participation of the median cord in the glial element formation, and the second is the origin of the neurilemma.

Baden (1936) suggested that the median cord participates in neither ganglionic formation nor other organic formation, and degenrates. It seems to be the general view, however, that the median cord takes part in the formation of the glial elements or neuropiles (Okada, 1960; Springer, 1967; Springer and Rutschky, 1969; Miyakawa, 1974b; etc.), and the result of the present study seems to agree with this view.

As for the origin of the neurilemma, there are three views, i.e., the first is the lateral cord origin (Nelson, 1915; Eastham, 1930; Roonwal, 1937; Ando, 1962; Ashhurst, 1965), the second is the median cord origin (Tiegs and Murray, 1938; Okada, 1960), and the third is the mesodermal origin (Baden, 1936; Larink, 1969). In P. pryeri, the peripheral ganglionic cells derived from the lateral cord seem to form the neurilemma.

iv) Sense organ - larval eyes

Panorpa pryeri

Middle in Stage 6, at the lateral body wall of the embryonic head, rudimental optic plates become evident,

and they are thicker than surrounding ectodermal parts and connected with rudimental postretinal fibers of lobi 1. Simultaneously the cell arrangement of developing optic plates begin to be irregular (Fig. 160).

In Stage 7, rudiments of the retinular and Semper's cells differentiate in the developing optic plates, and crystalline cones are formed by the Semper's cells (Fig. 161).

Middle in Stage 9, the developing crystalline cones become conspicuous (Fig. 171), because they are not stained with hematoxylin or eosin. Rudimantal rhabdoms are descernible beneath the crystalline cones. On the surface of the developing larval eyes, there is a corneal zone of 1 to 1.5μm-thick secreted by the corneagenous cells or primary pigment cells, and a basement membrane is distinguishable. As development proceeds, the cornea thickens to ca. 6μm-thick in maximum and that of the first instar larva shows slightly biconvex (Fig. 172). Judging from its staining character, the cornea is divided into three layers. The outer layer, ca. 4μm-thick, is transparent, the middle layer , ca. 1μm-thick, is stained with eosin and the inner layer is stained with hematoxylin. The eyes located near the posterior parts of the antennal bases consist of about thirty ommatidia severally. An ommatidium has four Semper's cells and eight retinular cells.

Bittacus laevipes and Panorpodes paradoxa

In B. laevipes, the rudimental postretinal fiber appears beneath the developing optic plate middle in Stage 5. The cell differentiation occurs in the optic plate which begins to thicken in Stage 7, and the developing crystalline cones are discernible in Stage 8.

The components in an ommatidium of the first instar larva (Fig. 173) are similar to those in P. pryeri.

In Pd. paradoxa, a rudimental postretinal fiber elongates from the lobus 1 of the protocerebrum to the future optic plate at the end of Stage 4 or the beginning of Stage 5 (Fig. 174). In Stage 6, the rudimental optic plate slightly thickens, though no cell differentiation is observed. Late in this stage, however, the postretinal fiber degenerates and the optic plate has no connection with the lobus 1, and then the optic plate becomes again thin (Fig. 175). As a result, the first instar larva of Pd. paradoxa has no larval eyes.

Discussion on this item

Generally speaking, larvae of the holometabolan insects have lateral ocelli or stemmata (Snodgrass, 1935; Paulus, 1979), and the embryogenesis of the stemmata seems to be fundamentally classified into two types. The first type is that the formation of the stemmata is accompanied with the ectodermal invagination of the deve-

loping optic plate, and invaginated ectodermal cells differentiate into retinular cells of the stmmata. This type is reported in the coleopteran Hydrophilus (Patten, 1887).

The second type is that without ectodermal invagination of the optic plate, and the plate thickens and the elements of the future stemmata including retinular cells occur within the developing optic plate. This type is known in the lepidopteran Ephestia kühniella (Busselmann, 1935) and Heliothis (Presser and Rutschky, 1957), and the mecopteran P. pryeri and B. laevipes, and moreover the compound eye formation of the hemimetabolan insects, i.e., Epiophlebia (Ando, 1957) and Oncopeltus (Butt, 1949) belongs to this type. The insects included in the second type are divided into two groups further. The first group has a typical ommatidium which has four Semper's cells and eight retinular cells, and Epiophlebia and Oncopeltus and other hemimetabolan insects belong to this type (Snodgrass, 1935). The second group includes the stemmata which has three Semper's cells and seven retinular cells (Ephestia, Busselmann, 1935; Heliothis, Presser and Rutschky, 1957).

The ommatidium of P. communis (Bierbrodt, 1942), P. pryeri and B. laevipes has four Semper's cells and eight retinular cells, so that they should be included in the first group of hemimetabolan insects. Paulus (1979) suggests that the stemmata of the second group mentioned

above is modified from the ommatidium of the hemimetabolan insects. Accordingly the larval eyes of P. communis, P. pryeri and B. laevipes are thought to be more akin to those of the hemimetabolans than those of the coleopterans on the manner of its development, and than those of the lepidopterans on the degree of the modification of the ommatidia.

In Pd. paradoxa, the first instar larva has no eyes, this fact already observed by Issiki (1959), and this character seems to be not palingenetic, but caenogenetic judging from the embryogenesis.

2) Mesodermal derivatives

i) Segmentation of inner layer, formation of coelomic sac and differentiation of splanchnic and somatic mesoderm

Panorpa pryeri

In Stage 4, mesodermal cells of the preoral region lie scattered in the protocephalic lobes (Fig. 156). Those of the gnathal segments begin to lie segmentally and expand laterally (Fig. 176) before the segmentation of the embryonic ectoderm while there exists a layer of mesodermal cells at the intersegmental regions. In the posterior part following the gnathal segments, however, the segmentation of the mesoderm does not yet occur in this stage, and the primary median mesoderm still distributes on the medioventral line of the embryo. The meso-

dermal cells of caudal end of the embryo exist in a large mass (Fig. 187).

In Stage 5, the segmentation of the mesoderm finally reaches to the tenth abdominal segment. Simultaneously paired coelomic sacs appear in the lateral sides of each segment from the mandibular to the third abdominal segment (Fig. 150).

Middle in Stage 5, coelomic sacs of the tenth abdominal segment are formed finally. In the part anterior to the mandibular segment, coelomic sacs are found only in the labral and antennal regions. Fig. 158 shows diagrammatically the distribution of the mesodermal cells and coeloms in the cephalognathal region.

In Stage 6, the ventral wall of the coelom begins to extend and lines the ectoderm of the embryo.
As development proceeds, the cells of the coelomic ventral wall scatter and become rudimental somatic mesodermal cells (Fig. 151). At the same time, the mesodrmal cells of the dorsal wall persist their original cell arrangement, and they are the future splanchnic mesoderm.

Panorpodes paradoxa, Bittacus laevipes and Boreus westwoodi

In Pd. paradoxa and B. laevipes, mesodermal cells distribute from the anterior end to the posterior end of

the embryo (Figs. 126, 177) middle in Stage 3, and in Stage 4, the segmentation of mesoderm begins before the ectodermal segmentation of the embryo.

In Pd. paradoxa, late in Stage 4, paired coelomic sacs are formed in each of the gnathal and following segments, and in Stage 5 in B. laevipes. In the cephalic region, coelomic sacs of the antenna and labrum are found, and in the abdominal segment the paired coelomic sacs are discernible in each of ten segments in the both species (Fig. 178).

The coelomic sacs of the gnathal and thoracic segments commence to differentiate into the developing somatic and splanchnic mesoderm in Stage 5 in Pd. paradoxa, and in Stage 6 in B. laevipes.

In Bo. westwoodi, the primary median mesoderm migrates laterally in Stage 4. As development advances, the segmentation of the mesoderm occurs in the gnathal and thoracic segments before the ectodermal metamerization of the embryo.

Late in Stage 4, the coelom formation begins (Fig. 155), and the wall of the coelom differentiates into the somatic and splanchnic mesoderm in Stage 5.

Discussion on this item

The segmentation of the mesoderm is generally prior to the metamerization of the ectoderm of the embryo (Johan-

nsen and Butt, 1941; Ando, 1962; Rempel and Chruch, 1969) and it is also true in P. pryeri, Pd. paradoxa, B. laevipes and Bo. westwoodi.

Concerning the differentiation of the somatic and splanchnic mesoderm, the splanchnic one arises from the coelomic dorsal wall, and the somatic one occurs from the ventral wall in general (Nelson, 1915; Bock, 1939; Luginbill. 1953; Sander, 1956; etc.), and the differentiation is undergone in the same way in P. pryeri, Pd. paradoxa, B. laevipes and Bo. westwoodi.

In the Hemimetabola, coelomic sacs often appear in the labral, antennal, intercalary and three gnathal segments in the cephalognathal region (Mellanby, 1936; Roonwal, 1937; Ando, 1962), and in the embryonic abdomen they are found as far as the tenth (Ando, 1962) or eleventh abdominal segment (Roonwal, 1937).

On the other hand, in the several Holometabola, coelomic sacs of the intercalary segment disappear (Trichoptera, Miyakawa, 1974c; Lepidoptera, Eastham, 1930; Shphonaptera, Kessel, 1939), and furthermore coelomic sacs of the mandibular and maxillary segments disappear in the coleopteran Calandra (Tiegs and Murray, 1938) and hymenopteran Athalia (Farooqi, 1963). In the trichopteran Stenopsyche (Miyakawa, 1974c) and siphonapteran Ctenocephalides (Kessel, 1939), coelomic sacs of the tenth abdominal segment do not appear during the embryonic development. In

P. pryeri, Pd. paradoxa, B. laevipes and Bo. westwoodi comparing with the hemimetabolan insects, only the coelomic sacs of the intercalary and eleventh abdominal segments disappear, so that in a point of the coelomic sac development, mecopteran insects seem to possess the more primitive character than those of holometabolan insects mentioned above.

ii) Circulatory system

a) Aorta

Panorpa pryeri

Middle in Stage 6, mesodermal cells located near the bases of the rudimentary antennae become membraneous and begin to elongate backward in the embryonic head (Fig. 179). This membraneous structure is to be a rudimental aorta.

In Stage 7, the developing aorta is found above the stomodaeum though it is not yet tubular (Fig. 166). Middle in Stage 8, the aorta gets a tubular form (Fig. 167). As development proceeds, the tube of the rudimental aorta grows backward and meets with the developing heart or dorsal blood vessel at the first thoracic segment.

In Pd. paradoxa and B. leavipes, the formation of the aorta is undergone in a similar process as in P. pryeri.

b) Heart, pericardial cells, dorsal diaphragm and blood cells

Panorpa pryeri

In Stage 6, median mesodermal cells situated on the ventral nerve cord migrate laterally, and there remains a small amount of mesodermal cells on the ganglia. Simultaneously, among the mesodermal cells on the ganglia there appear a few cells stained poorly with hematoxylin (Fig. 151). They are rudimental blood cells.

In Stage 7, there are observed the cells having large nuclei (ca. 6μm in diameter) stained lightly with hematoxylin are discernible at the lateral margin of the somatic mesoderm of thoracic and following segments (Fig. 180). They are the rudimental cardioblasts.

Middle in Stage 8, they change a crescent form in the transverse section. A few cells or future pericardial cells locate at the lateral side of the abdominal cardioblast (Fig. 181). Several cells of the somatic mesoderm existing at the ventral side of the developing splanchnic muscles become to be less stained with hematoxylin, and are arranged in a row (Fig. 181). They are considered to be the future dorsal diaphragm.

In Stage 9, the tubular heart appears on the mediodorsal line of the embryo from the first thoracic to the ninth abdominal segment. The vacuolated pericardial cells

(Fig. 182) are observed especially at the lateral sides of the heart from the second to the ninth abdominal segment, and in the same segments the well developed dorsal diaphragm exists.

Fig. 183 shows the heart, pericardial cells which are associated with fat bodies, and the dorsal diaphragm at the intersegmental region between the second and third abdominal segments in the first instar larva. The dorsal diaphragm contacts with the body wall only at the intersegmental regions. The pericardial cell has often two nuclei stained faintly with eosin, and its cytoplasm is little stained with hematoxylin. Fig. 184 shows the heart and its muscles, and ostial valves which exist in each segment from the fourth to the eighth abdominal ones. The blood cells are found especially in the head, heart and its circumference.

Panorpodes paradoxa and Bittacus laevipes

In Pd. paradoxa, cardioblasts first become discernible at the lateral margins of the somatic mesoderm of the thoracic and abdominal segments late in Stage 5 (Fig. 185), and in Stage 6 in B. laevipes.

In Stage 7, the nuclei of the cardioblasts become slightly large and are less stained with hematoxylin in B. laevipes (Fig. 148).

In Pd. paradoxa and B. laevipes, blood cells are

derived from the scattered median mesodermal cells, and the formation of the pericardial cells and dorsal diaphragm is essentially the same as those of P. pryeri.

Discussion on this item

In Stenopsyche (Miyakawa, 1974c), the aorta is formed from the labro-antennal coelom, and in Locusta (Roonwal, 1937), Pyrilla (Sander, 1956) and Epiophlebia (Ando, 1962) the aorta is derived from the antennal coelom. The origin of the aorta of P. pryeri, Pd. paradoxa and B. laevipes is the same as that of Locusta, Pyrilla and Epiophlebia. The cardioblasts originate from the lateral edges of the somatic mesoderm, and the dorsal diaphragm originates from the dorsal side of the somatic mesoderm in many insects (Eastham, 1930; Roonwal, 1937; Ando, 1962; Miyakawa, 1974c, etc.) and P. pryeri, Pd. paradoxa and B. laevipes.

As for the pericardial cells, they are derived from somatic mesodermal cells located at the lateral side of the cardioblasts in Locucta (Roonwal, 1937) and Melanoplus (Kessel, 1961), and they arise from the first thoracic to the eighth abdominal segment. In P. pryeri, pericardial cells appear associating with cardioblasts as in Locusta. They, however, do not appear in the thoracic segments.

The blood cells of P. pryeri, Pd. paradoxa and B. laevipes originate from the scattering primary mesodermal

cells as in Peiris (Eastham, 1930), Chrysopa (Bock, 1939), Pimpla turionellae (Bronskill, 1959), Chilo (Okada, 1960) and Stenopsyche (Miyakawa, 1974c), however in Epiophlebia (Ando, 1962) and Gerris (Mori, 1969), the blood cells are formed from the secondary median mesodermal cells which migrate from the lateral mesoderm.

iii) Suboesophageal bodies

Panorpa pryeri

Middle in Stage 5, mesodermal cells belonging to the intercalary segment are located beneath the developing midgut rudiment which elongates backward from the blind end of the stomodaeum. As development advances, the cells become to be apocytes (Fig. 164) and less staied with hematoxylin, and they are of the rudimental suboesophageal bodies. Then they migrate backward accompaning with the invagination of the rudimental anterior tentorium. At first they locate on the ventral side of the stomodaeum, then they surround it.

In the first instar larva, the suboesophageal bodies surrounding the stomodaeum are observed at the posterior region of the cranium. During the embryogenesis, the mitoses of the suboesophageal bodies are never found.

Panorpodes paradoxa and Bittacus laevipes

In Pd. paradoxa, the suboesophageal bodies develop

from the mesodermal cells the intercalary segment at the beginning of Stage 5, and in Stage 7 in B. laevipes, and they surround the lateroventral side of the stomodaeum at the posterior end of the cranium in the first instar larvae.

Discussion on this item

The suboesophageal bodies are found in the orthopteran, plecopteran, isopteran, mallophagen, coleopteran and lepidopteran insects (Johannsen and Butt, 1941). Also, they are known in the Trichoptera (Patten, 1884; Miyakawa, 1974c) and Diptera (Okada, 1960).

Patten (1884) suggested that the origin of the suboesophageal bodies is endodermal. Other many embryologists, however, reported that the bodies are mesodermal in origin. These bodies are derived from the mesodermal cells of the mandibular segment in Locusta (Roonwal, 1937), Melanoplus (Kessel, 1961) and lepidopteran Bombyx mori (Wada, 1955). They are formed from the mesodermal cells of the intercalary segment in Pieris (Eastham, 1930), Calandra (Tiegs and Murray, 1938), Chilo (Okada, 1960), and Stenopsyche (Miyakawa, 1974c).

Rempel and Church (1969) reported that the suboesophageal bodies are derived from the ectodermal proliferation of the intersegmental region between the intercalary and mandibular segments in Lytta, namely, ectodermal ori-

gin, and they emphasize the necessity for the re-examination of the origin of suboesophageal bodies.

These bodies, however, originate from the mesodermal cells which belong to the intercalary segment in P. pryeri, Pd. paradoxa and B. laevipes.

In Bombyx (Toyama, 1902; Wada, 1955), the suboesophageal bodies proliferate the blood cells. The suboesophageal bodies of P. pryeri, Pd. paradoxa and B. laevipes seem not to participate in the formation of the blood cells, because the author could not find the mitotical figures of those bodies during the embryogenesis as mentioned before.

iv) Gonads

Panorpa pryeri

In Stage 3, there are observed several large cells in the mesodermal cell mass of the caudal end of the embryo (Fig. 186). They seem to be rudimental germ cells.

Middle in Stage 4, fifteen to twenty germ cells are discernible on the mesodermal cell mass of the tenth abdominal segment (Fig. 187). In Stage 5, they begin to be round and less stained with hematoxylin, and migrate forward with the development of the proctodaeum (Fig. 188). Middle in Stage 5, they become to distribute from the sixth to the tenth abdominal segment. Middle in Stage 6, the germ cells located at the caudal end are

scattered, and the center of their distribution becomes to be in the seventh abdominal segment (Fig. 189). At this stage, one or two germ cells are observed on the ridges of the somatic mesoderm, namely, rudimental genital ridges in each of abdominal transverse sections (Fig. 190). In Stage 7, the distribution of the germ cells is limited to the sixth and seventh abdominal segments. They become a pair of cell masses surrounding by vacuolated mesodermal cells. These vacuolated cells become a cell strand which elongates backward from the germ cell mass. Middle in Stage 8, each of the germ cell masses becomes round, and takes their position in the sixth abdominal segment (Fig. 191). They are almost the same shape to the gonads of the first instar larva.

In the first instar larva, each gonad contains ca. 120 germ cells and is stained deeply with hematoxylin and eosin. The gonads and the ducts which run from the gonads to the eighth abdominal segment are associated with fat bodies.

Panorpodes paradoxa and Bittacus laevipoes

In Pd. paradoxa and B. laevipes, the manner of the gonad formation is similar to that of P. pryeri.

The rudimental germ cells become recognizable as a cluster which contains about a dozen cells slightly larger than the surrounding mesodermal cells on the tenth abdomi-

nal segment middle in Stage 4 in Pd. paradoxa, and in Stage 5 in B. laevipes (Fig. 192).

In the first instar larva, the gonads take their position near the posterior margin of the sixth abdominal segment in Pd. paradoxa, and of the fifth abdominal segment in B. laevipes, and have short ducts at their posterior end. Each gonad is composed of seven to eight germ cells in Pd. paradoxa, and their cytoplasm is stained faintly with eosin.

In Bo. westwoodi, about fifteen rudimental germ cells are found on the mesodermal cell mass of the tenth abdominal segment at the end of Stage 4.

Discussion on this item

Generally the germ cells make their appearance after the gastrulation of the embryo in many insects, and the position of the appearance is the anterior part of the abdomen in Bombyx (Miya, 1958), center of the abdomen in Ctenocephalides (Kessel, 1939) and posterior part of the abdomen in Epiophlebia (Ando, 1962), Lytta (Chruch and Rempel, 1971) and Stenopsyche (Miyakawa, 1974c). The latter case is true for P. pryeri, Pd. paradoxa, B. laevipes and Bo. westwoodi.

As development advances, the germ cells spread their distriubiton, namely, from the sixth to the eighth abdominal segment in Bombyx (Miya, 1958), from the fifth to the

sixth in Epiophlebia (Ando, 1962), and from the second to the seventh in Stenopsyche (Miyakawa, 1974c), though the germ cells do not migrate from the orignial position in Ctenocephalides (Kessel, 1939).

The germ cell strands on lateral sides of the embryonic abdomen metamerize temporarily, and take their position on each genital ridge, then they gather into a pair of cell masses, i.e., rudimental gonads (Miya, 1958; Ando, 1962; Church and Rempel, 1971; Miyakawa, 1974c). The author, however, failed to find the temporary segmentation of the germ cell strand in P. pryeri, Pd. paradoxa and B. laevipes.

v) Differentiation of muscles and fat bodies

Panorpa pryeri

In Stage 6, coelomic sacs of the each segment begin to break down and differentiate into the somatic and splanchnic mesoderm. In Stage 7, among the somatic mesoderm, there are the cells which have somewhat fibrous shape, and their cytoplasm is stained lightly with eosin (Fig. 147). They are developing mioblasts. At the same time, there are also found the cells which commence to migrate from the somatic mesoderm into the developing epineural sinus (Fig. 147). They are the rudimental fat bodies. As development advances, the rudimental fat bodies are vacuolated and stained slightly with eosin.

In the first instar larva, fat bodies mainly associate with the gonads, heart and midgut, and are observed in the thoracic and abdominal legs.

Panorpodes paradoxa and Bittacus laevipes

In Pd. paradoxa, the differentiation of the rudiments of the muscles and fat bodies from the somatic mesoderm occurs at the end of Stage 5, and middle in Stage 7 in B. laevipes.

In P. pryeri, Pd. paradoxa and B. laevipes, the differentiation and formation of the muscles and fat bodies are similar to those of many other insects (Nelson, 1915; Roonwal, 1937; Bock, 1939; Ando, 1962; Mori, 1969; etc.). Therefore, there are no special discussions for this item.

vi) Musculatures of thoracic and abdominal segments of first instar larvae

Panorpa pryeri

In the first instar larva, the main thoracic musculature is essentially the same in the three thoracic segments, and the main abdominal musculature is also the same in each of the abdominal segments except for that in the caudal one. Accordingly, Fig. 193 shows the main musculatures of the metathorax and first abdominal segment for the convenience of the comparison. The muscles of the anal legs is shown in Fig. 194.

Discussion on this item

It is noteworthy that in the first eight abdominal segmetns, there are the lateral muscles connecting to the inside of small processes as before mentioned (see p. 23), and they seem to be homologous with the thoracic lateral muscles connecting with the bases of thoracic legs (Fig. 193, arrow). No muscles concerning with the anal legs are likely to be homologous with those of the thoracic and abdominal segments.

3. Alimentary canal formation

i) Stomodaeum or foregut

Panorpa pryeri

At the end of Stage 4, a sharrow invagination of the stomodaeum appears in the center of the protocephalic lobes (Fig. 46). As development proceeds, the rudimental stomodaeum elongates backward, and its bottom appears flat middle in Stage 6 (Fig. 165). Middle in Stage 7, the developing stomodaeum further elongates and begins to narrow, and the bottom slightly evaginates into the lumen of the rudimental midgut (Fig. 133). Late in Stage 9, the closing membrane which is the border between the stomodaeum and midgut breaks and degenerates (Fig. 195). An infolding of the distal end of the stomodaeum forms the cardiac valve.

In the first instar larva, a long oesophagus follows the pharynx, and the proventriculus does not differentiate.

Panorpodes paradoxa, Bittacus laevipes, and Boreus westwoodi

In Pd. paradoxa and Bo. westwoodi, a sharrow invagination of the rudimental stomodaeum arises in the center of the head lobes late in Stage 4 (Figs. 70, 108), and middle in Stage 4 in B. laevipes (Fig. 86).

The further development of the stomodaeum of Pd. paradoxa and B. laevipes is essentially the same as that of P. pryeri. The proventriculus does not differentiate in these species, too.

ii) Proctodaeum or hindgut, and malpighian tubules

Panorpa pryeri

Middle in Stage 4, an apparently thickened amnion continues for a length of about 100μm from the posterior end of the embryo. The thickened amnion includes the future dorsal wall and the blind end of the proctodaeum (Fig. 187).

In Stage 5, the caudal end of the embryo begins to sink into the yolk, and the mesodermal cells first cover the lateral sides of the rudimental proctodaeum, and then the dorsal (Fig. 188). These mesodermal cells later differentiate into muscles surrounding the proctodaeum.

Middle in Stage 5, the developing proctodaeum is approximately at right angle to the posterior part of the embryo. Late in Stage 5, the blind end of the developing proctodaeum becomes thin (Fig. 196), and a sheet of the midgut epithelial rudiment is found on it. At the same time, three paired rudiments of the malpighian tubules evaginate from the anterior end of the proctodaeal wall (Fig. 196), and are situated at the comparable 1, 3, 5, 7, 9 and 11 o'clock positions.

Middle in Stage 6, the developing proctodaeum elongates forward and loops at its middle part. The looped part extends from the anterior end of the seventh abdominal segment, where the blind end of the proctodaeum is situated, to the posterior end of the eighth abdominal segment. Simultaneously, the malpighian tubules extend up to the second abdominal segment and turn back to the eighth one. As development proceeds, the blind end of the proctodaeum and the sheet of the midgut rudiment fuse with each other, and form a thick closing membrane middle in Stage 8. Late in Stage 9, the pyloric valve appears just behind the proximal part of the malpighian tubules, and the duodenal valve appears at the posterior end of the pylorus. The closing membrane breaks down just before hatching. The alimentary canal of the first instar larva is shown diagrammatically in Fig. 197.

Panorpodes paradoxa and Bittacus laevipes

The formation of the proctodaeum and malpighian tubules of Pd. paradoxa and B. laevipes undergoes basically in the same manner of that observed in P. pryeri.

The sinking of the developing proctodaeum into the yolk begins middle in Stage 4 in Pd. paradoxa, B. leavipes and Bo. westwoodi. The three pairs of the rudimental malpighian tubules occur from the blind end of the developing proctodaeum late in Stage 4 in Pd. paradoxa, and in Stage 6 in B. laevipes. The developing proctodaeum has a looped part middle in Stage 5 in Pd. paradoxa, and late in Stage 7 in B. laevipes.

iii) Midgut

Panorpa pryeri

Anterior midgut rudiment

At the end of Stage 4, a few proliferating cells in the posterior wall of the invaginating stomodaeum are distinctly observed. The anterior midgut rudimant arises from these cells (Fig. 198).

In Stage 5, from the whole region of the posterior wall of the developing stomodaeum, the anterior midgut rudiment elongates backward between the yolk and mesodermal cells (Fig. 199). The rudiment further develops by mitosis and it begins to fork at its distal end middle in Stage 5, but it is still a cell mass elongating from the

posterior stomodaeal wall.

As development advances, the rudiment separates bilaterally at its proximal region where it attaches with the stomodaeal wall, and assumes the form of a pair of ribbons. The distal ends of the rudiments reach up to the first thoracic segment.

Posterior midgut rudiment

In Stage 5, the arrangement of monolayered cells at the blind end of the future proctodaeum begins to be irregular, and a few cells of the posterior midgut rudiment appear there (Fig. 188). As development proceeds, these cells increase in number. As a result, a multilayered cell mass of the rudiment is formed on the blind end of the rudimental proctodaeum.

Middle in Stage 5, as the developing proctodaeum invaginates deeply, its blind end flattens. Then the cell mass of the posterior midgut rudiment (Fig. 196) elongates anteriorly as a pair of ribbons owing to mitosis as in the anterior midgut rudiment, and extends up to the eighth abdominal segment.

Further development of midgut rudiments

Middle in Stage 5, the paired ribbons of the anterior midgut rudiments reach up to the first thoracic segment, and of the posterior midgut rudiments extend up to the

eight abdominal segment. The ribbons of both rudiments elongate along the dorsal part of the coelomic sacs.

In Stage 6, the ribbons of the anterior and posterior midgut rudiments meet and fuse in the third or fourth abdominal segment, and as a result the rudiments continue between the bottoms of the stomodaeum and proctodaeum. Then the ribbons widen, covering the ventral side of the yolk, and the splanchnic mesoderm follows and lines them (Fig. 190).

In Stage 7, the ribbons become wider, and the ventral exposure of the yolk merely remains above the ventral nerve cord (Fig. 147). The splanchnic mesoderm commences to thin and becomes bilayered, and the epineural sinus is considerably enlarged above the ventral nerve cord, as a result of the remarkable consumption of the yolk.

Middle in Stage 8, the midgut rudiments completely cover the ventral side of the yolk (Fig. 200). As a result of the growth of the dorsolateral wall of the embryo, the midgut rudiments spread dorsally. Then they fuse on the dorsal side of the yolk, and the developing midgut assumes a complete tubular form.

Middle in Stage 9, the midgut epithelial cells are thicker on the dorsal side than on the ventral, and have many cytoplasmic processes that later differentiate into microvilli, in the distal parts of the cell (Fig. 182). Many regenerative cells are found in the thicker dorsal

epithelial cells more than in the ventral ones.

In the first instar larva, the epithelial cells have many vacuoles, and morphologically differentiate in each of the four regions of the midgut, i.e., Region I-IV (Fig. 197). In Region I (Fig. 201), the epithelial cells are somewhat irregular in height (20μm maximum), and Region II or middle part of the midgut (Fig. 202), they are of uniform height (ca. 20μm). In Region III of the midgut, they show a characteristic shape (Fig. 203). These cells (20 to 50μm in height) have no microvilli at their round distal ends. They seem to correspond to the cells of 'Type II' in the larval midgut of P. communis (Grell, 1938). In Region IV, there are taller cells (20 to 30μm in height).

Panorpodes paradoxa, Bittacus laevipes and Boreus westwoodi

The midgut formation of Pd. paradoxa and B. laevipes is the bipolar formation and proceeds principally in the same manner as that of P. pryeri as just mentioned.

The anterior midgut rudiment is derived from the bottom of the invaginating stomodaeum middle in Stage 4 in Pd. paradoxa and B. laevipes, and in Stage 4 in Bo. westwoodi (Figs. 204, 205).

The posterior midgut rudiment occurs from the blind end of the developing proctodaeum middle in Stage 4 in Pd. paradoxa, and in Stage 5 in B. laevipes, but in Bo.

westwoodi it does not yet appear in the stage.

In the first instar larva of B. laevipes, the midgut epithelial cells situated at the anterior part of the posterior half midgut have no microvilli. They seem to be comparable to these cells of Region III in P. pryeri, though their distal ends are not round.

In Pd. paradoxa, there are no epithelial cells which seem to be comparable to the cells of Region III of P. pryeri.

Discussion on this item will be given in "GENERAL DISCUSSION AND CONCLUSION".

4. The other structures and phenomena

i) Fate of embryonic envelopes

Panorpa pryeri

In Stage 4, the edge of the amnion covered the ventral surface of the embryo begins to spread laterally on the yolk mass from the cephalic to the thoracic region (Fig. 206). In Stage 5, the lateral spread of the original amnion occurs to the seventh abdominal segment (Fig. 207). As development proceeds, the amniotic spread almost covers the whole egg surface without the region near the caudal end of the embryo (Fig. 208). Middle in Stage 5, the embryo and yolk mass are covered completely with the spread amnion. Consequently at this time, the yolk mass is covered with the inner or dorsal amnion, and the outer

one situated just beneath the serosa. As the result of the final fusion of the double amnions, a few round cells of the inner amnion separate from the caudal end of the embryo into the space between the outer and inner amnions (Fig. 209). In Stage 7, the inner amniotic cells on the dorsal side of the egg become vacuolated and thick, and further thicken in Stage 8 (Fig. 210). This thickening part of the inner amnion becomes undistinguishable at the stage of the embryonic rotation. In Stage 9, the inner amnion disappears by the completion of dorsal closure of the embryo, but the outer amnion persists at the hatching.

Panorpodes paradoxa, Bittacus laevipes and Boreus westwoodi

In Pd. paradoxa and B. laevipes, the formation and fate of the inner and outer amnions are the same as those of P. pryeri.

The yolk mass is completely covered with the inner amnion middle in Stage 4 in Pd. paradoxa, late in Stage 4 in B. laevipes, and in Stage 5 in Bo. westwoodi. In Bo. westwoodi, there observes a thickening of the serosa at the anterodorsal part of the egg late in Stage 4 (Fig. 211).

Discussion on this item

As far as the author is aware, there are few papers in which described on the differentiation of the inner

and outer amnions. In some coleopteran insects, e.g., Brachyrhinus (Butt, 1936), Apion apricans and Polydrosus sericeus (Krzysztofowicz, 1960) both amnions are found. Therefore, the existence of the inner and outer amnions seems to be a character for the mecopteran P. pryeri, Pd. paradoxa, B. laevipes and Bo. westwoodi.

The similar phenomenon that the amnion covered a whole embryo persists till just before hatching is observed generally in the lepidopteran insects (Eastham, 1930; Presser and Rutschky, 1957; Okada, 1960; Anderson and Wood, 1968; Kobayashi, Tanaka, Ando and Miyakawa, 1981; etc.). In these lepidopteran insects, the amnion which is comparable to the outer amnion of the mecopteran insects mentioned above. In the Lepidoptera the continuous amnion is formed as the result of completion of the dorsal closure, and there remains the yolk in the space between the amnion and serosa. However this phenomenon is never seen in P. pryeri, Pd. paradoxa, B. laevipes and Bo. westwoodi. Although there are some differences of the amnion formation in the lepidopteran and mecopteran insects, it seems to be a significant character for the consideration on the relationship of these orders.

The partial thickening of the serosa in Bo. westwoodi resembles morphologically to the hydropyle cells or columnar serosa of the some heteropteran insects (Cobben, 1968; Mori, 1969, 1970; Madhavan, 1973).

ii) Formation of abdominal legs

Panorpa pryeri

In Stage 7, small paired processes, which consist of ectodermal cell masses (Fig. 212), first become evident above each ganglion of the first eight abdominal segments, and they are anlagen of abdominal legs. Middle in Stage 8, the paired cell masses commence to protrude cytoplasmic processes on the ventral surface of the embryo (Fig. 213).

In Stage 9, the paired cytoplasmic processes increase in size, and several nuclei migrate from the proximal part to the middle one in the develoiping abdominal legs (Fig. 214). As these nuclei move to the peripheral zone of the abdominal legs, a cavity appears within the leg. Fig. 215 shows the abdominal leg of the first instar larva.

Panorpodes paradoxa and Bittacus laevipes

In B. laevipes, paired small cell masses, namely, rudimental abdominal legs become recognizable on the first eight abdominal ganglia middle in Stage 7. The further development of the abdominal legs are essentially the same as those of P. pryeri.

In Pd. paradoxa, there are observed no abdominal legs during the embryonic development. However a small process is found at the center of the medioventral line of each of the first eight abdominal segments in the

first instar larva. This small process is formed as follows.

Late in Stage 6, a small cell mass in the ectoderm arises at the positions as just mentioned. Middle in Stage 7, these cell massses without those of the first and second abdominal segments begin to protrude cytoplasmic processes on the ventral surface of the embryo (Fig. 216).

As development proceeds, they elongate, the nuclei still stay at the proximal part of the processes. Fig. 217 shows the process of the first instar larva, and the process has several nuclei at the base, and their cytoplasm is stained lightly with eosin. On the other hand, the processes of the first and second abdominal segments become small pouches.

Discussion on this item

In the Holometabola, larval abdominal legs, prolegs or pseudopods are known in the Lepidoptera, Tenthredidae of the Hymenoptara and Blepharoceridae of the Diptera (Snodgrass, 1935; Matsuda, 1976).

The thoracic leg formation of the mecopteran insects starts as a slight thickening of the ectoderm (Fig. 218), and the thickening are transformed into the evagination which is filled with subsomitic mesodermal cells (Fig. 219). As development advances, lining mesodermal cells

differentiate into muscles and fat bodies (Fig. 220). The abdominal leg formation proceeds in the same manner of the thoracic leg formation mentioned above in the lepidopteran Diacrisia (Johannsen, 1929), hymeopteran Athalia (Farooqi, 1963) and dipteran Neocurupira chiltoni (Craig, 1967).

On the other hand, the abdominal leg formation of P. pryeri and B. laevipes is conspicuously different from the thoracic leg formation, and the formation is rather similar to the development of trichogen cells. These points seem to suggest that the abdominal legs of P. pryeri and B. laevipes are clearly different from the thoracic legs. Ando and Haga (1974) observed that no pleuropodia occur in the embryos of P. pryeri and B. mastrillii, and a pair of styliform appendages or abdominal legs is formed in the each of the first to the eighth abdominal segments along the medioventral line of grown embryos. They, however, did not refer to the homology of the thoracic and abdominal appendages.

In Pd. paradoxa, small processes on the medioventral line of the larval abdomen are similar to the abdominal legs, to some extent, in the manner of its formation.

iii) Formation of anal legs and telson

Panorpa pryeri

Late in Stage 5, the wall of the developing proctodaeum is very thick (Fig. 196), and the thickness persists till Stage 7. In Stage 7, the boundary between the posterior end of the tenth abdominal segment and the proctodaeum becomes distinct (Fig. 221). Middle in Stage 7, the wall of the proctodaeum commences to be thin except for the posterior end of the abdomen or telson (Fig. 222). At the same time, as the ganglion of the tenth abdominal segment migrates forwards, the posterior margin of the segment becomes a fold and surrounds the telson (Fig. 222). Late in Stage 7, the ectoderm of the telson begins to be thin, and several mesodermal cells which line the telson differentiate into muscles connecting with the distal end of the telson (Fig. 223). Four positions with which these muscles connect are the lateral and dorsolateral sides of the proctodaeal opening, and these points become ectodermal protrusions when development proceeds. They are the developing anal legs. After rotation of the embryo, these protrusions invaginate into the body cavity. Discussions for this item will be attempted later (see Chapter III, 'Interpretation on the metamerism in terminal region of the abdomen' in "GENERAL DISCUSSION AND CONCLUSION").

iv) Serosal cuticle

Panorpa pryeri

In Stage 5, there is a very thin envelope stained scarcely with hematoxylin between the serosa and chorion (Fig. 224). It is the serosal cuticle secreted by the serosa. Middle in this stage, it thickens slightly and has two or three layers stained faintly with hematoxylin (Fig. 225). In Stage 6, the cuticle composed of multi-layers becomes ca. 10μm-thick. The serosal nuclei are to be poorly stained with hematoxylin. In Stage 7, the cuticle is ca. 15μm-thick, and becomes 5 to 10μm-thick in Stage 9. The serosal nuclei indicate degenerating figures, though the amniotic nuclei are relatively apparent in Stage 9. The cytoplasm of the serosal cells becomes granular and stained faintly with eosin. The serosal cuticle persists just before hatching.

Panorpodes paradoxa, Bittacus laevipes and Boreus westwoodi

The serosal cuticle begins to be secreted late in Stage 2 in Pd. paradoxa, middle in Stage 3 in B. laevipes, and in Stage 4 in Bo. westwoodi. In Pd. paradoxa, the serosal cuticle reaches to the maximum thickness in Stage 6 (15μm), and in B. laevipes in Stage 5 (ca. 7μm).

Discussion on this item

The serosal cuticle is observed in many insects,

e.g., thysanuran Pedetontus unimaculatus (Machida, 1981a), Odonata (Ando, 1962), orthopteran Melanoplus (Slifer, 1937), plecopteran Pteronarcys proteus (Miller, 1940), hemipteran Pyrilla (Sander, 1956), coleopteran Lytta (Church and Rempel, 1971), etc.

As a role, it is considered that the serosal cuticle protects the egg together with the chorion. In some Odonata (Ando, 1962) and Pedetontus (Machida, 1981a, b), the serosal cuticle becomes a virtual protective membrane, because the chorion of these insects ruptures in the later embryonic development. The choria in P. pryeri and Pd. paradoxa do not rupture, but they are so thin and frail, so that the serosal cuticle in these species seems to have an important role for the protection of the egg contents.

In B. laevipes, however, the chorion is very thick (25μm in thickness) and its serosal cuticle is only a half thickness of those of P. pryeri and Pd. paradoxa.

v) Embryonic diapause

Bittacus laevipes

Early in Stage 6, the embryo commences to diapause for ca. 180 days. During the diapause, in the embryo no development of organs or little mitotical figures, and also no discernible consumption of the yolk are observed. In Stage 7, the embryo terminates the diapause, and the

mitotical figures are found in various regions of the embryo, especially in the ectoderm of the developing proctodaeum which begins to elongate remarkably from this stage (Fig. 226).

Discussion on this item

In Bombyx, the embryo enters the diapause in the stage when the inner layer formation just starts, and Okada (1971) noted the role of the chorion as to the control mechanism of the diapause. In the orthopteran Aulocara elliotti (Visscher, 1976), the embryo enters the diapause when the development of the central nervous system considerably proceeds, and she suggested that the diapause seems to be controled by the brain-corpora cardiaca complex in this species.

In B. laevipes, the diapausing embryo has a relatively developed brain, so that it seems to be possible that the developing brain controls the diapause of this species.

GENERAL DISCUSSION AND CONCLUSION

The results obtained in the present study have been discussed in each of the former items. Here, the subjects considered significant in the comparative embryology or morphology of insects will be further examined.

In this section, a term, Mecoptera will be used to represent P. pryeri, Pd. paradoxa, B. laevipes and Bo. westwoodi, and these species will be described by the names of the families to which they belong for the convenience of the description when no confusion will be supposed.

I. Alimentary canal formation

1. Stomodaeum and proctodaeum

The stomodaeum of the Mecoptera arises from a shallow invagination in the center of the protocephalic lobes of the embryo, and the manner of its formation is the same as in many insects (Johannsen and Butt, 1941; Anderson, 1972; Haget, 1977). On the other hand, in the Mecoptera the thickened amniotic part of the embryonic caudal end participates in the proctodaeum formation. This formation resembles to those in the Odonata (Ando, 1962), hemipteran Oncopeltus (Butt, 1949), Pyrilla (Sander, 1956), siphonapteran Ctenocephalides (Kessel, 1939), trichopteran Stenopsyche (Miyakawa, 1975) and lepidopteran Endoclita signifer (Kobayashi, Tanaka, Ando and Miyakawa, 1981). However the proctodaeum formation in the Meco-

ptera, which the future blind end of the proctodaeum originates from the thickened amniotic part, differs from those in the above species.

In the Mecoptera, it is also interesting that the pyloric valve is situated just behind the openings of the malpighian tubules, because the valve is generally found between the posterior end of the midgut and openings of the malpighian tubules (Snodgrass, 1935). As Grell (1938) suggests in the larva of P. communis, the existence of the duodenal valve, which is situated at the posterior end of the pylorus, seems to be also the characteristic of panorpid larvae, and the same is true for the Panorpodidae and Bittacidae, though the similar structure is seen in the cockroach, Blatta orientalis (Henson, 1944).

2. Midgut

In the apterygote insects (Collembola, Tetrodontophora bielanensis, Jura, 1966; Microcoryphia, Pedetontus, Machida and Ando, 1981), the midgut epithelium is wholly derived from the yolk cells or vitellophages, though in the Thysanura s.str., Lepisma saccharina (Sharov, 1953), both ends of the midgut epithelium are ectodermal in origin, i.e., the anterior end of the midgut originates in the cells derived from the posterior end of the stomodaeum, and the midgut posterior end is formed with the cells derived from the proctodaeal anteiror end.

In the Odonata (Ando, 1962), the epithelium of the midgut is formed by the yolk cells except those of both ends of the midgut, therefore the both ends are ectodermal in origin as in Lepisma (Sharov, 1953).

In some hemimetabolans, the midgut epithelium is formed by the cells or the outgrowths of the stomo- and proctodaeum, namely, bipolar formation (Hemiptera, Oncopeltus, Butt, 1949; Pyrilla, Sander, 1956), and the yolk cells participate together with the ectodermal bipolar formation of the midgut epithelium in the psocopteran Liposcelis (Goss, 1953) and embiopteran Haploembia solieri (Stefani, 1961). In the hemipteran Gerris (Mori, 1976), however, the midgut epithelium is formed only by the yolk cells.

In the holometabolan insects, as reviewed by Haget (1977), the midgut epithelial formation is basically bipolar (Neuroptera, Chrysopa, Bock, 1939; Coleoptera, Phyllophaga fervida, Luginbill, 1953; Hymenoptera, Mesoleius tenthredinis, Bronskill, 1964; Trichoptera, Stenopsyche, Miyakawa, 1975; Lepidoptera, Bombyx, Miya, 1976). In the Mecoptera, the formation is bipolar and commences as soon as the invagination of the stomo- and proctodaeum. It occurs in early developmental stage than in the above mentioned holometabolan species. However it is known that the formation begins in more early stage in the siphonapteran Ctenocephalides (Kessel, 1939) and dipteran

Dacus (Anderson, 1962). Although there are some differences in the time of appearance of the midgut rudiments in these species, they are ectodermal in origin, and the bipolar formation of the midgut seems to be general in the holometabolan embryogenesis.

There are some insects that show the bipolar formation of the midgut, but the inner layer (mesodermal) cells take part in the formation of the midgut rudiments. For example, the megalopteran Sialis lutaria (Strindberg, 1915), coleopteran Donacia crassipes (Hirschler, 1909), and lepidopteran Catocala nupta (Hirschler, 1928), and moreover the midgut is formed only by the median mesodermal cells in the coleopteran Phyllobius glaucus (Jura, 1956). It is of particular interest that the mesodermal cells participate in the midgut formation of megalopteran Sialis, which are thought to be one of the most primitive groups in the Holometabola together with the Mecoptera. The data on Sialis, however, need to be re-examined.

II. Homology in larval abdominal legs and thoracic legs

According to Berlese's theory, the first instar larvae of hemimetabolan insects have only thoracic legs (oligopod), and when the holometabolan larvae hatch they have legs on the thoracic and abdominal segments (polypod). Hinton (1958) considered that the larval abdominal legs of the panorpoid insects (Mecoptera, Trichoptera,

Lepidoptera, Siphonaptera and Diptera) are secondary adaptive structures and not homologous with the thoracic legs. Recently, Matsuda (1976), gave an attention to the position of abdominal legs in insect embryos, and suggested that the larval abdominal legs are serially homologous with the thoracic legs.

Then the author attempts to homology in the larval abdominal legs and the thoracic ones in the Mecoptera comparing with other holometabolan insects which have larval abdominal legs. The author will recognize the abdominal legs homologous with the thoracic legs when the following two criteria are satisfied. The first is that in each segment paired abdominal legs must be arranged in a row with the thoracic legs. The second is that the abdominal legs must develop histologically in the same manner as that of the thoracic legs, at least in their early and middle development.

In the holometabolan insects, the abdominal legs or apppendages are found in larval stages of the Megaloptera, Lepidoptera, Tenthredidae of Hymenoptera and Blepharoceridae of Diptera.

In the larvae of lepidopteran Diacrisia (Johannsen, 1929), hymenopteran Athalia (Farooqi, 1963) and dipteran Neocurupira (Craig, 1967), the abdominal legs are arranged in a row with the thoracic legs, and the formation of abdominal legs are similar to that of the thoracic legs.

The larval abdominal legs of these insects satisfy the above two criteria so that the author recognize which they are to be homologous with the thoracic legs.

In the coleopteran Lytta (Chruch and Rempel, 1971) and neuropteran Chrysopa (Bock, 1939), the abdominal appendages occur only in the first abdominal segment, and disappear during the embryonic stage. These appendages are the pleuropodia.

In the megalopteran Protohermes grandis, Miyakawa (1979) mentioned on the abdominal appendages of the embryo as follows, "The abdominal segments have two pairs of swellings. The median ones immediately lateral to the ventral nerve cord are small and homotopous with the pleuropodia. These median swellings later disappear. The lateral swellings are conspicuous structures located between the median swellings and tracheal pits, and they later give rise to the abdominal filaments or tracheal gills". In this species, median swellings seem to be homologous with the thoracic legs judging from his description that the median ones are homotopous with the pleuropodia, because the pleurpodia are generally thought to be homologous with the thoracic legs (Wheeler, 1890; Hussey, 1926; Machida, 1981a). Consequently the larval abdominal appendages or filaments of Protohermes are not considered to be homologous with the thoracic legs.

In the mecopteran P. pryeri and B. laevipes, on the

ventral surface of the embryonic abdomen there appear two pairs of the processes, i.e., median and lateral processes, on the first eight abdominal segments (Figs. 54 and 94). The lateral processes are located at the positions comparing to those of thoracic legs, and persists in the first instar larva. The median processes are located on each of the abdominal ganglia and become abdominal legs. The abdominal leg formation is considerably different from that of the thoracic legs (see Chapter VII, 4, ii, 'Formation of abdominal legs' in "OBSERVATIONS").

Furthermore in the first instar larva of P. pryeri, there are the abdominal lateral muscles, connecting with the lateral processes mentioned above, and they seem to be homologous with the lateral muscles associated with the thoracic legs (Fig. 193, arrow). From these observations, the author concludes that the median processes or so-called larval abdominal legs of P. pryeri and B. laevipes are not homologous with the thoracic legs.

In conclusion, in many cases the larval abdominal legs of holometabolan insects are thought to be homologous with the thoracic legs as mentioned by Matsuda (1976). In some cases, e.g., in Protohermes (Miyakawa, 1979), P. pryeri and B. laevipes, however, the larval abdominal legs or filaments seem to be not homologous with the thoracic legs as suggested by Hinton (1958).

III. Interpretation on the metamerism in terminal region of the abdomen

Concerning the metamerism in terminal region of the insect abdomen, Heymons, in his embryological works on hemimetabolan insects (1895, 1896), regarded the telson or twelfth abdominal segment which consists of the subanal and supraanal lobes, despite the lack of segmental ganglia, coelomic sacs and appendages. On the other hand, Snodgrass (1935) suggested that "In most insects no trace of a twelfth segment is to be found, and the periproct (=telson) must be supposed to be represented, if at all, by a circumanal membrane at the end of the eleventh segment". Matsuda (1976), however, from the elaborate examinations on the studies concerned with the segmentation of the insect abdomen, concluded that, supporting Heymons' view, the abdomen consists of the eleven segments and telson (=the twelfth abdominal segment) in the lower insects (Thysanura-Pterygota). Recently, Machida (1981a, b), from his embryological study on the thysanuran Pedetontus, denied Snodgrass' view, and supported one proposed by Heymons (1895, 1896) and Matsuda (1976).

As mentioned above, it seems to be general that the telson is not derived from the eleventh abdominal segment in the Thysanura and Hemimetabola. In P. pryeri, the telson is located around the opening of the proctodaeum (see Chapter VII, 4, iii, 'Formation of anal legs and

telson' in "OBSERVATIONS"), but it is not derived from the posterior part of the tenth abdominal segment.

In P. pryeri, the problem is that the rudimental eleventh abdominal segment exists or not in the posterior part of the tenth abdominal segment. In this species, the eleventh abdominal ganglia and coelomic sacs never appear during the embryonic stage (see Chapter VII, 1, iii, a, 'Ventral nerve cord' and 2, i, 'Segmentation of inner layer, formation of coelomic sacs, and differentiation of splanchnic and somatic mesoderm' in "OBSERVATIONS"), while there is a possibility that the eleventh abdominal mesodermal cells are involved in the large mesodermal mass of the tenth abdominal segment. The author, however, can not deny the possibility that the rudimental eleventh abdominal segment exists in the posterior end of the tenth abdominal segment for the following reasons.

In the first instar larva of P. pryeri, the caetotaxy of the first nine abdominal segments is fundamentary same. That of the tenth abdominal segment is also similar to the other abdominal segments without the additional three pairs of spines which occur on the posterior margin of the tergum (Fig. 17, arrow) as in P. klugi (=japonica) (Miyake, 1912), P. nuptialis (Byers, 1963), P. folsa and ten species of Panorpa and Neopanorpa (Yie, 1951). This group of the spines is never found on the first nine abdominal segments, and seems to be regarded

as that of the eleventh abdominal segment. Furthermore in P. communis (Rottmar, 1966), the imaginal disk of the pupal eleventh abdominal segment is formed in the posterior part of the prepupal tenth abdominal segment.

Judging from these data, the tenth abdominal segment of P. pryeri is thought to contain the rudimental eleventh abdominal segment in its posterior part. Consequently the author considers that the abdomen of P. pryeri consists of ten segment and telson, and the rudimental eleventh abdominal segment is to be hidden in the tenth abdominal segment.

In Pd. paradoxa, Issiki (1959) reported that the abdomen of the first instar larva apparently consists of eleven segments, and on the eleventh abdominal tergum there are found three pairs of spines. The author, however, failed to find the distinguishable intersegmental suture at the posterior part of the tenth abdominal segment of its first instar larvae. Moreover in the embryo of this species he also could not find the ganglia and coelomic sacs of the eleventh abdominal segment (Fig. 178).

The abdomen of the first instar larva of Pd. paradoxa is composed of ten segments and telson, but the vestigial eleventh abdominal segment is possibly involved in the posterior part of the tenth abdominal segment as in P. pryeri, since there are three extra pairs of the spines on the posterior margin of the tenth abdominal tergum

(Fig. 227, arrow) pointed out by Issiki (1959).

Matsuda (1976) regarded the larval anal legs of Panorpa as caenogenetically modified cerci of the eleventh abdominal segment. The anal legs of P. pryeri are, however, directly derived from the telson (see Chapter VII, 4, iii, 'Formation of anal legs and telson' in "OBSERVATIONS"), and hence the author believes that these of P. pryeri are not cerci of the eleventh abdominal segment.

IV. Phylogenetic consideration on mecopteran families from embryological aspects

Up to the present day, some embryologists have attempted to examine the phylogenetic relationship of the insects by means of the comparative embryology. According to Johhansen and Butt (1941), in the hemimetabolan and holometabolan insects, the types in the formation of germ bands and the relation in their length to the egg form have no significance for the phylogenetic research. Sharov (1957, 1966) explained the phylogenetic relationship between the thysanuran and pterygote insects in point of the manner of the embryonic envelope formation. Krzysztofowicz (1966) studied the coleopteran embryogenesis included three families and 28 species, and suggested the significance of the embryonic envelope formation and the liquified yolk existing between the amnion and serosa for the comparison of these families.

Ando (1962) investigated the embryology of seven families of the Odonata, and divided them into two groups by the germ band types in relation to the yolk, i.e., the partially invagination type (Cordulegasteridae and Libellulidae) and invaginated type (the remaining families). He also showed the relationship of the seven families by means of the comparative embryological data agrees with the taxonomical ones of the Odonata. Cobben (1968, 1978) studied the eggs, architecture of the shell, gross embryology and eclosion of the Heteroptera in detail, and used the types of blastokinesis of embryos as a character for the phylogenetical studies on ten heteroptaran superfamilies.

Recently the relationship of the Trichoptera and lower Lepidoptera was examined as for the germ rudiment formation, and it was suggested the close affinity betweeen these orders (Ando and Tanaka, 1976; Ando and Kobayashi, 1978; Ando and Tanaka, 1980; Kobayashi and Ando, 1981; Akaike, Ishii and Ando, 1982; Kobayashi and Ando, 1982).

From the results quoted above, there are some cases in which the data from the comparative embryology gave imporpant criteria for the study of the insect phylogeny, when one investigates the embryology of the insects situated on the phylogenetical divergent point, and compares the results obtaining in the early and middle stages of

the embryonic development.

Therefore the author attempts to examine the relationship of the mecopteran families by means of the comparative embryology.

1. Ooplasm

In general there is a tendency that eggs of the lower pterygote as in the Hemimetabola are poor in the ooplasm (periplasm and reticuloplasm) compared with the amuont of the yolk, on the contrary, the ooplasm is rich in the higher pterygote eggs as in the Holometabola (Krause, 1939, 1961; Anderson, 1972; Ando, 1981).

In the Mecoptera, the eggs of the Bittacidae are poor in ooplasm compared with the amount of the yolk, and these of the Panorpodidae and Panorpidae are rich in ooplasm, and these of the Boreidae are nearly intermediate in the relative amount. Especially in the Bittacidae, little reticuloplasm is found in their eggs. One may think the egg character of the Bittacidae as an effect of the egg hibernation. Ando (1973), however, denied the supposition quoting the case of hibernatant and nonhibernatant eggs in the Odonata which exibit almost the same characteristics concerning the relative amount of the ooplasm and yolk. If the diapause effects on the nature of the eggs, the accumulation of the yolk for the food during the winter is considered. However, at least, the amount of the eosi-

nophilic yolk in the Bittacidae is not so different from that of the Boreidae (see Chapter I, 'Observation and organization of newly laid eggs' in "OBSERVATIONS"), and there is not distinguishable consumption of the yolk during the diapause (see Chapter VII, 4, v, 'Embryonic diapause' in "OBSERVATIONS"). Consequently the nature of eggs of the Bittacidae seems to be not caenogenetic, but palingenetic as suggested by Ando (1973), and this nature is likely to be more primitive than that of eggs of the Boreidae, Panorpodidae and Panorpidae.

2. Inner layer formation

As discussed in Chapter VI, in lower hemimetabolan insects, the inner layer formation is carried out only the cell proliferation along the median line of the embryo. On the other hand, there are few holometabolan insects in which the inner layer is formed only by the above-mentioned manner, i.e., proliferating type, and in almost all other holometabolans the inner layer is formed by the invagination of the middle plate along the median line, i.e., the invaginating type.

In the Mecoptera, the inner layer of the Bittacidae is formed by the proliferating type, and that of the Boreidae, Panorpodidae and Panorpidae is formed by the invaginating type, so that the Bittacidae is likely to be more primetive than the other three families in this aspect.

3. Type of germ band

Krause (1939) classified the germ band of the insects into three types. The first type is that the germ band includes only the future protocephalic and gnathal regions at first, and the future thoracic and abdominal regions develop from the posterior end of the germ band as it elongates. He termed it as the short germ type. On the contrary, the germ band, which includes all of the future protocephalic, gnathal, thoracic and abdominal regions from the beginning, is termed the long germ type. The germ band, which includes the future protocephalic, gnathal and thoracic regions at first, is termed the semilong germ type. He suggested that the short germ type is often found in hemimetabolans, e.g., Odonata, Orthoptera and Hemiptera, and the long germ type is found in higter holometabolans, e.g., Diptera and Hymenoptera. The semilong germ type is found in some coleopterans.

In the Mecoptera, the germ band of the Panorpidae is regarded as the semilong germ type and those of the other three families are regarded as the short germ one (Fig. 228), hence the germ band of the Panorpidae is thought to be more derived type than that of the other families.

4. Germ band or germ rudiment formation

In several species of the coleopteran Chrysomelidae, Zakhvatkin (1968) observed that the eggs of Leptinotarsa

decemlineata and Phyllodecta vitellinae are rich in yolk and poor in ooplasm, and germ bands are formed on the surface of the eggs, namely, the superficial type of the germ band. On the contrary, the eggs of Galerucella lineola and Chalcoides aurata are rich in ooplasm and not so rich in yolk, and their germ bands sink into the yolk at first, that is the invaginated type. Therefore he concluded that the relative amount of the yolk and ooplasm determines the type of the early embryogenesis.

In the Mecoptera, the germ band formation of the Bittacidae, Boreidae and Panorpidae is the superficial type, and the germ band or rudiment formation of the Panorpodidae is the immersed type which the invaginatd germ rudiment leaves from the egg periphery and sinks into the yolk completely. Concerning the considerable difference in the formation between the Panorpodidae and Panorpidae, though they have similar ooplasm-rich eggs, the author thinks that the affinity of these two families is not so close.

5. Genealogical tree of the Mecoptera based on embryological characters

Finally, the foregoing conclusions from the present study are summed up in the figure on the following page.

GENEALOGICAL TREE OF THE EUMECOPTERA

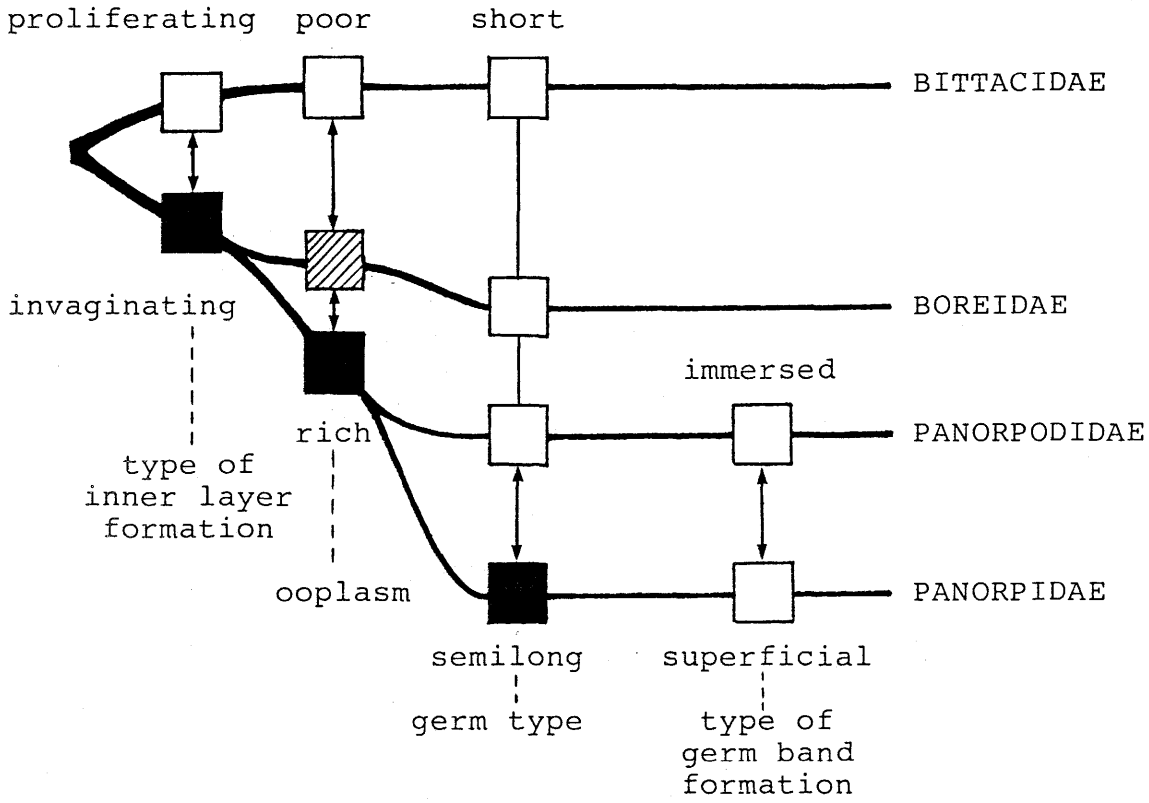

The genealogical tree of the four eumecopteran families based on the embryological characters, proposed by the author, does not agree with one concluded by Penny (1975). He considered that the Boreidae and Panorpodidae branched after their common ancestor branched from the ancestor of the Panorpidae, because only the Boreidae and Panorpodidae have scarabaeiform larvae in the eumecopteran families. The tree proposed by the author, however, agrees with the mecopteran genealogical tree suggested by Mickoleit (1978) based on the comparative morphology of exoskeleton of the female genitalia, and also agrees with that suggested by Willmann (1981) from that of the

exoskeleton of the male genitalia. While according to the embryological data, the author can not favor Hinton's proposal (1958) that, from the morphological difference of the larval cranium, maxilla and labium, the Boreidae is to be separated from the mecopteran families and to be established as a new order, Neomecoptera.

SUMMARY

1. The comparative embryolgy of nine species of the Mecoptera, representing four families belonging to the suborder Eumecoptera is studied.
2. Especially the entire embryonic development of Bittacus laevipes, Panorpodes paradoxa and Panorpa pryeri is described, and the early and middle development of Boreus westwoodi is also described.
3. The egg shape of B. laevipes is spherical, and that of Bo. westwoodi, Pd. paradoxa and P. pryeri is oval.
4. The eggs of B. laevipes and Bo. westwoodi have micropyles at both poles.
5. The newly laid eggs show the metaphasic figure of the first maturation division. The egg of P. pryeri has the polar granule at the posterior end of the egg periphery.
6. The egg of B. laevipes is poor in ooplasm, while the eggs of Pd. paradoxa and P. pryeri are rich, and the quantity of the oolpasm of Bo. westwoodi is intermediate to that of B. laevipes and P. pryeri.
7. The egg periods are ca. 270 days in B. laevipes, ca. 33 days (21°C) in Pd. paradoxa, and ca. 150 hr (21°C) in P. pryeri.
8. The very thin blastoderm is formed in B. laevipes and Bo. westwoodi. The thick blastoderm is formed and the inner periplasm is found in Pd. paradoxa and P. pryeri.

9. The external features of embryos of four species, and the first instar larvae of B. laevipes, Pd. paradoxa and P. pryeri are described in detail.

10. The embryonic period is devided into eight stages in Pd. paradoxa and P. pryeri, and nine in B. laevipes.

11. The very small germ disk is formed on the ventral sureface of the egg in B. laevipes.

12. The germ rudiment formation of Pd. paradoxa is of the so-called immersed type, and the germ band formation of B. laevipes, Bo. westwoodi and P. pryeri is of the superficial one.

13. The germ band of B. laevipes, Bo. westwoodi and Pd. paradoxa is classified into the short germ type, and that of P. pryeri is the semilong germ type.

14. The inner layer formation is of the so-called proliferating type in B. laevipes, and of the invaginating type in Bo. westwoodi, Pd. paradoxa and P. pryeri.

15. In the cephalognathal region, the ectodermal invaginations are six pairs. Moreover, the single invagination appears on the median line of the labrum.

16. The single invagination of the ectoderm arises on the medioventral line at the intersegmental region between the ninth and tenth abdominal segments in B. laevipes, Pd. paradoxa and P. pryeri, and it is the future anal gland.

17. The formation of the corpora allata and prothoracic

glands is described in B. laevipes.

18. The tracheal invaginations appear in the mesothorx to the eighth abdominal segments. The spiracles of the mesothorax shift to the posterior margin of the prothorax, and the metathoracic ones are disappear later.

19. The oenocytes occur in the ectoderm at the posteromedial position of spiracles of the first eight abdominal segments in B. laevipes, Pd. paradoxa and P. pryeri.

20. The ventral nerve cord consists of sixteen paris of ganglion, one for each segment from the mandibular to the tenth abdominal.

21. The median cord has the neuroblasts which participate into the ganglion formation in B. laevipes, Pd. paradoxa and P. pryeri.

22. The neurilemma is originated from the outer cells of the lataral cord in B. laevipes, Pd. paradoxa and P. pryeri.

23. The brain consists of three pairs protocerebral ganglia(lobus 1, 2, and 3+3'), the antennal ganglia (=deutocerebrum), and the intercalary ganglia (=tritocerebrum).

24. The stomatogastric nervous system is derived from three evaginations of the stomodaeal roof in B. laevipes, Pd. paradoxa and P. pryeri.

25. The larval eyes of B. laevipes and P. pryeri are the compound eyes and their formation is described. The

optic plate of Pd. paradoxa becomes vestigial during the embryonic stage, and the first instar larva has no eyes.

26. The coelomic sacs are formed eighteen pairs, one for each of the labral, antennal, three gnathal, three thoracic, and ten abdominal segments.

27. The aorta is formed by the antennal mesodermal cells in B. laevipes, Pd. paradoxa and P. pryeri.

28. The heart, pericardial cells, and dorsal diaphragm are derived from the lateral walls of coeloms in the thoracic and abdominal regions in B. laevipes, Pd. paradoxa and P. pryeri.

29. The blood cells are originated from the primary median mesoderm in B. laevipes, Pd. paradoxa and P. pryeri.

30. The suboesophageal bodies arise from the mesodermal cells of the intercalary segment in B. laevipes, Pd. paradoxa and P. pryeri.

31. The formation of the gonads is described in B. laevipes, Pd. paradoxa and P. pryeri.

32. The fat bodies and body muscles differentiate from the lateral walls of the coeloms.

33. The musculatures of the thoracic and abdominal segments of the first instar larva are described in P. pryeri.

34. The stomodaeum and proctodaeum are formed in the usual manner as ectodermal invaginations.

35. The three pairs of the malpighian tubules evaginate from the blind end of the proctodaeum in B. laevipes, Pd. paradoxa and P. pryeri.

36. The anterior and posterior midgut rudiments are derived from the proliferating cells of the stomodaeal and proctodaeal blind ends severally. Therefore the midgut epithelium is entirely ectodermal in origin.

37. The duodenal valve is formed at the middle part of the proctodaeum.

38. The midgut epithelium of the first instar larva is classified into four regions from the morphological characters of the cells in P. pryeri.

39. The amnion of the embryo spreads laterally, and differentiates into the outer and inner amnions.

40. The thickened serosa appears near the anterior pole of the egg in Bo. westwoodi, and the serosal cuticle is formed in B. laevipes, Bo. westwoodi, Pd. paradoxa and P. pryeri.

41. The embryos of B. laevipes diapause for ca. 180 days.

42. The formation of the abdominal legs is described in B. laevipes and P. pryeri, and the legs are not homologous with the thoracic legs.

43. The formation of the anal legs and telson is described in P. pryeri. The anal legs are formed from the part of the telson, and seem not to be modified cerci

of the eleventh abdominal segment.

44. The tenth abdominal segments of Pd. paradoxa and P. pryeri are likely to involve the vestigial eleventh abdominal segments.

45. The relationship of the four mecopteran families is discussed, and the genealogical tree is given based on the present embryological data. The Bittacidae is thought to be most primitive, and the Panorpidae seems to be the most derived family in the four mecopteran families.

ACKNOWLEDGEMENTS

The author wishes to express his hearty thanks to Prof. Dr. Hiroshi Ando of Sugadaira Montane Research Center, Uneversity of Tsukuba for his constant guidance as well as invaluable suggestion and advice given to the author in the course of proceeding the work. Thanks also due to Prof. Dr. Koichi Sekiguchi and Dr. Kazuo Haga of University of Tsukuba for their valuable suggestion and constant encouragement. The author is especially thankful to Dr. Ryuichi Matsuda of the Biosystematics Research Institute, Canadian Department of Agriculture for his valuable suggestions of the morphological accounts of insects. The author also thankful to Prof. Dr. George Byers of University of Kansas, U.S.A., and Prof. Dr. Gerhard Mickoleit and Dr. Erika Mickoleit of University of Tübingen, F.R.G., for their kindly offering forign mecopteran materials to the author.

Also for the valuable advices and constant encouragement given to the author, he wishes to express his acknowledgements to Professors Drs. Masukichi Okada, Toshihide Ichimura and Mitsuo Chihara of University of Tsukuba, Drs. Ichiroku Hayashi and Seiji Tokumasu of Sugadaira Montane Research Center, University of Tsukuba. In referring to the literature the author is indebted to Dr. Tsukane Yamasaki of the Natural Sciense Museum (Nat. Hist.), Tokyo, and Dr. Hajime Mori of Tokyo Metropolitan

University. Finally the author wishes to express his thanks to the staffs of Sugadaira Montane Research Center, Dr. Ryuichiro Machida and Mr. Tohru Kishimoto of University of Tsukuba for their kindness in helping in many sides.

LITERATURE CITED

*indirect citation

Akaike, M., Ishii, M. and Ando, H. 1982. The formation of germ rudiment in the caddisflies, Gryphotaelius admorsus MacLachlan and Neosererina crassicornis Ulmer (Integripalpia, Trichoptera) and its phylogenetic significance. Pro. Jap. Soc. Zool., (22):46-52.

Anderson, D. T. 1962. The embryology of Dacus tryoni (Frogg.)[Diptera, Trypetidae(=Tephritidae)], the Queensland fruit-fly. J. Embryol. Exp. Morphol., 10:248-292.

Anderson, D. T. 1972. The development of hemimetabolous insects, pp. 95-163. The development of holometabolous insects, pp. 165-242. In S. J. Counce and C. J. Waddington (eds.), Developmental Systems: Insects. Vol. 1, Academic Press, New york.

Anderson, D. T. and Wood, E. C. 1968. The morphology basis of embryonic movements in the light brown apple moth, Epiphyas postvittana (Walk.)(Lepidoptera: Tortricidae). Aust. J. Zool., 16:763-793.

Ando, H. 1957. A comparative study on the development of ommatidia in Odonata. Sci. Rep. Tokyo Kyoiku Daigaku, Sec. B, 8:174-216.

Ando, H. 1960. Studies on the early embryonic development of a scorpion fly, Panorpa pryeri MacLachlan (Mecoptera, Panorpidae). Sci. Rep. Tokyo Kyoiku Daigaku, Sec. B, 9:227-242.

Ando, H. 1962. The Comparative Embryology of Odonata with Special Reference to a Relic Dragonfly Epiophlebia superstes Selys. Jap. Soc. Promot. Sci., Tokyo.

Ando, H. 1973. Old oocytes and newly laid eggs of scorpion-flies and hanging-flies (Mecoptera: Panorpidae and Bittacidae). Sci. Rep. Tokyo Kyoiku Daigaku, Sec. B, 15:163-187.

Ando, H. 1981. Embryology and phylogeny in insects, pp. 33-49. In S. Ishii (ed.), Recent Advance in Entomology. Tokyo University Press, Tokyo (in Japanese).

Ando, H. and Haga, K. 1974. Studies on the pleuropodia of Embioptera, Thysanoptera and Mecoptera. Bull. Sugadaira Biol. Lab. Tokyo Kyoiku University, (6):1-8.

Ando, H. and Kobayashi, Y. 1978. The formation of germ rudiment in the primitive moth, Neomicropteryx nipponensis Issiki (Micropterygidae, Zeugloptera, Lepidoptera) and its phylogenetic significance. Proc. Jap. Soc. Syst. Zool., (15):47-50.

Ando, H. and Suzuki, N. 1977. On the embryonic development of larval compound eyes of the scorpion-fly, Panorpa pryeri MacLachlan (Mecoptera, Panorpidae). Proc. Jap. Soc. Syst. Zool., (13):81-84.

Ando, H. and Tanaka, M. 1976. The formation of germ rudiment and embryonic membranes in the primitive moth, Endoclyta excrescens Butler (Hepialidae, Monotrysia, Lepidoptera) and its phylogenetic significance. Proc.

Jap. Soc. Syst. Zool., (12):52-55.

Ando, H. and Tanaka, M. 1980. Early embryonic development of the primitive moths, Endoclyta signifer Walker and E. excrescens Butler (Lepidoptera: Hepialidae). Int. J. Insect Morphol. Embryol., 9:67-77.

Ashhurst, D. E. 1965. The connective tissue sheath of the locust nervous system: its development in the embryo. Quart. J. Micro. Sci., 106:61-73.

Baden, V. 1936. Embryology of the nervous system in the grasshopper, Melanoplus differentialis (Acrididae; Orthoptera). J. Morphol., 60:159-188.

Bierbrodt, E. 1942. Der Lavenkopf von Panorpa communis L. und seine Verwandlung, mit besonderer Berücksichtigung des Gehirns und der Augen. Zool. Jahr., Anat., 68:49-136.

Bock, E. 1939. Bildung und Differenzierung der Keimblätter bei Chrysopa perla (L.). Z. Morphol. Ökol. Tiere, 27:615-702.

Bronskill, J. F. 1959. Embryology of Pimpla turionellae (L.) (Hymenoptera: Ichneumonidae). Can. J. Zool., 37:655-688.

Bronskill, J. F. 1964. Embryogenesis of Mesoleius tenthredinis Morl. (Hymenoptera: Ichneumonidae). Can. J. Zool., 42:439-453.

Busselmann, A. 1935. Bau und Entwicklung der Raupenocellen der Mehlmotte Ephestia kühniella Zeller. Z. Mor-

phol. Ökol. Tiere, 29:218-228.

Butt, F. H. 1936. The early embryological developmeny of the parthenogenetic alfalfa snout beetle, Brachyrhinus ligustici L. Ann. Entomol. Soc. Amer., 24:1-13.

Butt, F. H. 1949. Embryology of the milkweed bug, Oncopeltus fasciatus (Hemiptera). Mem. Cornell Univ. Agri. Exp. Stn., 283:3-43.

Byers, G. W. 1963. The life history of Panorpa nuptialis (Mecoptera: Panorpidae). Ann. Entomol. Soc. Amer., 56:142-149.

Church, N. S. and Rempel, J. G. 1971. The embryology of Lytta viridana Le Conte (Coleoptera: Meloidae). VI. The appendiculate, 72-h embryo. Can. J. Zool., 49:1563-1570.

Cobben, R. H. 1968. Evolutionary Trende in Heteroptera. Part I. Eggs, Architecture of the Shell, Gross Embryology and Eclosion. Agri. Res. Rep., Wageningen.

Cobben, R. H. 1978. Evolutionary Trends in Heteroptera. Part II. Mouthpart-structures and Feeding Strategies. H. Veenman & Zonen B. V., Wageningen.

Cooper, K. W. 1974. Sexual biology, chromosomes, development, life histories and parasites of Boreus, especially of B. notoperates. A southern California Boreus. II. (Mecoptera: Boreidae). Psyche, 81:84-120.

Craig, D. A. 1967. The eggs and embryology of some New Zealand Blepharoceridae (Diptera, Nematocera) with

reference to the embryology of other Nematocera. Trans. Roy. Soc. N. Z., Zool., 18:191-206.

Dorn, A. 1972. Die endokrinen Drüsen im Embryo von Oncopeltus fasciatus Dallas (Insecta, Heteroptera). Z. Morphol. Tiere, 71:52-104.

Eastham, L. 1927. A contribution to the embryology of Pieris rapae. Quart. J. Micro. Sci., 71:353-394.

Eastham, L. 1930. The embryology of Pieris rapae. Organogeny. Phil. Trans. Roy. Soc., B, 219:1-50.

Farooqi, M. M. 1963. The embryology of the mustard sawfly Athalia proxima Klug. (Tenthredinidae, Hymenoptera). Aligarh Musl. Univ. Publs., 6:1-68.

Gassner, G., III. 1963. Notes on the biology and immature stages of Panorpa nuptialis Gerstaecker (Mecoptera: Panorpidae). Texas J. Sci., 15:142-154.

Goss, R. J. 1953. The advanced embryology of the book louse, Liposcelis divergens Badonnel (Psocoptera; Liposcelidae). J. Morphol., 92:157-206.

Grell, K. G. 1938. Der Darmtraktus von Panorpa communis L. und seine Anhänge bei Larve und Imago. Zool. Jahrb., Anat., 64:1-84.

Haget, A. 1977. L'embryologie des insectes, pp. 1-262, 279-387. In P. P. Grassé (ed.), Traité de Zoologie. Vol. 8, fasc. 5B, Masson, Paris.

Hennig, W. 1981. Insect Phylogeny. John Wiley & Sons, Chichester, New York.

Henson, H. 1944. The development of the malpighian tubules of Blatta orientalis (Orthoptera). Proc. Roy. Entomol. Soc. London, (A) 19:73-91.

Heymons, R. 1895. Die Embryonalentwicklung von Dermapteren und Orthopteren unter Besonderer Berücksichtigung der Keimblätterbildung. Gustav Fischer, Jena.

Heymons, R. 1896. Grundzüge der Entwickelung und des Körperbaues von Odonaten und Ephemerieden. Anhang Abhandl. Kgl. Akad. Wiss., Berlin.

Hinton, H. E. 1958. The phylogeny of the panorpoid orders. Ann. Rev. Entomol., 3:181-206.

Hinton, H. E. 1981. Biology of Insect Eggs. 3 vols., Pergamon Press, Oxford.

Hirschler, J. 1909. Die Embryonalentwicklung von Donacia crassipes. Z. Wiss. Zool., 92:627-744.

Hirschler, J. 1928. Embryogenese der Insekten, pp. 570-824. In C. Schröder (ed.), Handbuch der Entomologie. I, Gustav Fischer, Jena.

Hussey, P. B. 1926. Studies on the pleuropodia of Belostoma flumineum Say and Ranatra fusca Palisot de Beauvous, with a discussion of these organs in other insects. Entomol. Amer., 7:1-81.

Ishii, T. 1937. Notes on the life-history of Bittacus nipponicus Navas. Shokubutsu oyobi Dôbutsu (Zoology and Botany), Tokyo, 5:24-28 (in Japanese).

Issiki, S. 1959. Mecoptera, pp. 123-125. pl. 231. In

A. Kawada (ed.), Illustrated Insect Larvae of Japan. Hokuryûkan, Tokyo (in Japanese).

Johannsen, O. A. 1929. Some phases in the embryonic development of Diacrisia virginica Fabr. (Lepidoptera). J. Morphol. Physiol., 48:493-541.

Johannsen, O. A. and Butt, F. H. 1941. Embryology of Insects and Myriapods. McGraw-Hill, New York.

Jura, C. 1956. Embryogenesis of the alimentary system of the weevil, Phyllobius glaucus Scop. (Curculionidae, Coleoptera). Zool. Pol., 7:155-176.

Jura, C. 1966. Origin of the endoderm and embryogenesis of the alimentary system in Tetrodontophora bielanensis (Waga)(Collembola). Acta Biol. Cracov. Zool., 9:95-102.

Kessel, E. L. 1939. The embryolgy of fleas. Smithsonian Misc. Coll., 98:1-78.

Kessel, R. G. 1961. Cytological studies on the suboesophageal body cells and pericardial cells in embryos of the grasshopper, Melanoplus differentialis (Thomas). J. Morphol., 109:289-321.

Kobayashi, Y. and Ando, H. 1981. The embryonic development of the primitive moth, Neomicropteryx nipponensis Issiki (Lepidoptera, Micropterygidae): Morphogenesis of the embryo by external observation. J. Morphol., 169: 49-59.

Kobayashi, Y. and Ando, H. 1982. The early embryonic

development of the primitive moth, Neomicropteryx nipponensis Issiki (Lepidoptera, Micropterygidae). J. Morphol., 172: 259-269.

Kobayashi, Y., Tanaka, M., Ando, H. and Miyakawa, K. 1981. embryonic development of alimentary canal in the primitive moth, Endoclita signifer Walker (Lepidoptera, Hepialidae). Kontyû, 49:641-652.

Krause, G. 1939. Die Eitypen der Insekten. Biol. Zent., 59:495-536.

Krause, G. 1961. Preformed ooplasmic reaction system in insect eggs. Symposium on "Germ cells and Development". Institut Int. d'Embryologie and Fondazione A. Baselli (1960), 302-337.

Krzysztofowicz, A. 1960. Comparative investigations on the embryonic development of the weevils (Coleoptera, Curculionidae), and an attempt to apply them to the systematics of this group. Zool. Pol., 10:2-27.

Larink, O. 1969. Zur Entwicklungsgeschichte von Petrobius brevistylis (Thysanura, Insecta). Helgoländer Wiss. Meeresunters., 19:111-155.

Luginbill, P., Jr. 1953. A contribution to the embryology of the may beetle. Ann. Entomol. Soc. Amer., 46:505-528.

Machida, R. 1981a. External features of embryonic development of a jumping bristletail, Pedetontus unimaculatus Machida (Insecta, Thysanura, Machilidae). J.

Morphol., 168:339-355.

Machida, R. 1981b. The embryology of the jumping bristletail Pedetontus unimaculatus Machida (Insecta, Microcoryphia, Machilidae). pp. 225 (The Doctoral Thesis, University of Tsukuba).

Machida, R. and Ando, H. 1981. Formation of midgut epithelium in the jumping bristletail Pedetontus unimaculatus Machida (Archaeognatha: Machilidae). Int. J. Morphol. Embryol., 10:297-308.

Madhavan, M. M. 1974. Structure and function of the hydropyle of the egg of the bug, Sphaerodema molestum. J. Insect Physiol., 20:1341-1349.

Matsuda, R. 1965. Morphology and Evolution of the Insect Head. Mem. Amer. Entomol. Inst., No. 4.

Matsuda, R. 1970. Morphology and Evolution of the Insect Thorax. Mem. Can. Entomol., No. 76.

Matsuda, R. 1976. Morphology and Evolution of the Insect Abdomen. Pergamon Press, Oxford.

Mellanby, H. 1936. The later embryology of Rhodnius prolixus. Quart. J. Micro. Sci., 79:1-42.

Mickoleit, G. 1978. Die phylogenetischen Beziehungen der Schnabelfliegen-Familien aufgrund morphologischer Ausprägung der weiblichen Genital- und Postgenitalsegmente (Mecoptera). Entomol. Germ., 4:258-271.

Miller, A. 1940. Embryonic membranes, yolk cells, and morphogenesis of the stonefly Pteronarcys proteus Newman

(Plecoptera; Pteronarcidae). Ann. Entomol. Soc. Amer., 33:437-477.

Miya, K. 1958. Studies on the embryonic development of the gonad in the silkworm, Bombyx mori L. Part 1. Differentiation of germ cells. J. Fac. Agri., Iwate Univ., 3:436-467.

Miya, K. 1976. Ultrastructural changes of embryonic cells during organogenesis in the silkworm, Bombyx mori. II. The alimentary canal and the malpighian tubules. J. Fac. Agri., Iwate Univ., 13:95-122.

Miya, K. and Abe, T. 1966. The early embryology of Epilachna vigintioctomaculata Motschulsky (Coccinellidae, Coleoptera), including some observations on the later development. J. Fac. Agri., Iwate Univ., 7:277-289.

Miyakawa, K. 1973. The embryology of the caddisfly Stenopsyche griseipennis MacLachlan (Trichoptera: Stenopsychidae). I. Early stages and changes in external form of embryo. Kontyû, 41:413-435.

Miyakawa, K. 1974a. The embryology of the caddisfly Stenopsyche griseipennis MacLachlan (Trichoptera: Stenopsychidae). II. Formation of germ band, yolk cells and embryonic envelopes, and early development of inner layer. Kontyû, 42:64-73.

Miyakawa, K. 1974b. The embryology of the caddisfly Stenopsyche griseipennis MacLachlan (Trichoptera: Stenopsychidae). III. Organogenesis: Ectodermal derivatives.

Kontyû, 42:305-324.

Miyakawa, K. 1974c. The embryology of the caddisfly Stenopsyche griseipennis MacLachlan (Trichoptera: Stenopsychidae). IV. Organogenesis: Mesodermal derivatives. Kontyû, 42:451-466.

Miyakawa, K. 1975. The embryology of the caddisfly Stenopsyche griseipennis MacLachlan (Trichoptera: Stenopsychidae). V. Formation of alimentary canal and other structures, general consideration and conclusion. Kontyû, 43:55-74.

Miyakawa, K. 1979. Embryology of the dobsonfly, Protohermes grandis Thunberg (Megaloptera: Corydalidae). I. Changes in external form of the embryo during development. Kontyû, 47:367-375.

Miyake, T. 1912. The life-history of Panorpa klugi M'Lachlan. J. Coll. Agri., Imp. Univ. Tokyo, 4:117-139.

Mori, H. 1969. Normal embryogenesis of the waterstrider, Gerris paldum insularis Motschulsky, with special reference to midgut formation. Jap. J. Zool., 16:53-67.

Mori, H. 1970. The distribution of the columnar serosa of eggs among the families of Heteroptera, in relation to phylogeny and systematics. Jap. J. Zool., 16:89-98.

Mori, H. 1976. Formation of the visceral musculature and origin of the midgut epithelium in the embryos of Gerris paludum insularis Motschulsky (Hemiptera: Gerridae). Int. J. Insect Morphol. Embryol., 5:117-125.

Nelson, J. A. 1915. The embryology of the Honey Bee. Princeton Univ. Press, Princeton, N. J.

Okada, M. 1960. Embryonic development of the rice stemborer, Chilo suppressalis. Sci. Rep. Tokyo Kyoiku Daigaku, Sec. B, 9:243-296.

Okada, M. 1971. Role of the chorion as a barrier to oxygen in the diapause of the silkworm, Bombyx mori L. Experientia, 27:658-660.

Paterson, N. F. 1932. A contribution to the embryological development of Euryope terminalis. Part 2. Organogeny. S. African J. Sci., 29:414-448.

Patten, W. 1884. The development of phryganids, with a preliminary note of Blatta germanica. Quart. J. Micro. Sci., 24:549-602.

Patten, W. 1887. Studies on the eyes of arthropods. I. Development of the eyes of Vespa, with observations on the ocelli of some insects. J. Morphol., 1:193-226.

Paulus, H. F. 1979. Eye structure and the monophyly of the Arthropoda, pp. 299-383. In A. P. Gupta (ed.), Arthropod Phylogeny. Van Nostrand Reinhold Company, New York.

Penny, N. D. 1975. Evolution of the extant Mecoptera. J. Kansas Entomol. Soc., 48:331-350.

Pilgrim, R. L. C. 1972. The aquatic larva and the pupa of Choristella phylpotti Tillyard, 1917 (Mecoptera: Nannochoristidae). Pac. Insects, 14:151-168.

Presser, B. D. and Rutschky, C. W. 1957. The embryonic development of the corn earworm, Heliothis zea (Boddie) (Lepidoptera, Phalaenidae). Ann. Entomol. Soc. Amer., 50:133-164.

Ramamurty, P. S. 1964a. On the contribution of the follicle epithelium to the deposition of yolk in the oocyte of Panorpa communis (Mecoptera). Exp. Cell Res., 33: 601-605.

Ramamurty, P. S. 1964b. Distribution of RNA in the ooplasm of the scorpion fly. Sci. Cul., 30:459-461.

Raminani, L. and Cupp, E. W. 1978. Embryology of Aedes aegypti (L.)(Diptera: Culicidae): Organogenesis. Int. J. Insect Morphol. Embryol., 7:273-296.

Rempel, J. G. and Church, N. S. 1969. The embryology of Lytta viridana Le Conte (Coleoptera, Meloidae). V. The blastoderm, germ layers, and body segments. Can. J. Zool., 47:1157-1171.

Rempel, J. G. and Church, N. S. 1971. The embryology of Lytta viridana Le Conte (Coleoptera, Meloidae). VII. Eighty-eight to 132 h: the appendages, the cephalic apodemes, and head segmentation. Can. J. Zool., 49: 1571-1581.

Rempel, J. G. and Church, N. S. 1972. The embryology of Lytta viridana Le Conte (Coleoptera, Meloidae). VIII. The respiratory system. Can. J. Zool., 50:1547-1554.

Rempel, J. G., Heming, B. S. and Church, N. S. 1977. The

embryology of Lytta viridana Le Conte (Coleoptera, Meloidae). IX. The central nervous system, stomatogastric nervous system, and endocrine system. Quaest. Entomol., 13:5-23.

Roonwal, M. L. 1936. Studies on the embryology of the African migratory locust, Locusta migratoria migratorioides R. and F. I. The early development, with a newly theory of multiphased gastrulation among insects. Phil. Trans. Roy. Soc. London, Ser. B, 226:391-421.

Roonwal, M. L. 1937. Studies on the embryology of the African migratory locust, Locusta migratoria migratorioides R. and F. II. Organogeny. Phil. Trans. Roy. Soc. London, Ser. B, 227:175-244.

Rottmar, B. 1966. Über Züchtung, Diapause und postembryonale Entwicklung von Panorpa communis L. Zool. Jahrb., Anat., 83:497-570.

Sander, K. 1956. The early embryology of Pyrilla perpusilla Walker (Homoptera), including some observations on the later development. Aligarh Musl. Univ. Publs. Zool., Indian Insect Types, 4:1-61.

Setty, L. R. 1931. The biology of Bittacus stigmaterus Say (Mecoptera, Bittacidae). Ann. Entomol. Soc. Amer., 24:467-484.

Setty, L. R. 1940. Biology and morphology of some north American Bittacidae (Order Mecoptera). Amer. Midl. Nat., 23:257-353.

Shafiq, S. A. 1954. A study of the embryonic development of the gooseberry sawfly, Pteronidea ribessii. Quart. J. Micro. Sci., 95:93-114.

*Sharov, A. G. 1953. Razvitiye schetinokhvostok (Thysanura, Apterygota) v svyzi s problemoi filogenii nasekomykh. Trud. Inst. Morfol. Zhivotynykh, 8:63-127.

*Sharov, A. G. 1959. O sisteme pervichnobeskrylykh nasekomykh. Trud. Inst. Morfol. Zhivotnykh, 27:175-186.

Sharov, A. G. 1966. Basic Arthropodan Stock with Special Reference to Insects. Pergamon Press, Oxford.

Slifer, E. H. 1937. The origin and fate of the membranes surrounding the grasshopper egg, together with some experiments on the source of the hatching enzyme. Quart. J. Micro. Sci., 79:493-507.

Snodgrass, R. E. 1935. Principles of Insect Morphology. McGraw-Hill, New York.

Springer, C. A. 1967. Embryology of the thoracic and abdominal ganglia of the large milkweed bug, Oncopeltus fasciatus (Dallas), (Hemiptera, Lygaeidae). J. Morphol., 122:1-18.

Springer, C. A. and Rutschky, C. W., III. 1969. A comparative study of the embryological development of the median cord in Hemiptera. J. Morphol., 129:375-400.

Stefani, R. 1961. La formazione dei foglietti embryonali, l'origine dell'epitelio intestinale e la determinazione della linea germinale femrninile vell'Haploembia soli-

eri. Caryologia, 14:1-30.

*Steiner, P. 1930. Studien an Panorpa communis L. Z. Morphol. Ökol. Tiere, 17:1-67.

Striebel, H. 1960. Zur Embryonalentwicklung der Termiten. Acta Trop., 17:193-260.

Strindberg, H. 1915. Hauptzüge der Entwicklungsgeschichte von Sialis lutaria L. Zool. Anz., 46:167-185.

*Strübing, H. 1950. Beiträge zur Biologie von Boreus hyemalis L. Zool. Beitr., (N. F.), 1:51-110.

Suzuki, N. and Ando, H. 1981. Alimentary canal formation of the scorpion fly, Panorpa pryeri MacLachlan (Mecoptera: Panorpidae). Int. J. Insect Morphol. Embryol., 10:345-354.

Suzuki, N., Shimizu, S. and Ando, H. 1981. Early embryology of the alderfly, Sialis mitsuhashii Okamoto (Megaloptera: Sialidae). Int. J. Insect Morphol. Embryol., 10:409-418.

Tiegs, O. W. and Murray, F. V. 1938. The embryonic development of Calandra oryzae. Quart. J. Micro. Sci., 80:159-284.

Tillyard, R. J. 1935. The evolution of the scorpion-flies and their derivatives. Ann. Entomol. Soc. Amer., 28: 1-45.

Toyama, K. 1902. Contribution to the study of silkworm. I. On the embryology of the silkworm. Bull. Coll. Agri., Tokyo Imp. Univ., 5:73-118.

Ullmann, S. L. 1964. The origin and structure of the mesoderm and the formation of the coelomic sacs in Tenebrio molitor L. (Insecta, Coleoptera). Phil. Trans. Roy. Soc. London, Ser. B, 248:245-277.

Ullmann, S. L. 1967. The development of the nervous system and other ectodermal derivatives in Tenebrio moritor L. (Insecta, Coleoptera). Phil. Trans. Roy. Soc. London, Ser. B, 252:1-25.

Visscher, S. N. 1976. The embryonic diapause of Aulocara elliotti (Orthoptera, Acrididae). Cell Tiss. Res., 174:433-452.

Wada, S. 1955. Zur Kenntnis der Keimblätterherkunft der Subösophagealkörpers am Embryo des Seidenraupe, Bombyx mori L. J. Seric. Sci. Jap., 24:114-117 (in Japanese with German summary).

Wheeler, W. M. 1889. The embryology of Blatta germanica and Coryphora decemlineata. J. Morphol., 3:291-386.

Wheeler, W. M. 1890. On the appendages of the first abdominal segment of embryo insects. Trans. Wisconsin Acad. Sci. Arts and Letters., 8:87-140.

Willmann, R. 1981. Das Exoskelett der männlichen Genitalien der Mecoptera (Insecta). II. Die phylogenetischen Beziehungen der Schnabelfliegen-Familien. Z. Zool. Syst. Evolut. -forsch., 19:153-174.

Withycombe, C. L. 1922. On the life-history of Boreus hyemalis L. Trans. Entomol. Soc. London, 1921:312-318.

Wolf, K. 1961. Erste entwicklungsgeschichtliche Beiträge zum Eitypus Panorpa (Mecoptera). pp. 77 (Zulassungsarbeit, Zool. Inst., Univ. Würzburg).

Yie, S. 1951. The biology of Formosan Panorpidae and morphology of eleven species of their immature stages. Mem. Coll. Agri. Nat. Taiwan Univ., 2:1-111.

Zakhvatkin, Y. A. 1968. Sravnitelbnaia embriologiia Chrysomelidae. Zool. Zh., 47:1333-1342.

ABBREVIATIONS USED IN THE FIGURES

a, amnion

a1-10, first to tenth abdominal segments

ac, amniotic cavity

af, amniotic fold

ag, antennal ganglion

ag1-10, first to tenth abdominal ganglia

al, abdominal leg

amr, anterior midgut rudiment

an, anus

ang, anal gland

anl, anal leg

ant, anterior tentorium

apc, amnioproctodaeal cavity

ar, aorta

at, antenna

atm, antennal mesoderm

atr, atrium of spiracle

b, brain

b1-3, protocephalic buldges 1 to 3

bc, blood cell

bdc, blastoderm cell

bep, blind end of proctodaeum

bm, basement membrane

bz, budding zone

c, cuticle

ca, corpus allatum

cb, cardioblast

cc, crystalline cone

cca, corpus cardiacum

ceb, central body of tentorium

ch, chorion

cn, cleavage nucleus

cnt, connective

coc, corneagenous cell

con, conjunctiva

cor, cornea

cos, common duct of salivary glands

cox, coxopodite

cp, cytoplasmic process

cr, cytoplasmic reticulum or reticuloplasm

cra, cranium

cs, coelomic sac

cse, columnar serosa

ct, coxa of thoracic leg

ctr, commissure of tritocerebrum

cv, cardiac valve

da, developing aorta

dc, deutocerebrum

dcm, degenerating closing membrane

dd, dorsal diaphragm

dm, distribution of mesodermal cells

dn, developing neurilemma

dp, dorsal process

dv, duodenal valve

e, eye

ea, embryonic area

ec, ectoderm

eea, extraembryonic area

ema, extensor mandibular apodeme

es, epineural sinus

est, evagination of stomatogastric nervous system

et, egg tooth

fb, fat body

fg, frontal ganglion

fm, first maturation division of female nucleus

fma, flexor mandibular apodeme

gc, germ cell

gd, germ disk

gi, ganglion of intercalary segment

gr, germ rudiment

gri, genital ridge

gs, granular substance

h, heart

hg, hypocerebral ganglion

ia, inner amnion

ic, intercalary segment

il, inner layer

ip, inner periplasm

ipg, invagination of prothoracic gland

isg, invagination of salivary gland

l, lumen

l1-3, lobi 1 to 3 of protocerebrum

la, labral apodeme

lg, lamina ganglionaris

li, labium

lig, labial segment

lp, lateral plate

lpa, lateral process of abdominal segment

ls, lateral spread of amnion

mc, mesodermal cell

md, mandible

mdc, median cord

mdg, mandibular ganglion

mdl, medioventral line

mds, mandibular segment

me, midgut epithelium

med, medulla

ml, median line

mp, micropyle

mpc, mitotical figure of proctodaeal cell

mpl, middle plate

mt, malpighan tubule

mu, muscle

mv, microvilli

mvl, medioventral line

mx, maxilla

mxa, maxillary apodeme

mxg, maxillary ganglion

mxs, maxillary segment

nb, neuroblast

nbm, neuroblast of median cord

ne, neurilemma

ng, neural groove

np, neuropile

oa, opening of amniotic fold

oam, outer amnion

oe, oesophagus

oec, oenocyte

og, outer ganglionic cell

ol, optic lobe

op, optic plate

ov, ostial valve

pb, polar body

pc, protocorm

pcc, pericardial cell

pce, protocerebrum

pcl, protocephalon or protocephalic lobe

pd, proctodaeum

pg, primitive groove

pgl, prothoracic gland

pl, periplasm

pmr, posterior midgut rudiment

pn, paracardiac nerve

pog, polar granule

prf, postretinal fiber

pt, posterior tentorium

pv, pyloric valve

pw, proctodaeal wall

ra, rudimental amnion

rc, regenerative cell

rd, ridumental dorsal process

rdd, rudimental dorsal diaphragm

re, rudimental eye

rec, retinular cell

rg, rudimental gonad

rh, rhabdom

ria, round cell of inner amnion

rmt, rudimental malpighian tubule

rn, recurrent nerve

rng, rudimental neural groove

rop, rudimental optic plate

rpf, rudimental postretinal fiber

rs, rudimental serosa

s, serosa

sb, suboesophageal body

sc, serosal cuticle

sd, stomodaeum

sdu, salivary duct

sec, Semper's cell

sg, salivary gland

sm, second maturation division of female pronucleus

smu, splanchnic muscle

som, somatic mesoderm

sp, spiracle

spc, small process on cranium

spm, splanchnic mesoderm

sr, stomodaeal roof

stn, stomatogastric nervous system

sz, spermatozoon

t, tentorium

t1-3, first to third thoracic segments

tc, tritocerebrum

te, telson

ter, tergum

tgl-3, first to third thoracic ganglia

tll-3, first to third thoracic legs

tp, telopodite

tr, trachea

trc, trichogen cell

tri, tracheal invagination

v, vacuole

vtt, vestigial tracheal trunk

y, yolk or yolk granule

yc, yolk cell (= yolk nucleus)

yca, yolk cell aggregation

EXPLANATION OF FIGURES

1. Newly laid egg of P. pryeri.
2. Close-up of Fig. 1 showing lateral side of shell.
3. Anterior pole of egg of P. pryeri.
4. Newly laid egg of Pd. paradoxa.
5. Anterior pole of egg of Pd. paradoxa.

Scales = 100µm (Figs. 1, 4) and 10µm (Figs. 2, 3, 5).

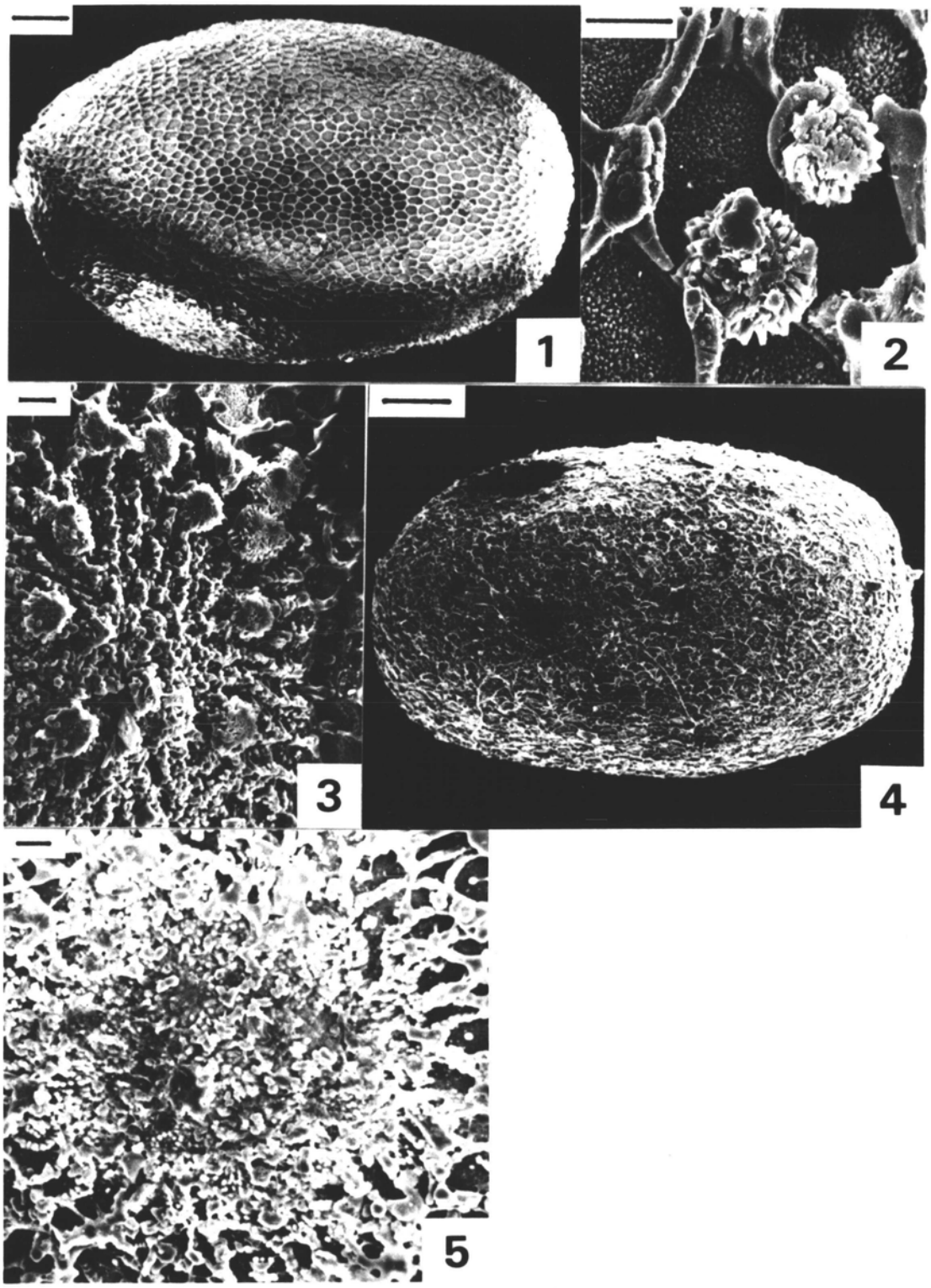
1
2
3
4
5

EXPLANATION OF FIGURES

6. Newly laid egg of B. laevipes.

7. Honeycombed pattern of shell of B. laevipes. Granular substance on egg surface is removed.

8. Anterior pole of egg of B. laevipes showing micropyles.

9. Newly laid egg of Bo. westwoodi.

10. Anterior pole of egg of Bo. westwoodi showing micropyles.

11. First instar larva of P. pryeri.

Scales = 100µm (Fig. 6), 10µm (Fig. 7), 5µm (Figs. 8, 10), 50µm (Fig. 9) and 500µm (Fig. 11).

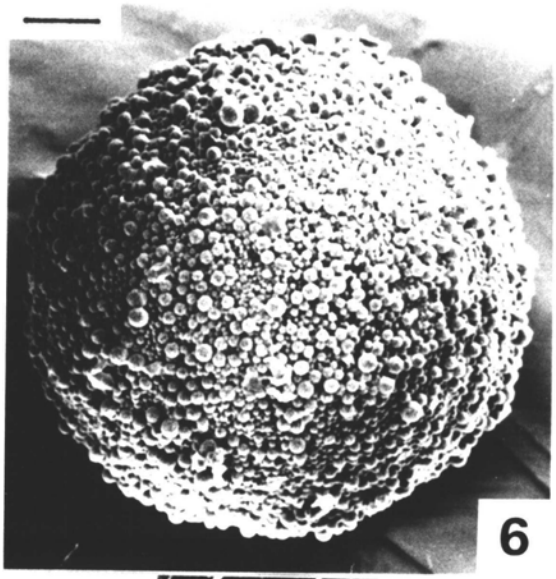

6

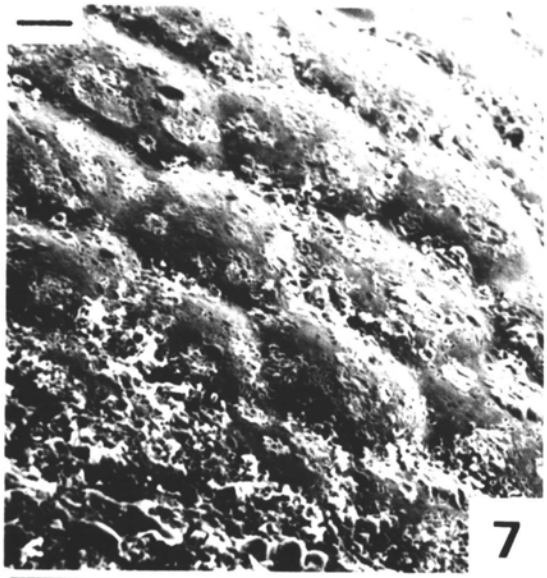

7

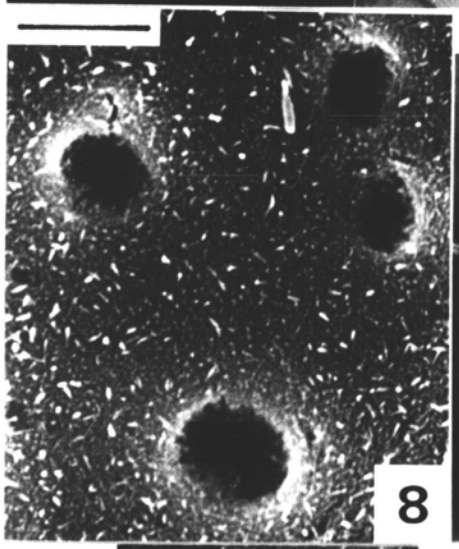

8

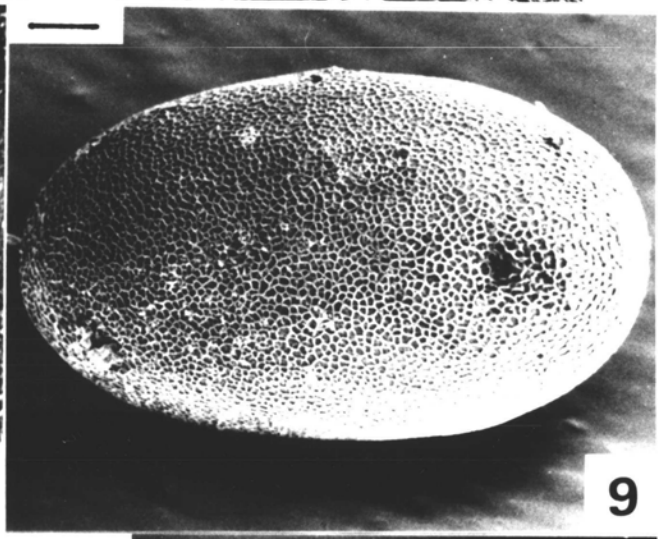

9

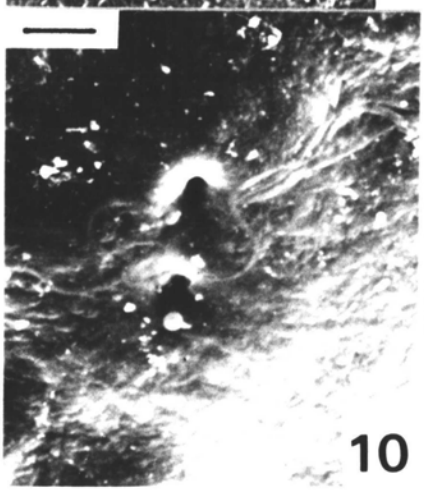

10

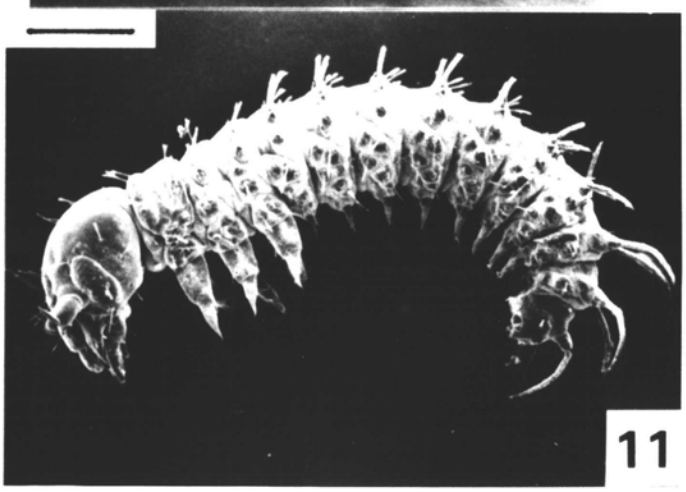

11

EXPLANATION OF FIGURES

12. First instar larva of Pd. paradoxa.

13. Small ventral process of third abdominal segment of first instar larva of Pd. paradoxa.

14. First instar larva of B. laevipes.

15. Larval eye of B. laevipes.

16. First instar larva of Bo. wedtwoodi.

17. Laterodorsal view of tenth abdominal segment of first instar larva of P. pryeri. Arrows show three pairs of spines which belong to vestigial eleventh abdominal segment.

Scale = 500µm (Figs. 12, 14, 16), 10µm (Figs. 13, 15) and 50µm (Fig. 17).

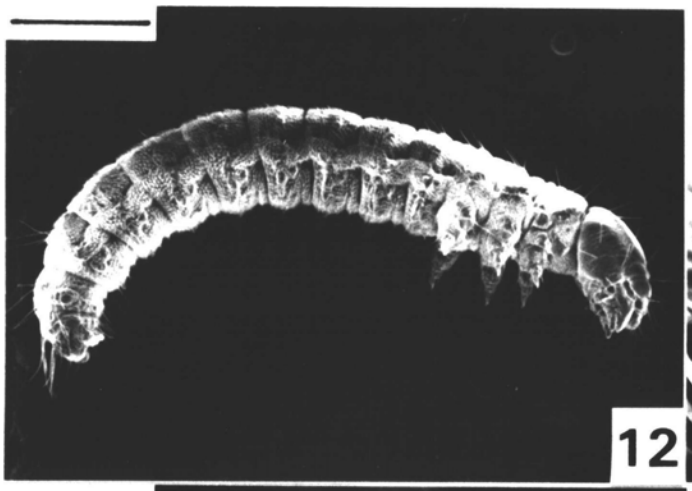

12

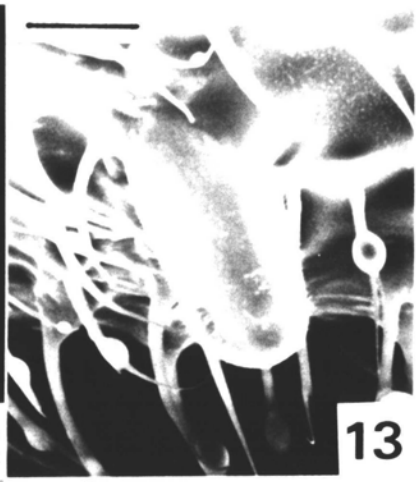

13

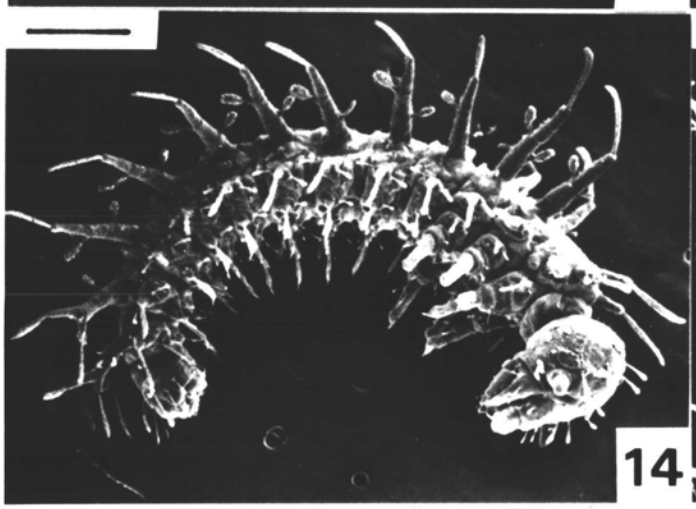

14

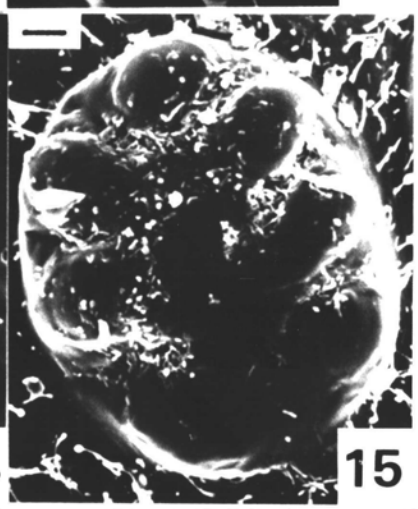

15

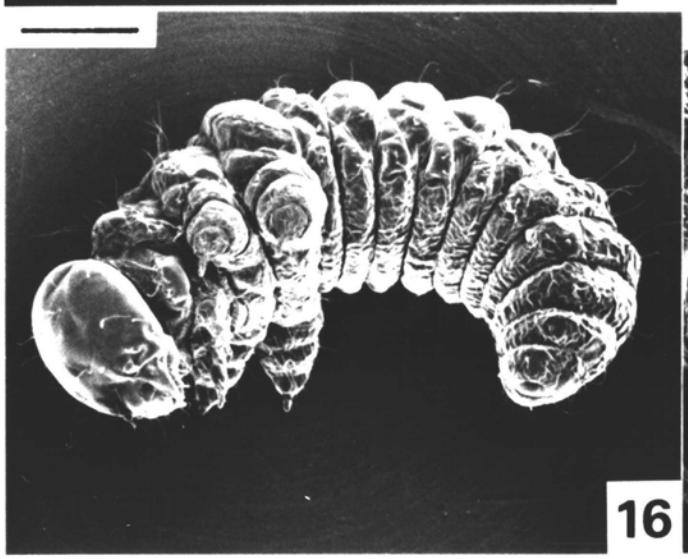

16

17

EXPLANATION OF FIGURES

18. Part of transverse section of egg of P. pryeri, showing second maturation division of female pronucleus early in Stage 1.

19. Part of longitudinal section of egg of P. pryeri, showing polar granule early in Stage 1.

20. Part of transverse section of egg of Pd. paradoxa early in Stage 1.

21. Part of transverse section of egg of Pd. paradoxa, showing first maturation division of female pronucleus early in Stage 1.

22. Part of transverse section of egg of B. laevipes, showing first maturation division of female pronucleus early in Stage 1.

Scales = 50μm.

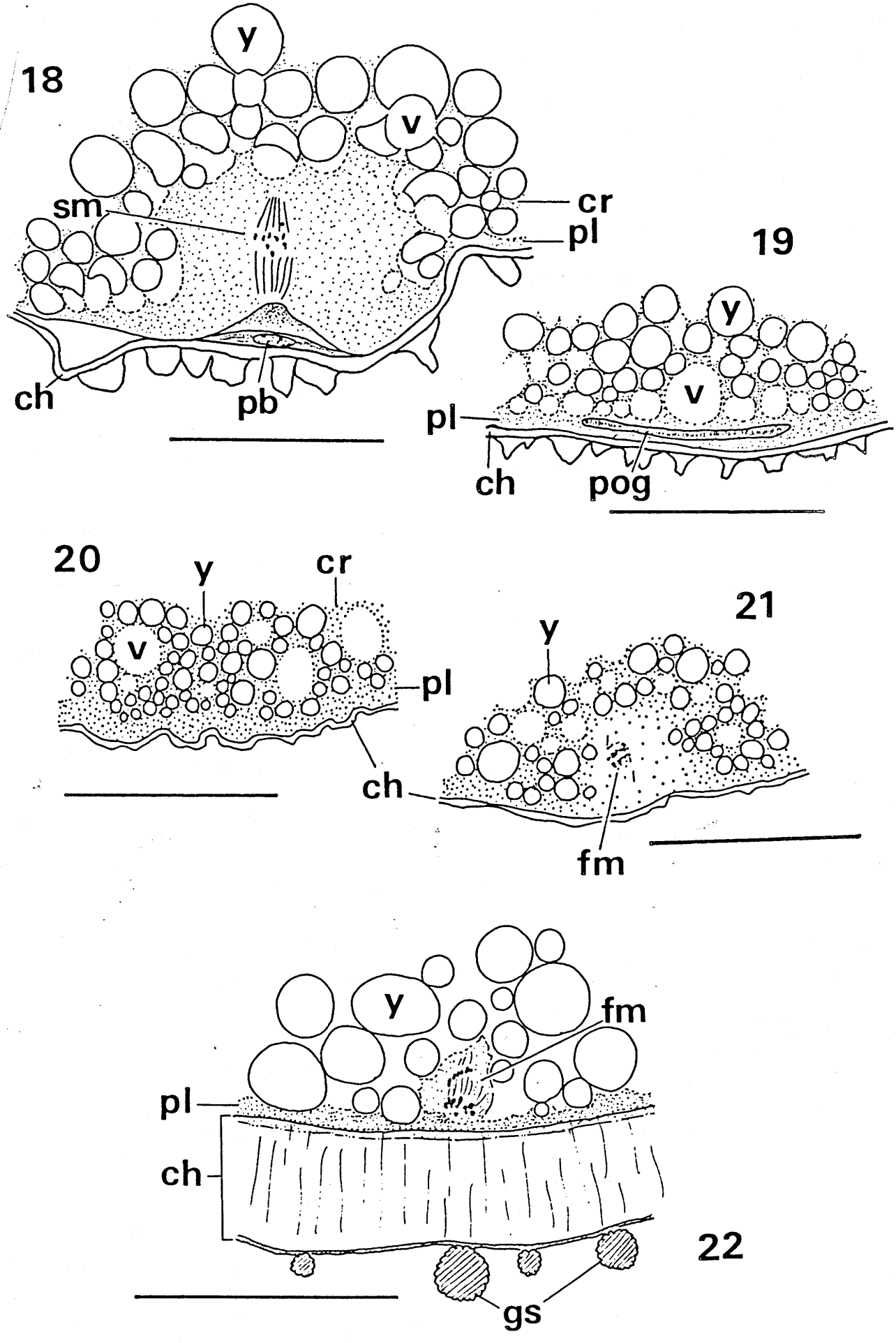
18
y
v
sm
cr
pl
ch
pb
19
y
v
pl
ch
pog
20
y
cr
v
pl
ch
21
y
fm
22
y
fm
pl
ch
gs

EXPLANATION OF FIGURES

23. Longitudinal section of chorion through anterior (A) and Posterior (B) poles of egg of Bo. westwoodi.
24. Part of transverse section of egg of Bo. westwoodi early in Stage 1.
25. Part of transverse section of egg of P. pryeri, showing spermatozoon.
26. Part of longitudinal section of egg of P. pryeri in Stage 1.
27. Part of longitudinal section of egg of P. pryeri in Stage 1.
28. Part of transverse section of egg of Pd. paradoxa early in Stage 1.
29. Part of longitudinal section of egg of Pd. paradoxa late in Stage 1.

Scales = 50μm.

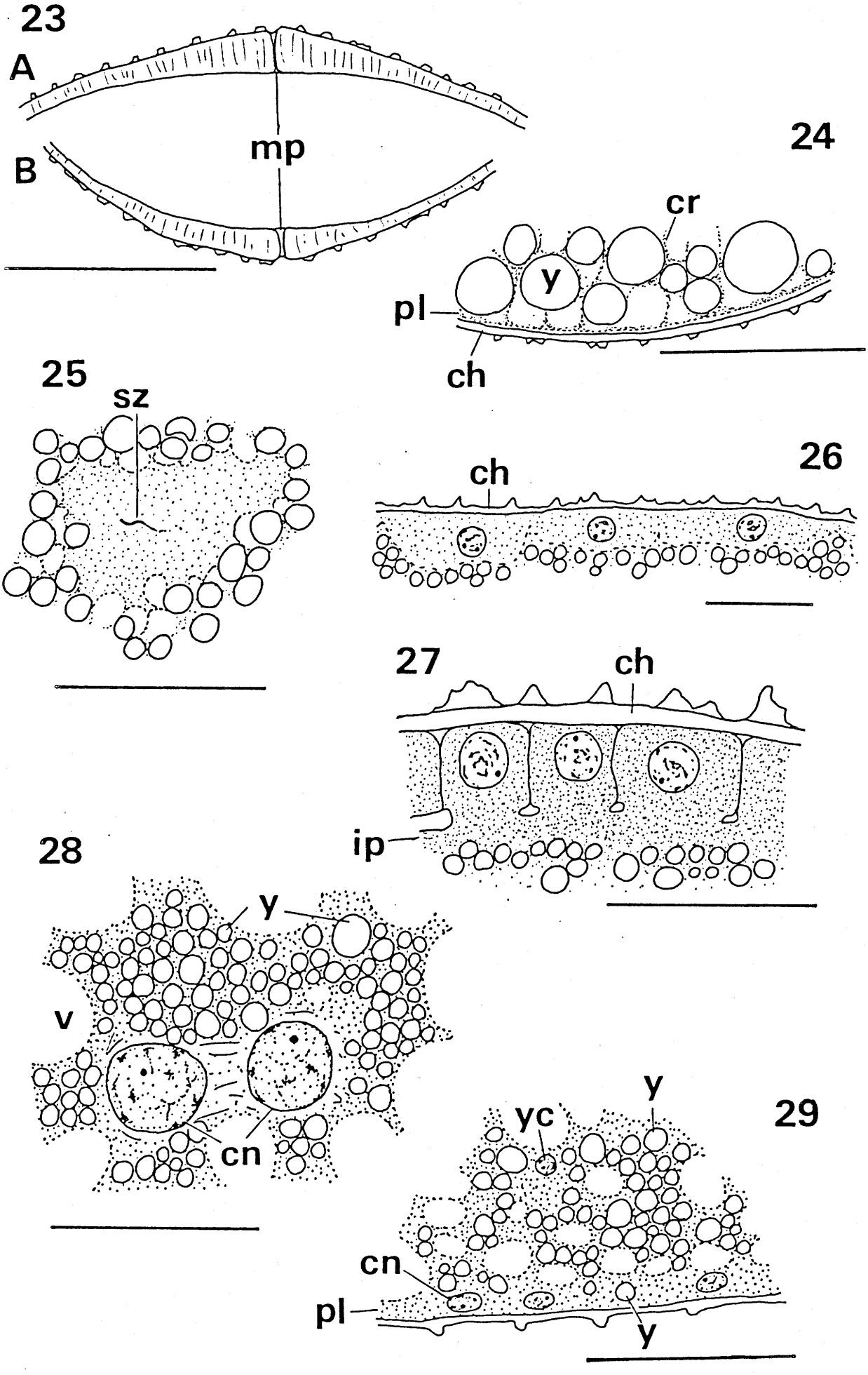
23
A
mp
B
24
cr
y
pl
ch
25
sz
26
ch
27
ch
ip
28
y
v
cn
29
y
yc
cn
pl
y

EXPLANATION OF FIGURES

30. Blastoderm cells in Pd. paradoxa late in Stage 1.

31. Cleavage nuclei at egg periphery in B. laevipes in Stage 1.

32. Blastoderm cells in B. laevipes late in Stage 1.

33, 34, 35. Consecutive stages of blastoderm formation in Bo. westwoodi during Stage 1.

Scales = 50μm.

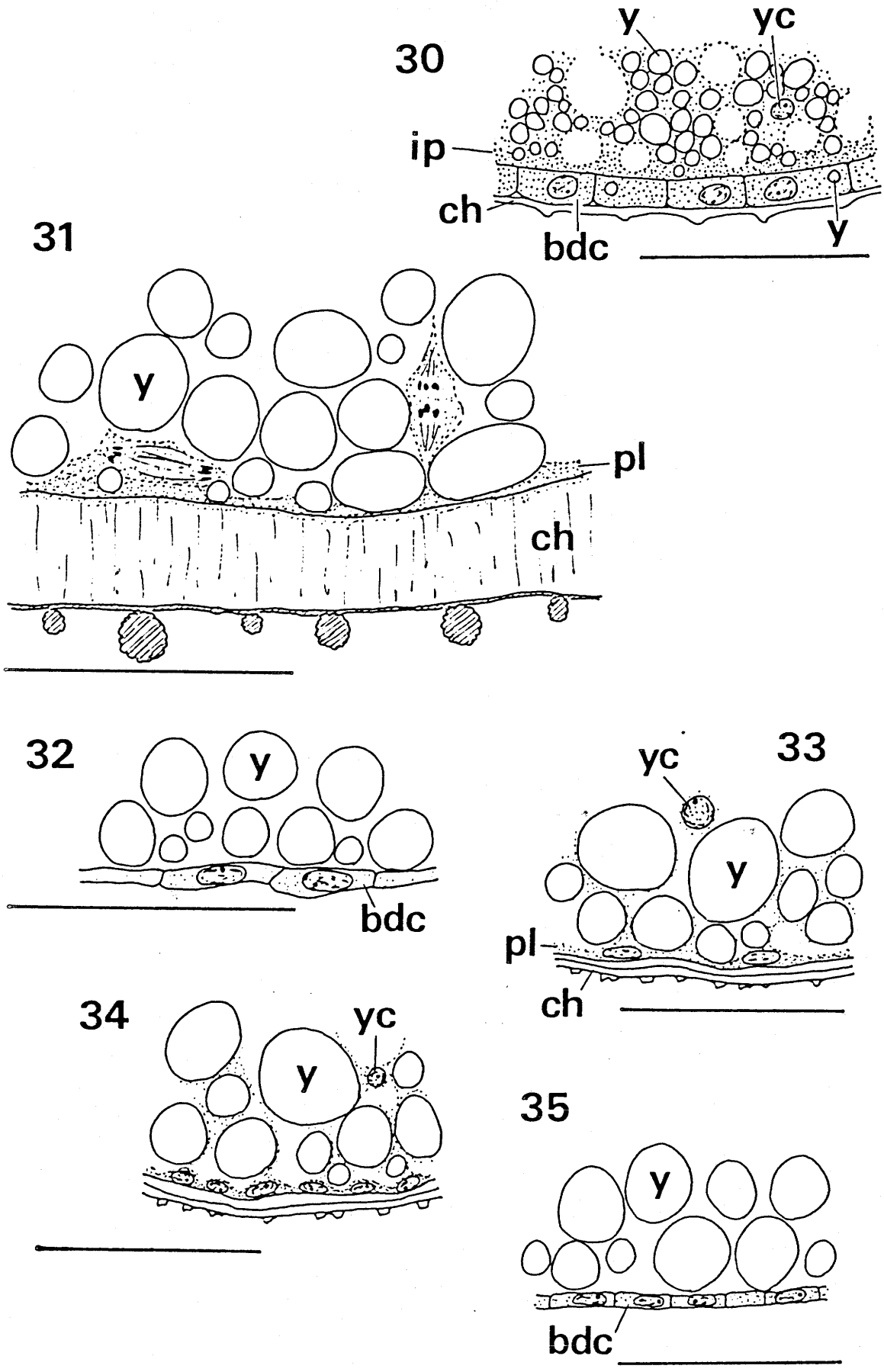
30
y
yc
ip
ch
bdc
y
31
y
pl
ch
32
y
bdc
33
yc
y
pl
ch
34
yc
y
35
y
bdc

EXPLANATION OF FIGURES

36. Cells of embryonic area in P. pryeri early in Stage 2.
37. Cells of extraembryonic area in P. pryeri early in Stage 2.
38. Lateral view of egg of P. pryeri late in Stage 2.
39. Ventral view of germ band of P. pryeri late in Stage 2.
40. Ventral view of germ band of P. pryeri early in Stage 3.
41. Lateral view of germ band of P. pryeri early in Stage 3.
42. Ventral view of germ band of P. pryeri late in Stage 3.
43. Ventral view of germ band of P. pryeri early in Stage 4.
44. Ventral view of germ band of P. pryeri early in Stage 4.

Scales = 50μm (Figs. 36, 37) and 500μm (Figs. 38-44). Arrows indicate the position of the caudal end of the germ bands.

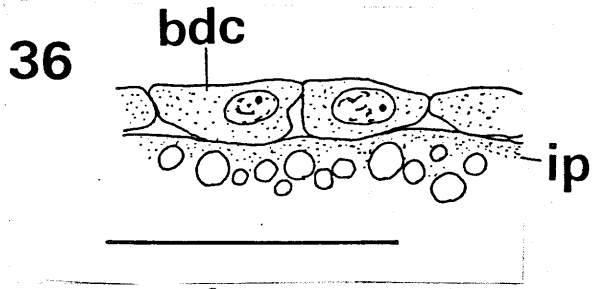
36
bdc
ip

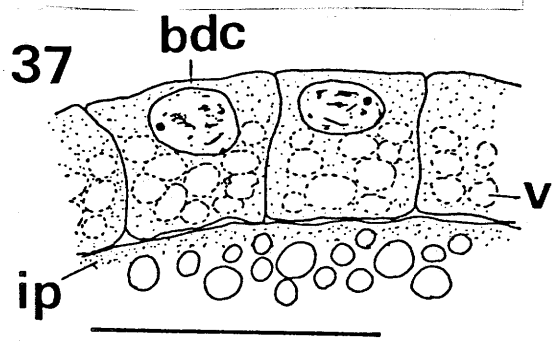
37
bdc
v
ip

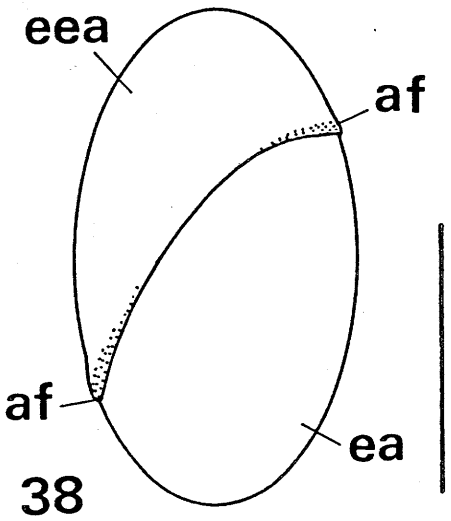
eea
af
af
ea
38

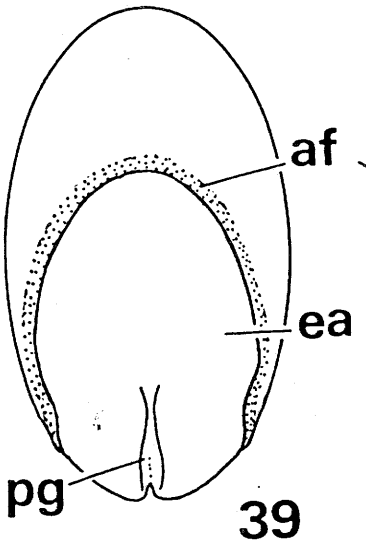
af
ea
pg
39

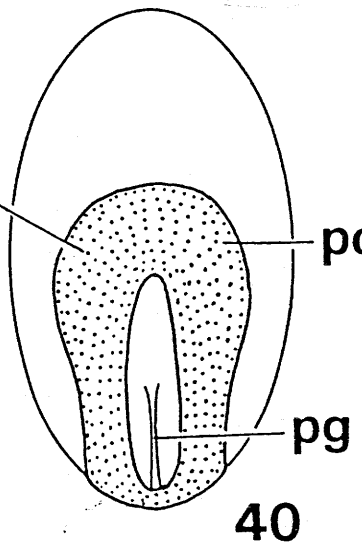
pcl
pg
40

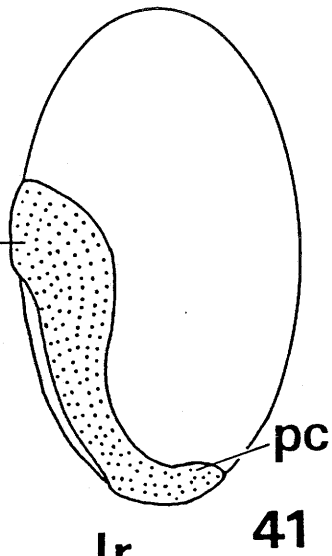
pc
41

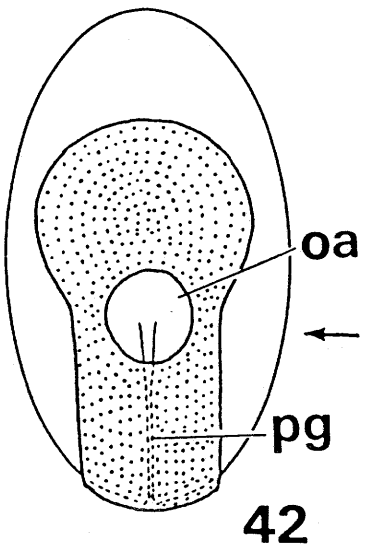
oa
pg
42

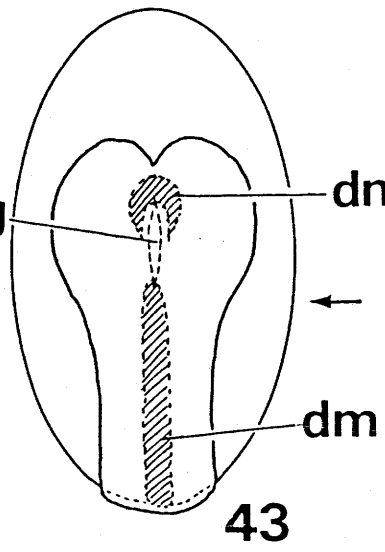
pg
dm
dm
43

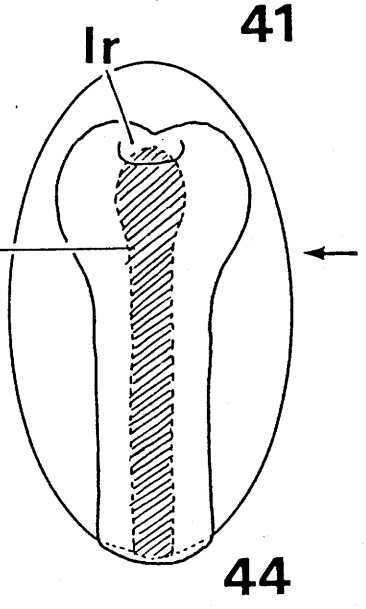
lr
44

EXPLANATION OF FIGURES

45. Ventral view of embryo of P. pryeri in Stage 4.

46. Ventral view of embryo of P. pryeri late in Stage 4.

47. Ventral view of embryo of P. pryeri early in Stage 5.

48. Dorsal view of embryo of P. pryeri early in Stage 5.

49. Ventral view of embryo of P. pryeri late in Stage 5.

50. Ventral view of embryo of P. pryeri early in Stage 6.

51. Ventral view of embryo of P. pryeri in Stage 6.

52. Lateral view of embryo of P. pryeri in Stage 6.

Scale = 500μm.

Arrows indicate the position of the caudal end of the embryos.

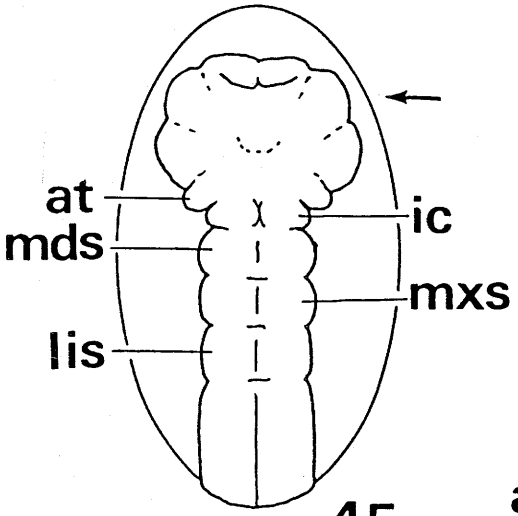

45

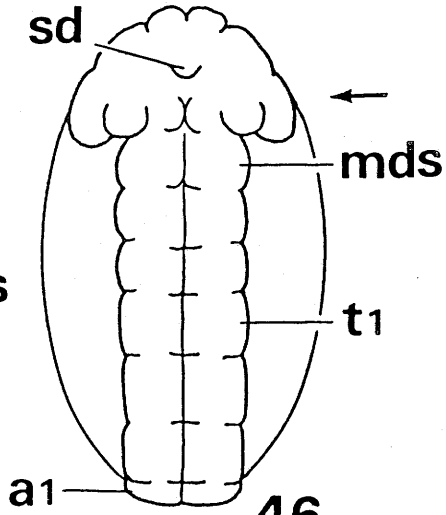

46

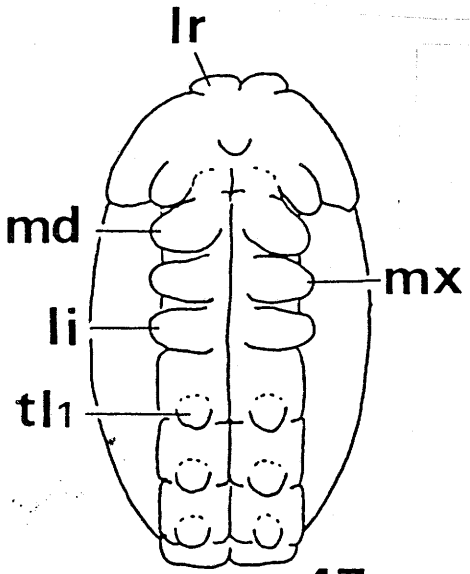

47

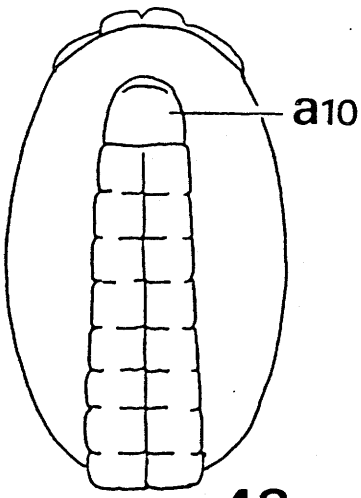

48

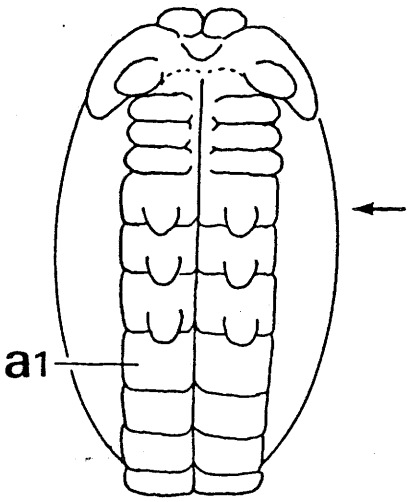

49

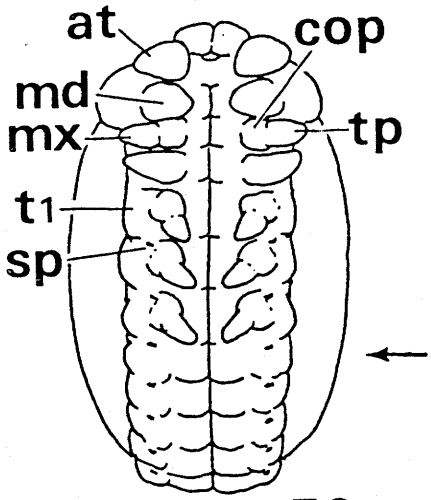

50

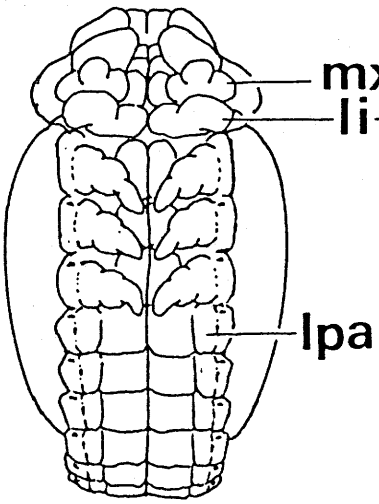

51

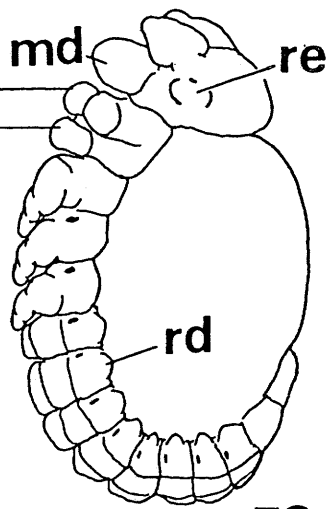

52

EXPLANATION OF FIGURES

53. Lateral view of embryo of P. pryeri in Stage 7.

54. Lateroventral view of third thoracic to second abdominal segments of embryo of P. pryeri in Stage 7.

55. Lateral view of embryo of P. pryeri early in Stage 8.

56. Ventral view of embryo of P. pryeri in Stage 8.

57. Ventral view of embryo of P. pryeri early in Stage 9.

58. Lateral view of embryo of P. pryeri late in Stage 9.

Scale = 500µm.

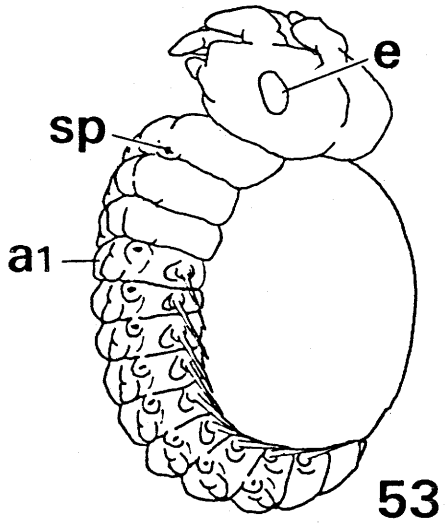

53

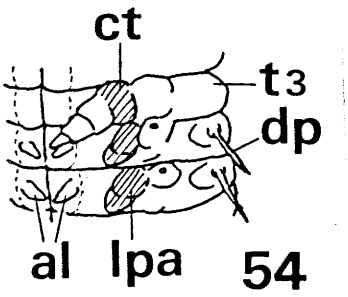

54

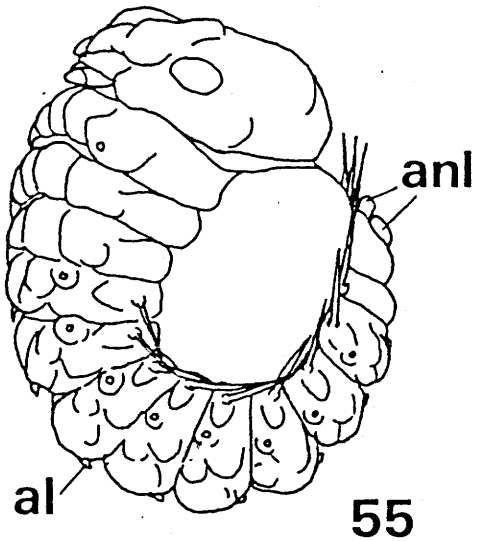

55

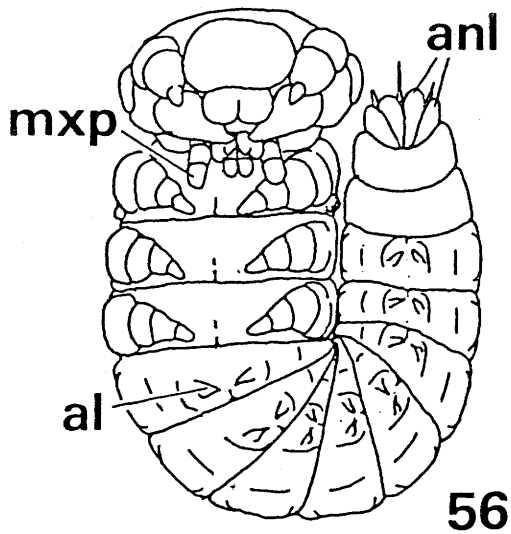

56

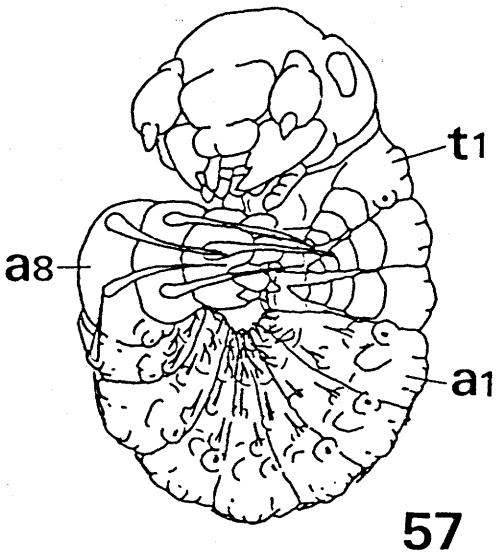

57

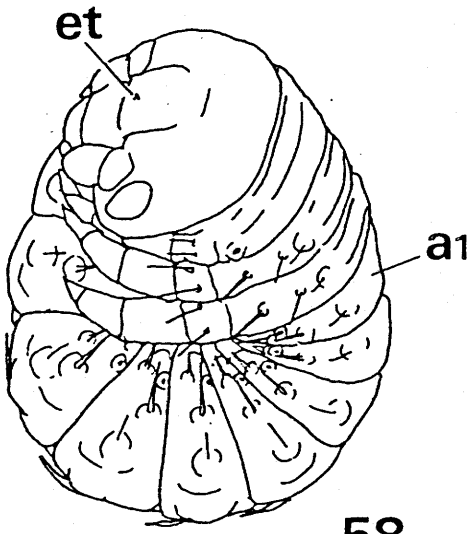

58

EXPLANATION OF FIGURES

59. Longitudinal section of egg of Pd. paradoxa early in Stage 2.

60. Longitudinal section of egg of Pd. paradoxa early in Stage 2.

61. Longitudinal section through posterior part of egg of Pd. paradoxa early in Stage 2.

62. Longitudinal section through posterior part of egg of Pd. paradoxa in Stage 2.

Scales = 100µm (Figs. 59, 60) and 50µm (Figs. 61, 62).

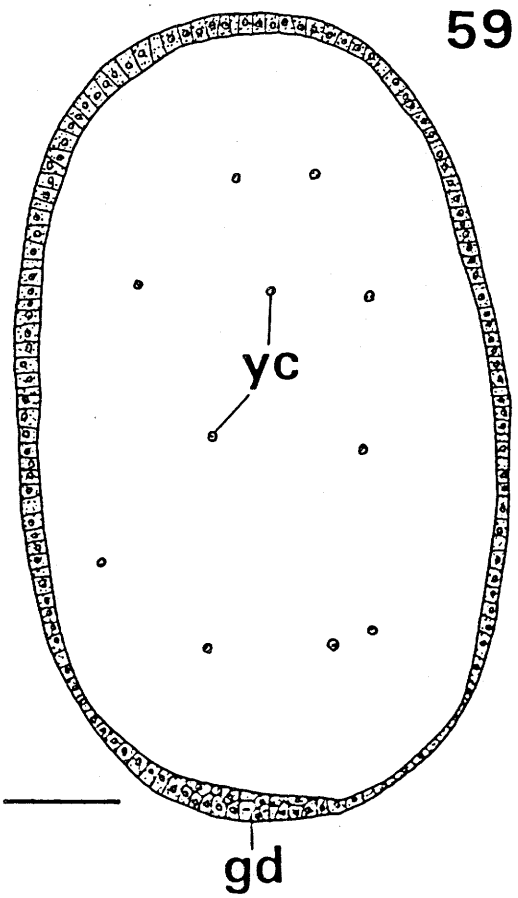
59
yc
gd

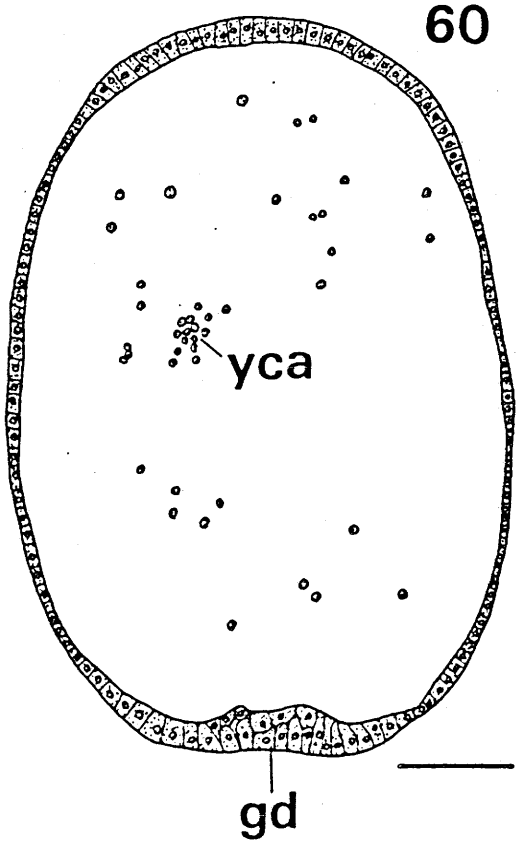
60
yca
gd

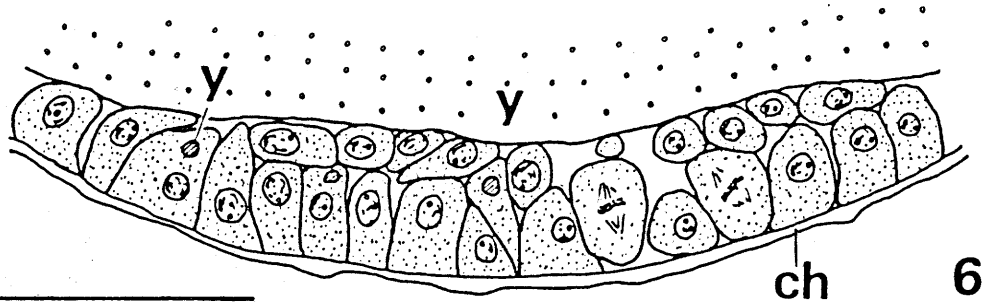
y
y
ch
61

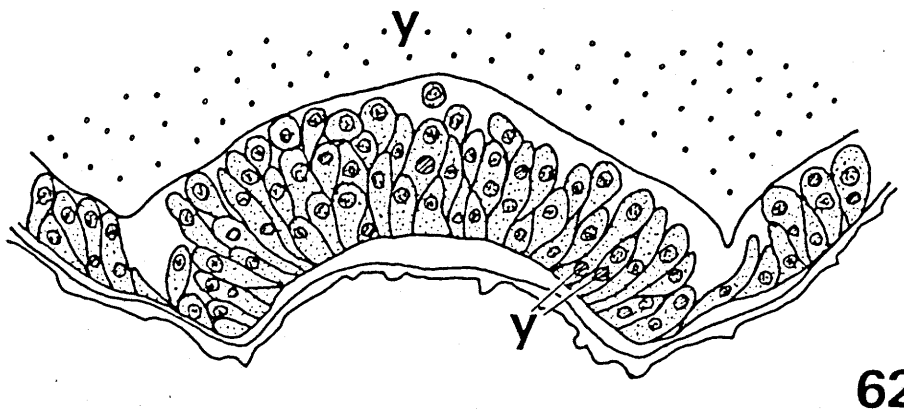
y
y
62

EXPLANATION OF FIGURES

63, 65, 66, 67. Diagrams showing consecutive stages of germ band formation of Pd. paradoxa during Stage 2 (Figs. 63, 65) and 3 (Figs. 66, 67).

64. Transverse section through germ rudiment of Pd. paradoxa late in Stage 2.

68. Lateral view of germ band of Pd. paradoxa early in Stage 4.

69. Lateral view of embryo of Pd. paradoxa late in Stage 4.

Scales = 100μm.

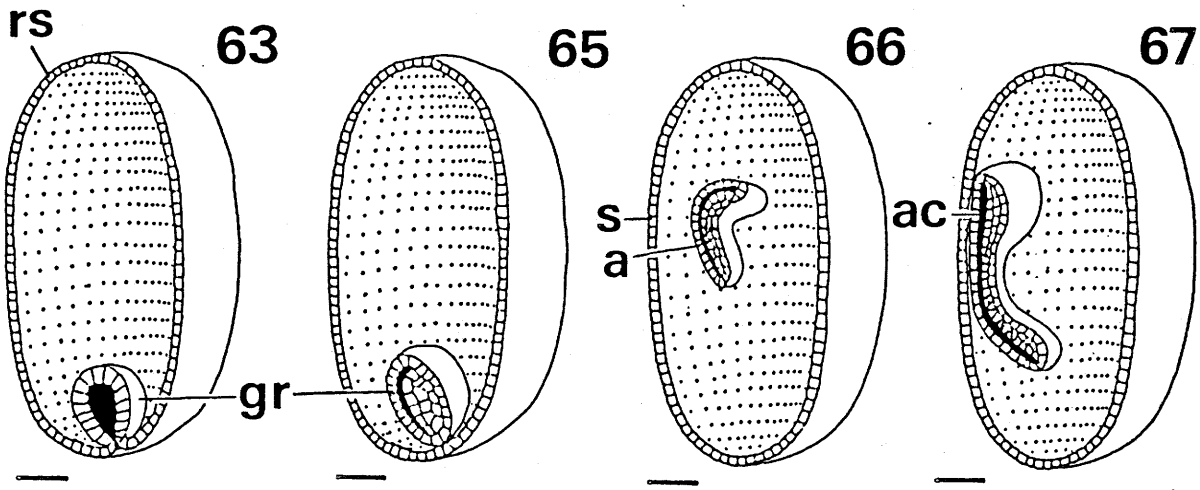
rs
63
gr
65
66
s
a
67
ac

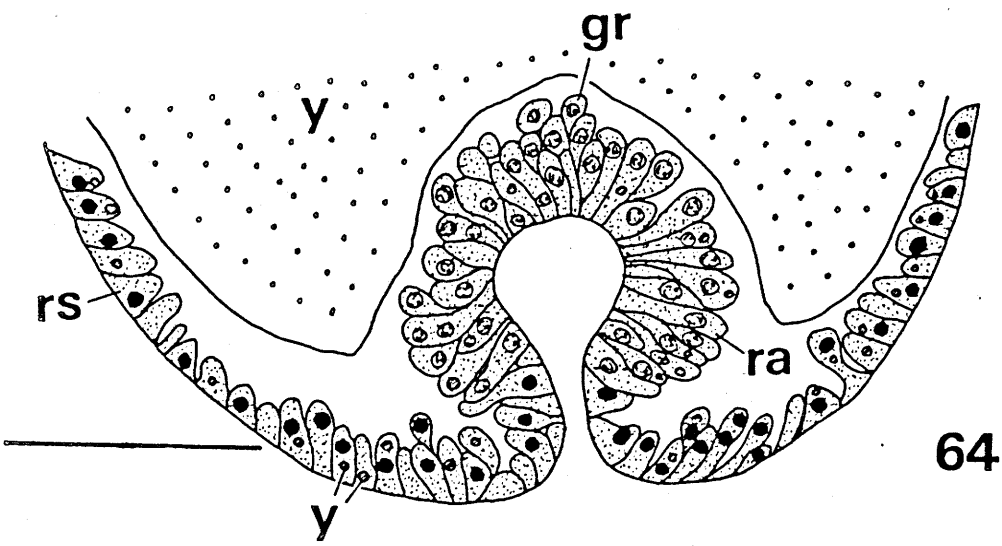
gr
y
rs
ra
y
64

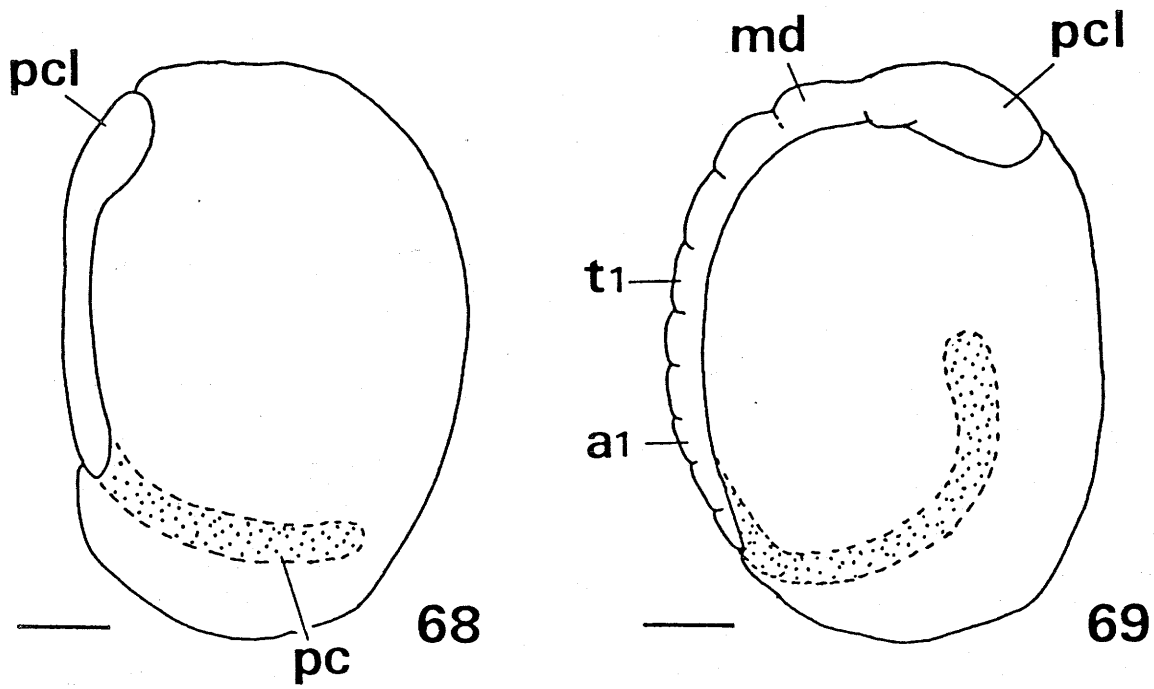
pcl
md
pcl
t1
a1
pc
68
69

EXPLANATION OF FIGURES

70. Frontal view of embryo of Pd. paradoxa late in Stage 4.

71. Lareral view of embryo of Pd. paradoxa early in Stage 5.

72. Ventral view of embryo of Pd. paradoxa early in Stage 5.

73. Lareral view of embryo of Pd. paradoxa late in Stage 5.

74. Lateral view of embryo of Pd. paradoxa early in Stage 6.

75. Ventral view of third thoracic to second abdominal segments of embryo of Pd. paradoxa early in Stage 6.

Scale = 100μm.

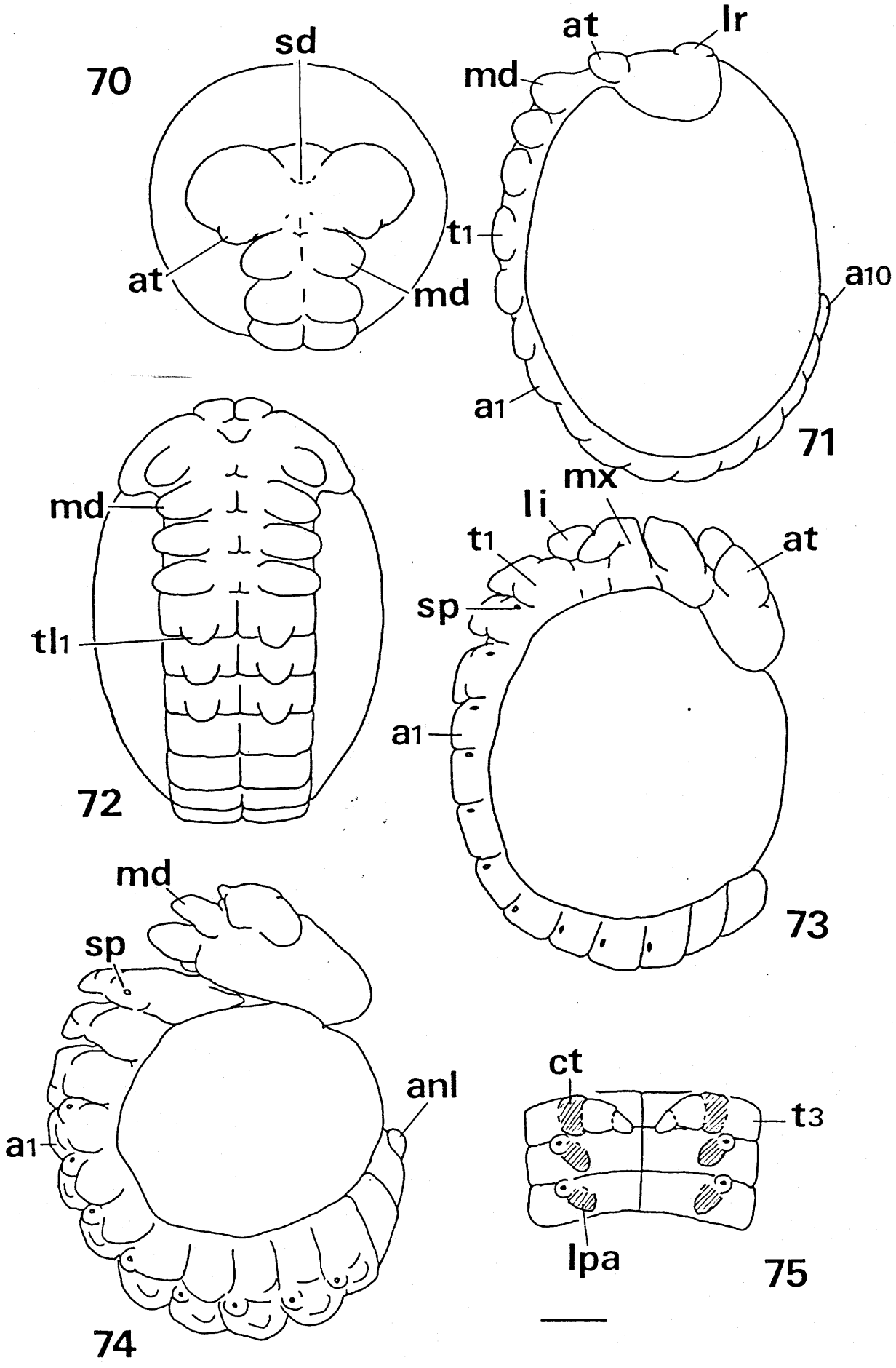
70
sd
at
md
71
at
lr
md
t1
a10
a1
72
md
tl1
73
mx
li
t1
at
sp
a1
74
md
sp
anl
a1
75
ct
t3
lpa

EXPLANATION OF FIGURES

76. Lateral view of embryo of Pd. paradoxa late in Stage 6.

77, 78, 79. Diagrams showing consecutive stages of revolution of embryo of Pd. paradoxa during Stage 7.

80. Ventral view of embryo of Pd. paradoxa in Stage 8.

Scales = 100µm (Figs. 76, 80).

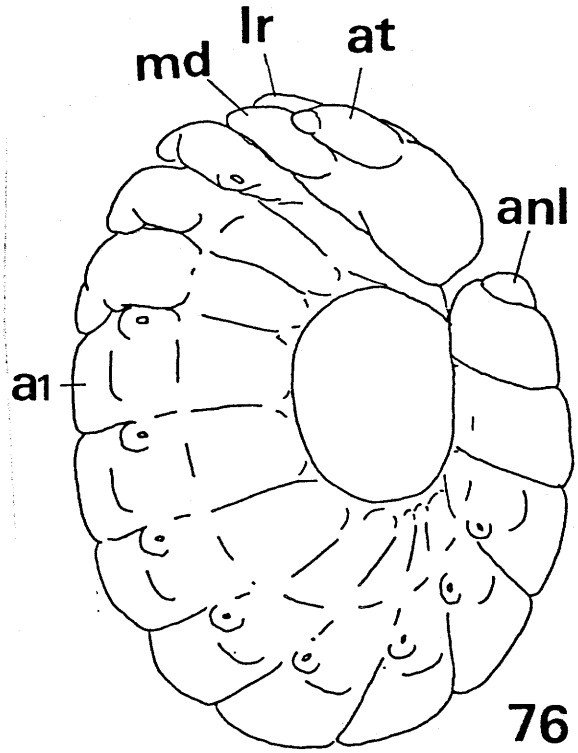

76

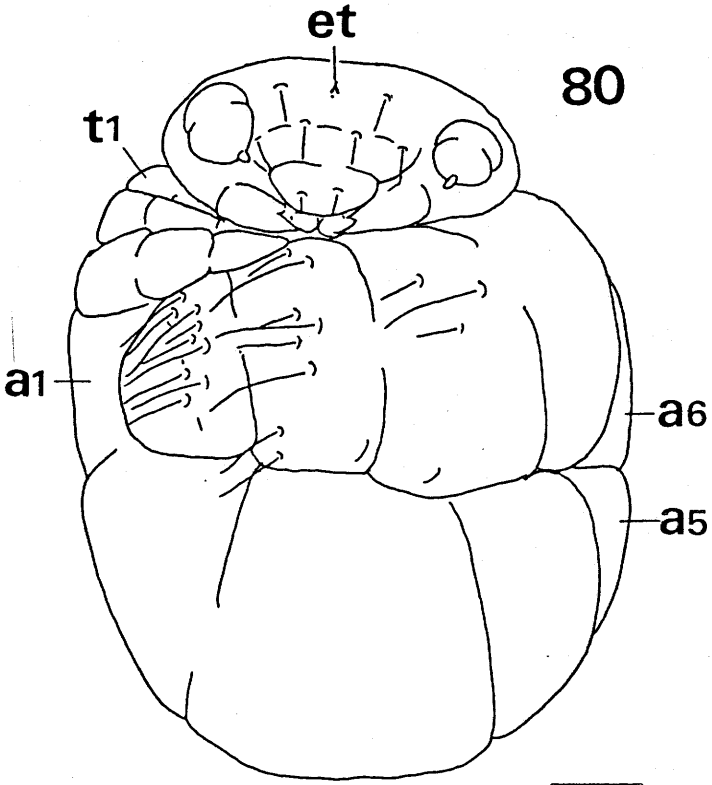

80

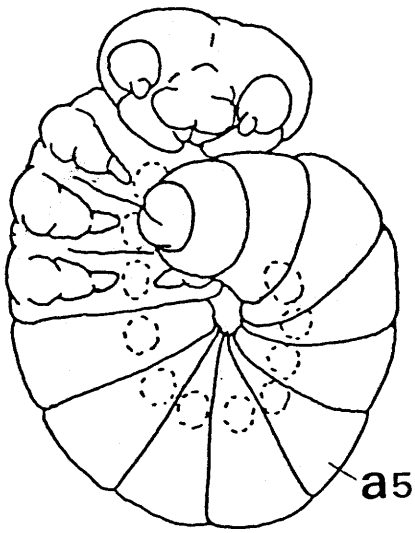

78

77

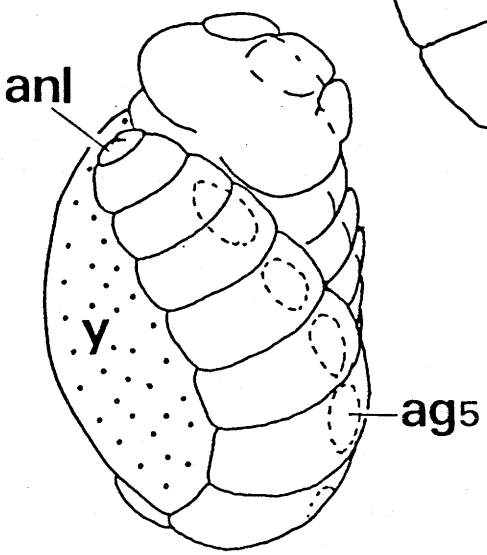

79

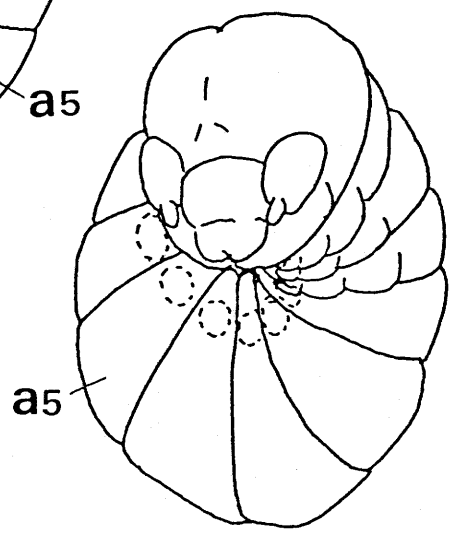

EXPLANATION OF FIGURES

81. Ventral view of germ disk of B. laevipes in Stage 2.

82. Ventral view of germ disk of B. laevipes early in Stage 3.

83. Ventral view of germ band of B. laevipes in Stage 3.

84. Ventral view of germ band of B. laevipes late in Stage 3.

85. Ventral view of germ band of B. laevipes early in Stage 4.

86. Ventral view of embryo of B. laevipes in Stage 4.

87. Ventral view of embryo of B. laevipes late in Stage 4.

88. Frontal view of embryo of B. laevipes late in Stage 4.

89. Lateral view of embryo of B. laevipes late in Stage 4.

Scale = 500μm.

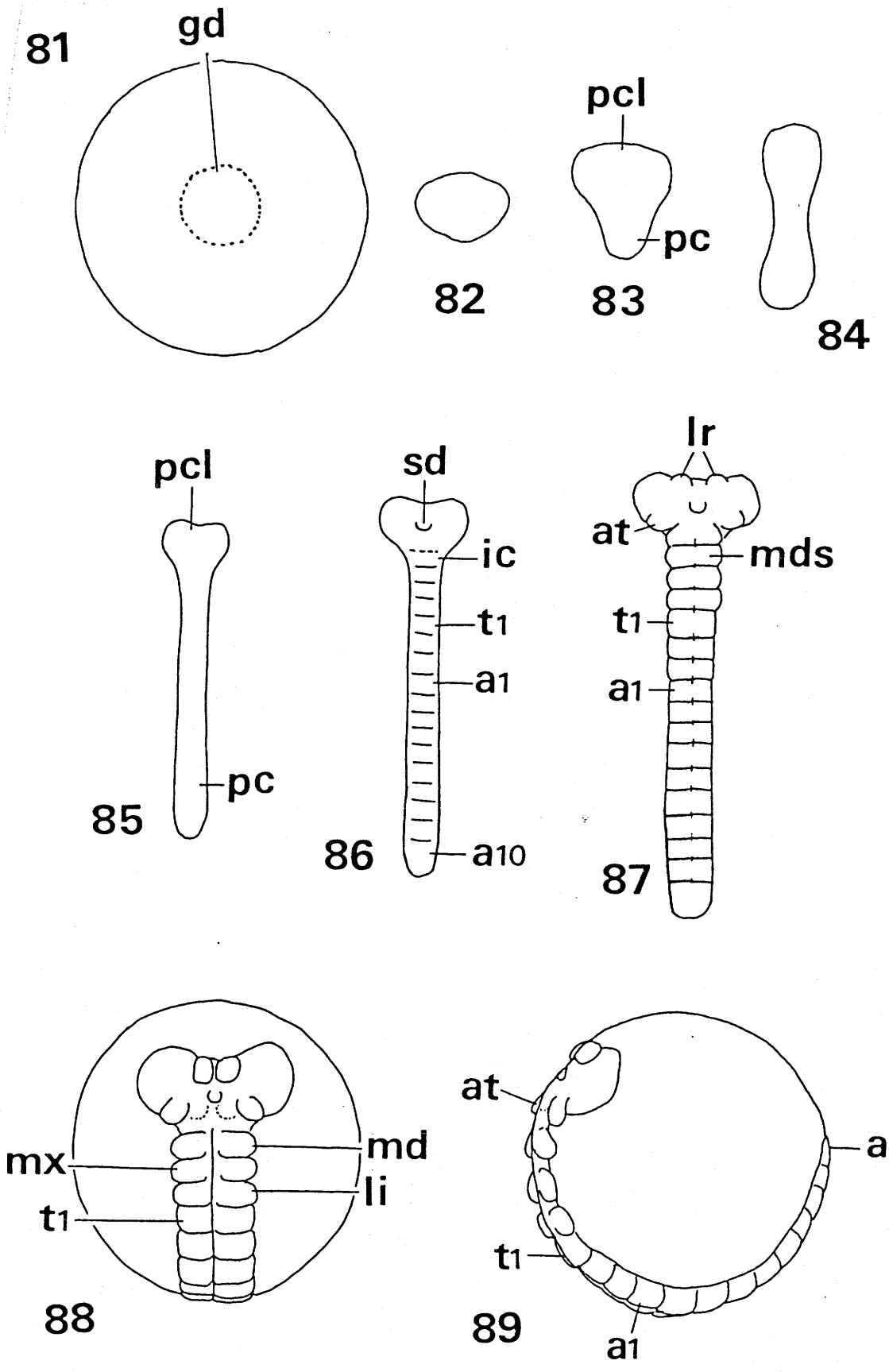
81
gd
82
pcl
pc
83
84
pcl
pc
85
sd
ic
t1
a1
a10
86
lr
at
mds
t1
a1
87
mx
md
li
t1
88
at
a10
t1
a1
89

EXPLANATION OF FIGURES

90. Frontal view of embryo of B. laevipes early in Stage 5.

91. Frontal view of embryo of B. laevipes in Stage 5.

92. Frontal view of embryo of B. laevipes in Stage 6.

93. Frontal view of cephalognathal region of embryo of B. laevipes early in Stage 7.

94. Frontal view of cephalognathal region, and third thoracic and first abdominal segments of embryo of B. laevipes in Stage 7.

95. Frontal view of embryo of B. laevipes in Stage 7.

96. Frontal view of embryo of B. laevipes late in Stage 7.

Scale = 500µm.

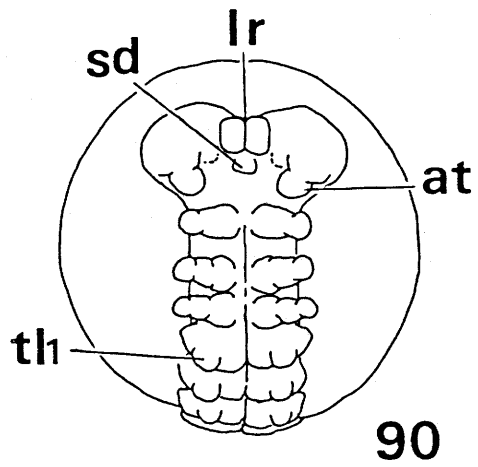

90

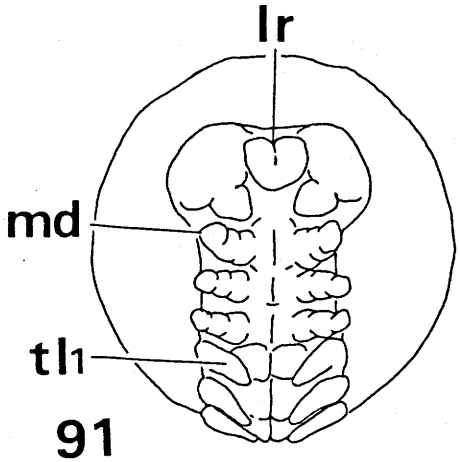

91

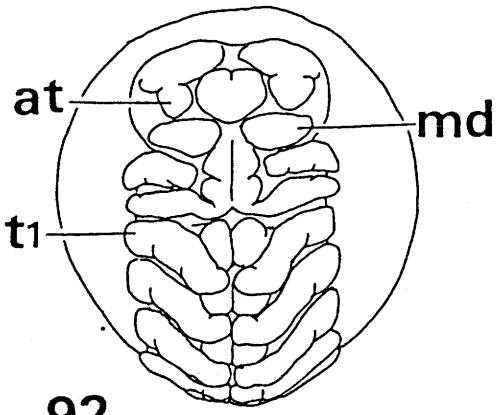

92

93

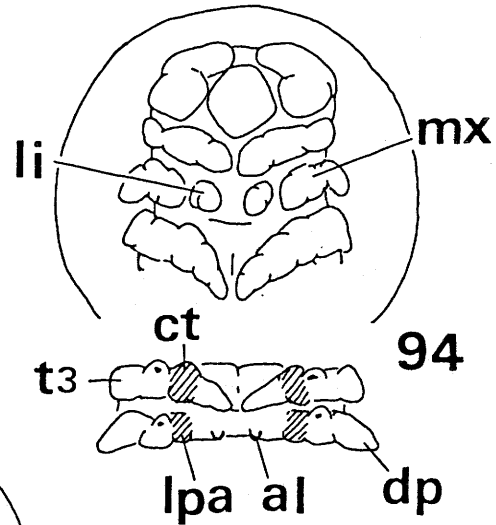

94

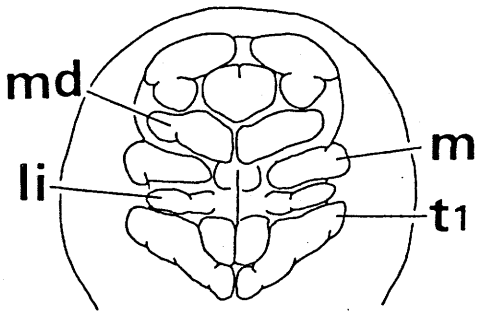

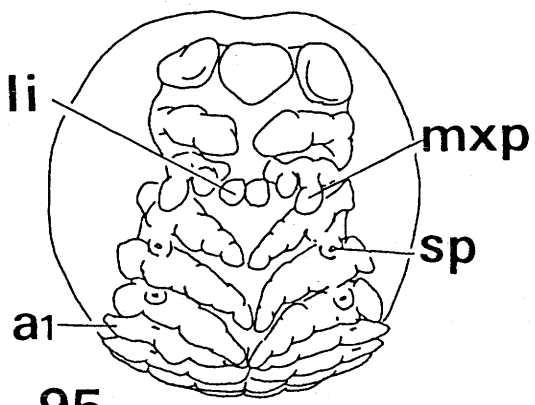

95

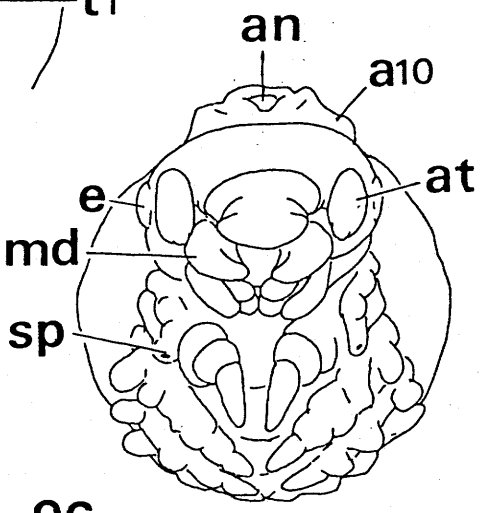

96

EXPLANATION OF FIGURES

97. Lateral view of embryo of B. laevipes early in Stage 8.

98. Lateral view of embryo of B. laevipes in Stage 8.

99. Lateral view of embryo of B. laevipes in Stage 8.

100. Lateral view of embryo of B. laevipes late in Stage 8.

101. Full grown embryo of B. laevipes in Stage 9.

Scale = 500µm.

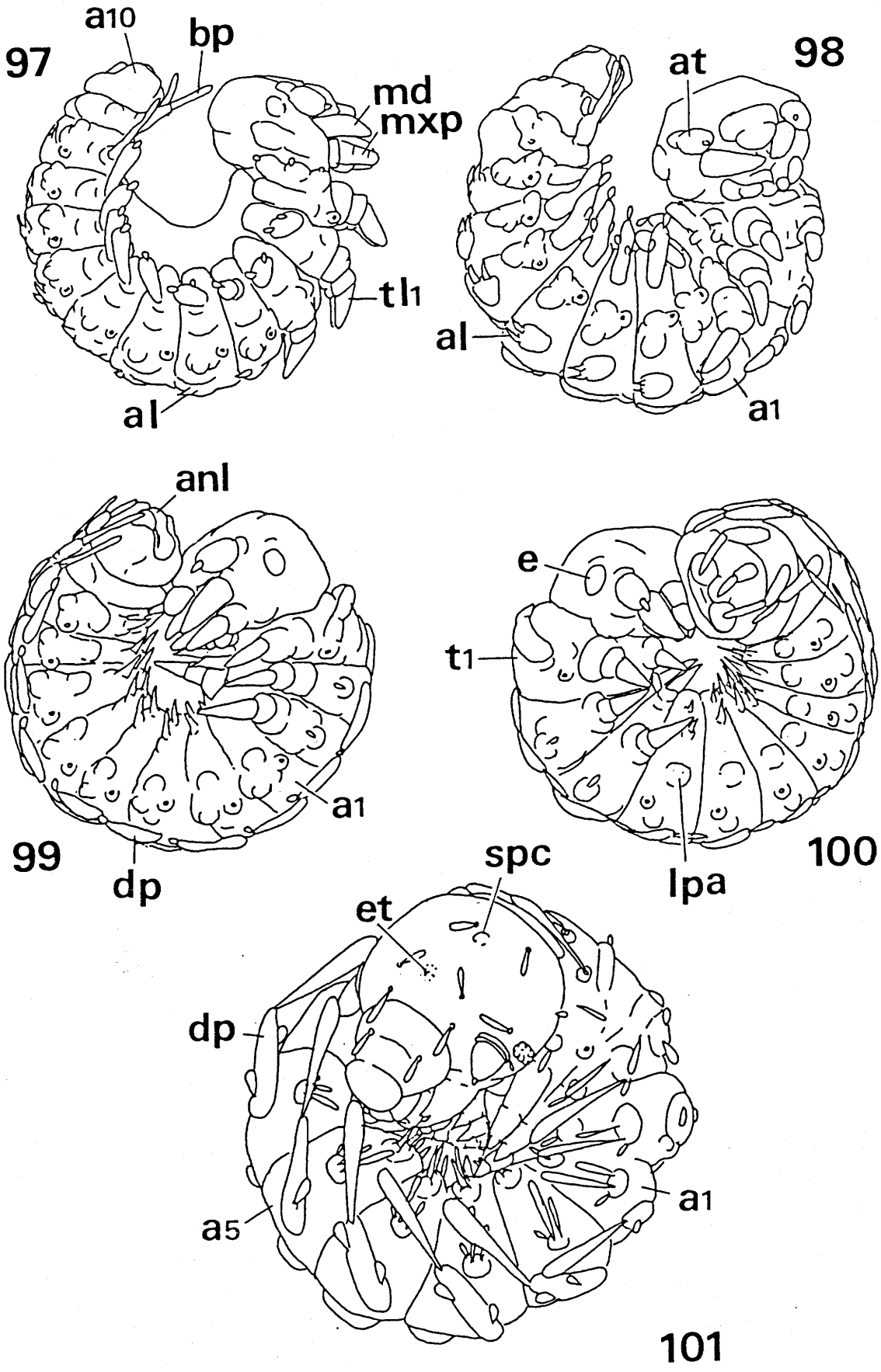
97
a10
bp
md
mxp
tl1
al
98
at
al
a1
anl
a1
99
dp
e
t1
lpa
100
spc
et
dp
a1
a5
101

EXPLANATION OF FIGURES

102. Sagittal section of small process in the cranium of first instar larva of B. laevipes.

103. Ventral view of egg of Bo. westwoodi in Stage 2.

104. Part of transverse section through embryonic area of egg of Bo. westwoodi in Stage 2.

105. Ventral view of germ band of Bo. westwoodi early in Stage 3.

106. Transverse section through germ band of Bo. westwoodi early in Stage 3.

107. Ventral view of germ band of Bo. westwoodi late in Stage 3.

Scales = 50μm (Figs. 102, 104, 106) and 100μm (Figs. 103, 105, 107).

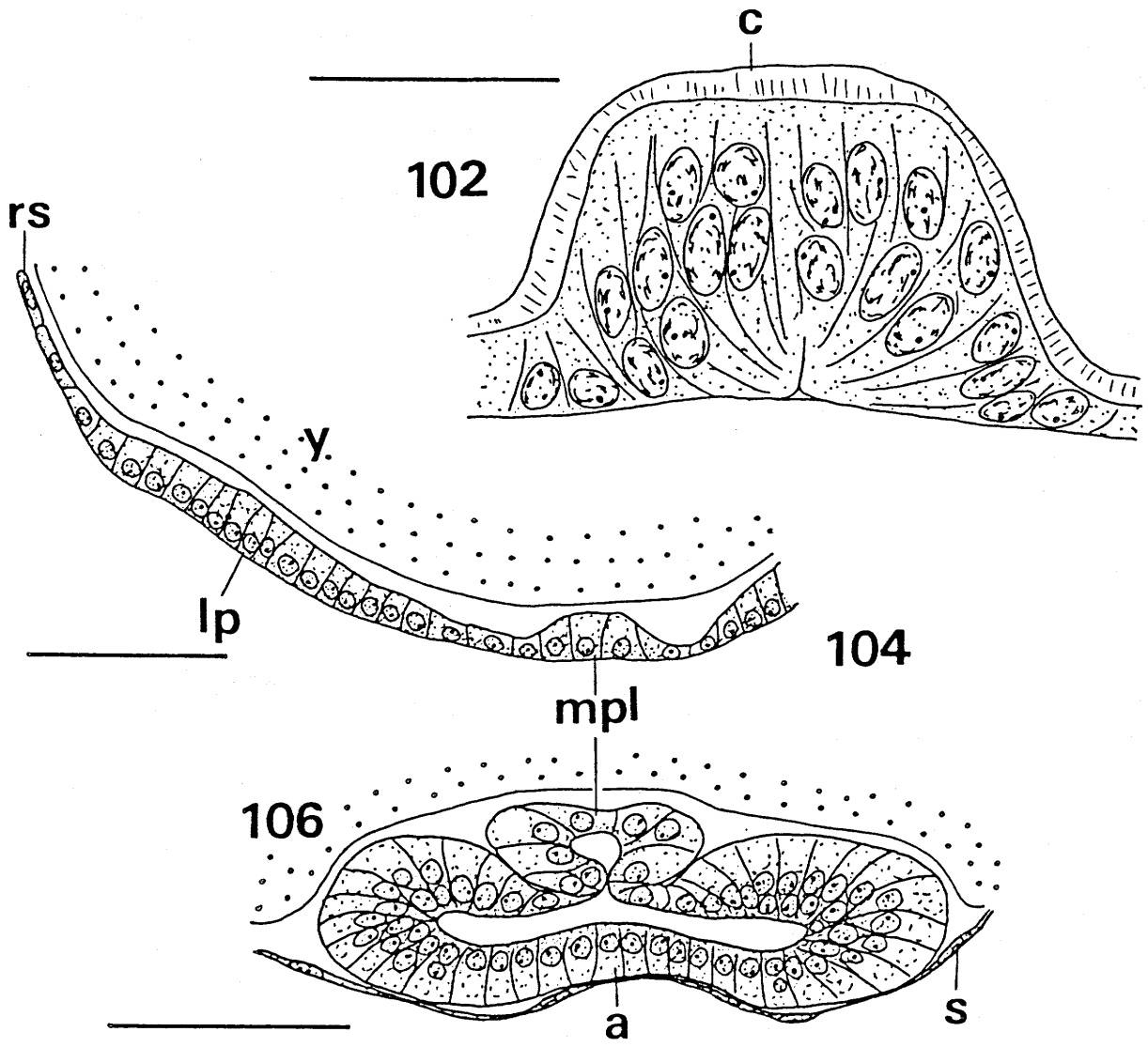
c
102
rs
y
lp
104
mpl
106
a
s

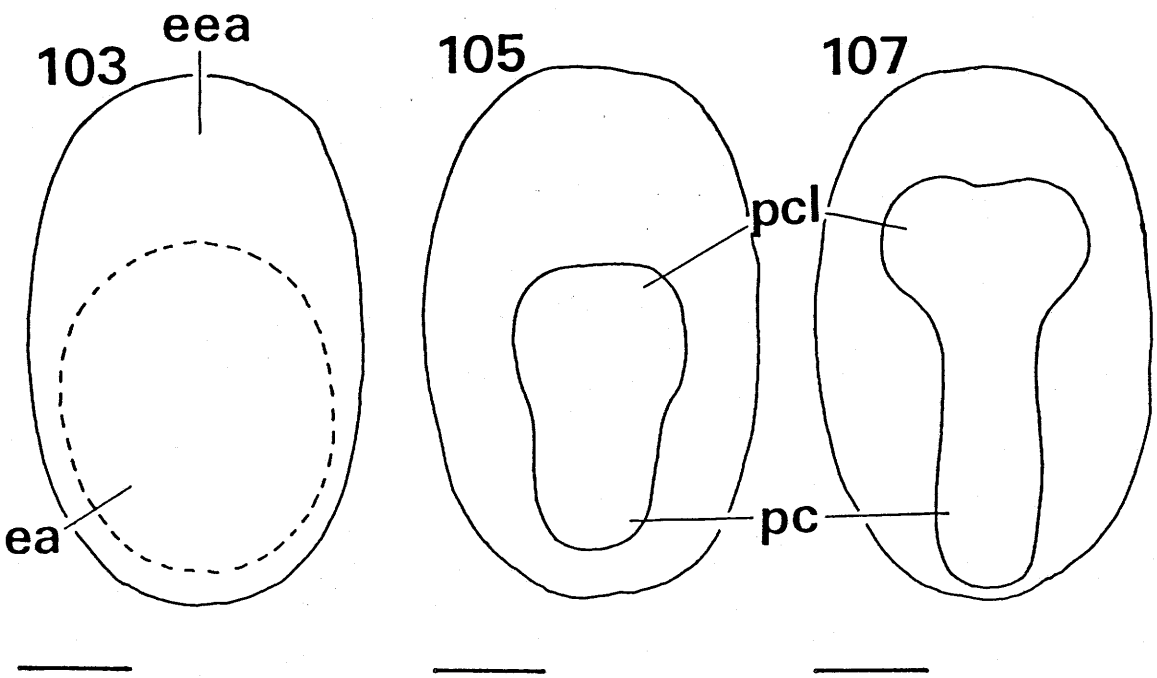
103
eea
ea
105
pcl
pc
107

EXPLANATION OF FIGURES

108. Ventral view of embryo of Bo. westwoodi in Stage 4.

109. Ventral view of embryo of Bo. westwoodi early in Stage 5.

110. Posterior part of abdomen of embryo of Bo. westwoodi early in Stage 5.

111. Lateral view of embryo of Bo. westwoodi late in Stage 5.

112. Ventral view of embryo of Bo. westwoodi late in Stage 5.

Scale = 100μm.

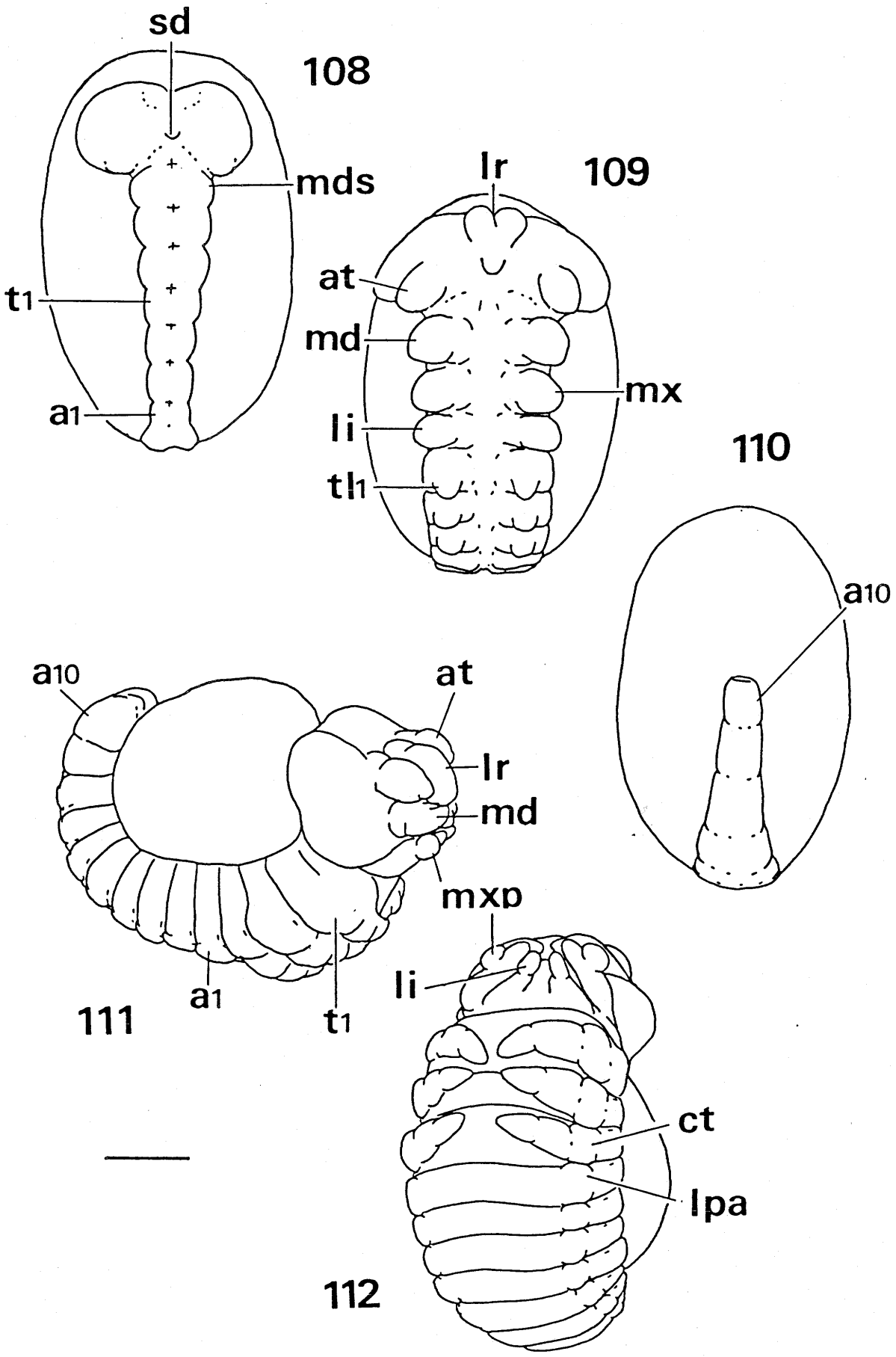
sd
108
mds
t1
a1
lr
109
at
md
mx
li
tl1
110
a10
a10
at
lr
md
mxp
li
a1
t1
111
ct
lpa
112

EXPLANATION OF FIGURES

113. Change of egg size of P. pryeri, Pd. paradoxa and B. laevipes. R = time of revolution of embryo.

114. Outlines of newly laid (broken line) and full grown (solid line) eggs of P. pryeri (A), Pd. paradoxa (B) and B. laevipes (C).

Scale = 500μm.

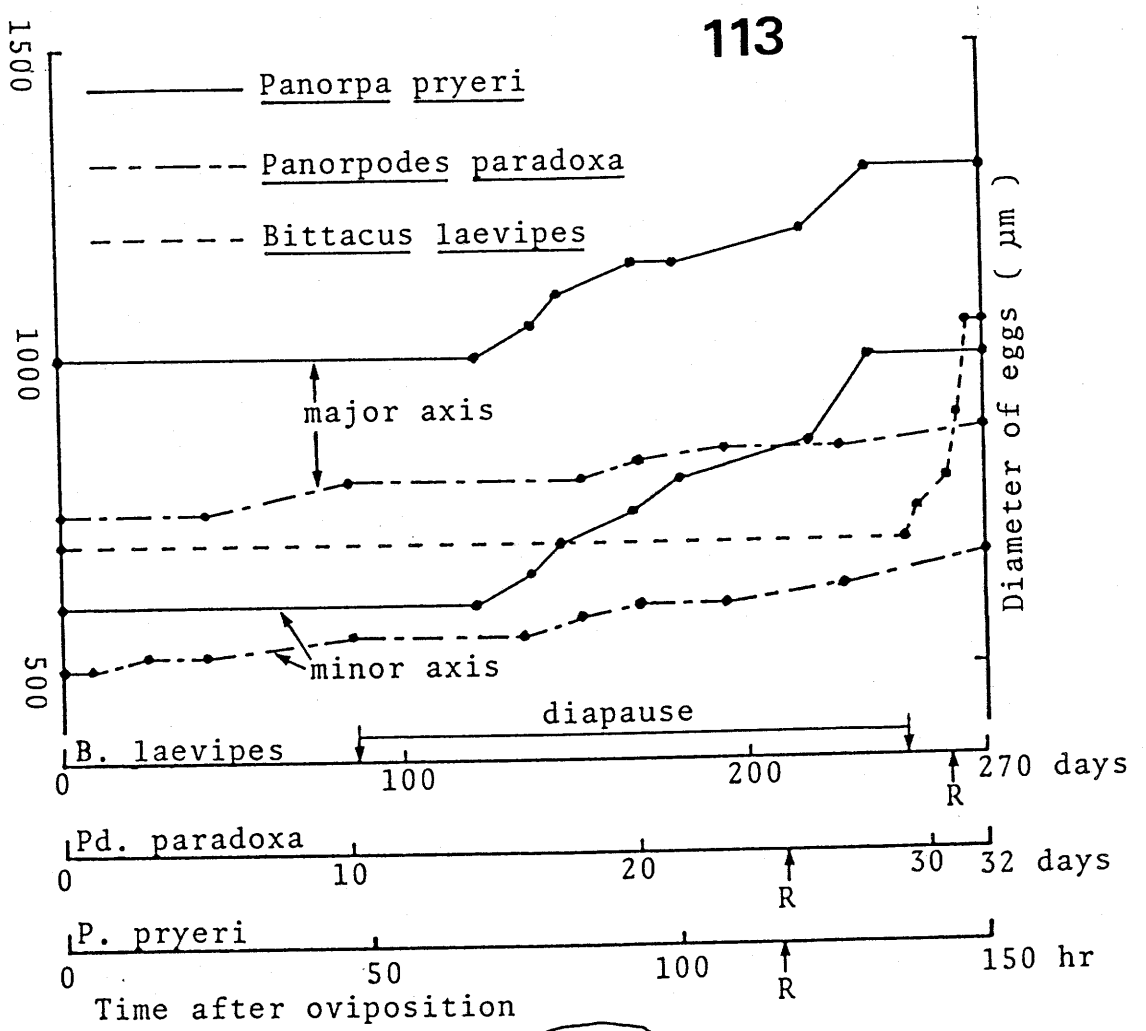
113
1500
1000
500
Panorpa pryeri
Panorpodes paradoxa
Bittacus laevipes
major axis
minor axis
Diameter of eggs (µm)
diapause
B. laevipes
0
100
200
R
270 days
Pd. paradoxa
0
10
20
R
30
32 days
P. pryeri
0
50
100
R
150 hr
Time after oviposition

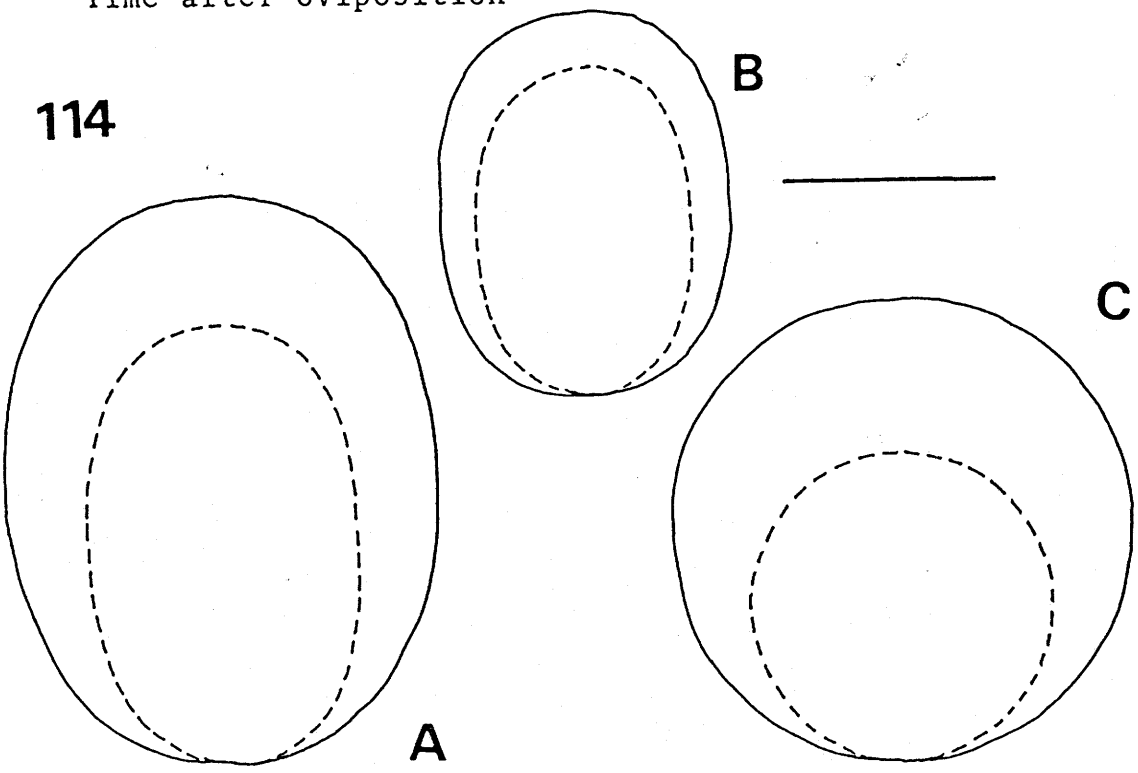
114
B
C
A

EXPLANATION OF FIGURES

115. Transverse section through middle part of egg of P. pryeri in Stage 2.

116. Longitudinal section of posterior part of egg of P. pryeri late in Stage 2.

117. Diagrams of transverse sections through middle part of eggs of P. pryeri, showing the germ band and embryonic envelope formation. The parenthesized number indicates the number of cells. A, Stage 2; B, Stage 3.

Scales = 100μm.

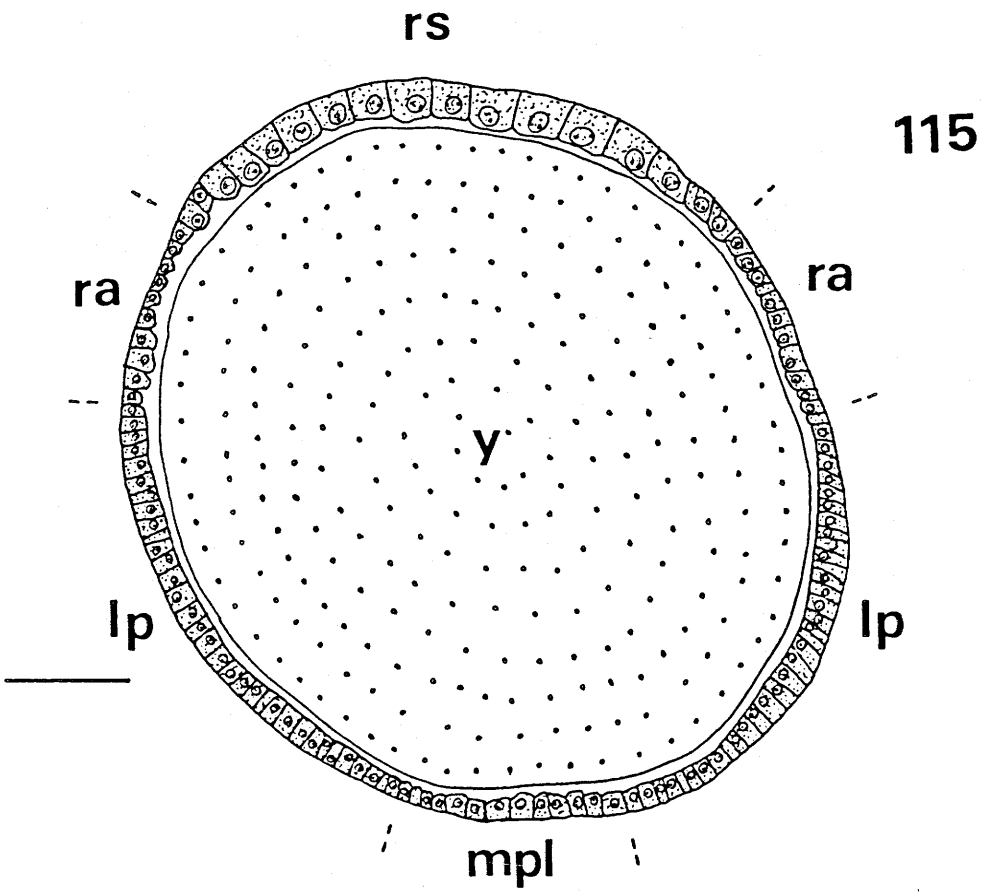
rs
115
ra
ra
y
lp
lp
mpl

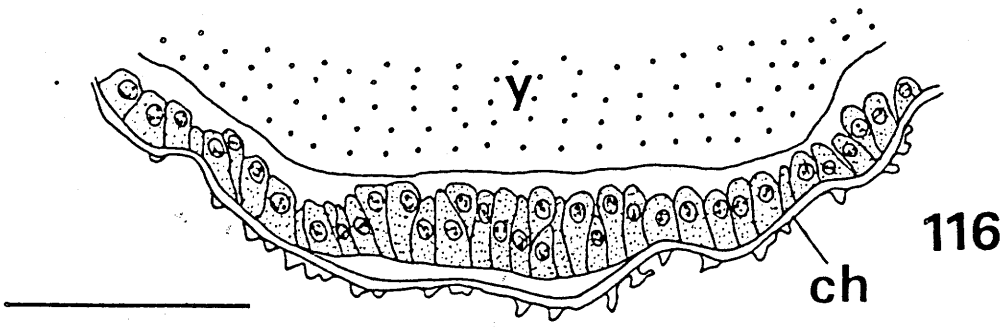
y
116
ch

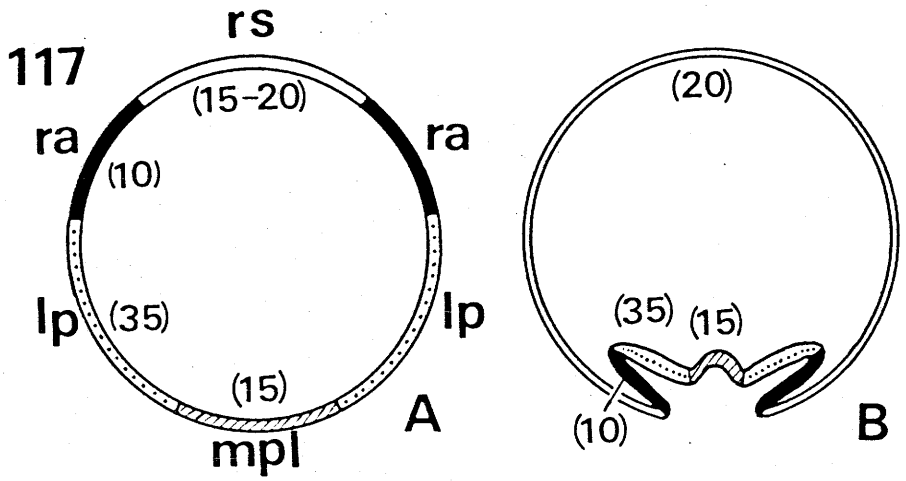
117
rs
(15–20)
ra
ra
(10)
lp
(35)
lp
(15)
A
mpl
(20)
(35)
(15)
(10)
B

EXPLANATION OF FIGURES

118. Part of transverse section through preoral region of germ band of P. pryeri early in Stage 3.

119. Part of transverse section through preoral region of germ band of P. pryeri in Stage 3.

120. Transverse section through abdominal region of germ band of P. pryeri in Stage 3.

121. Part of transverse section through preoral region of germ band of P. pryeri late in Stage 3.

122. Transverse section through germ rudiment of Pd. paradoxa late in Stage 2.

Scales = 50μm.

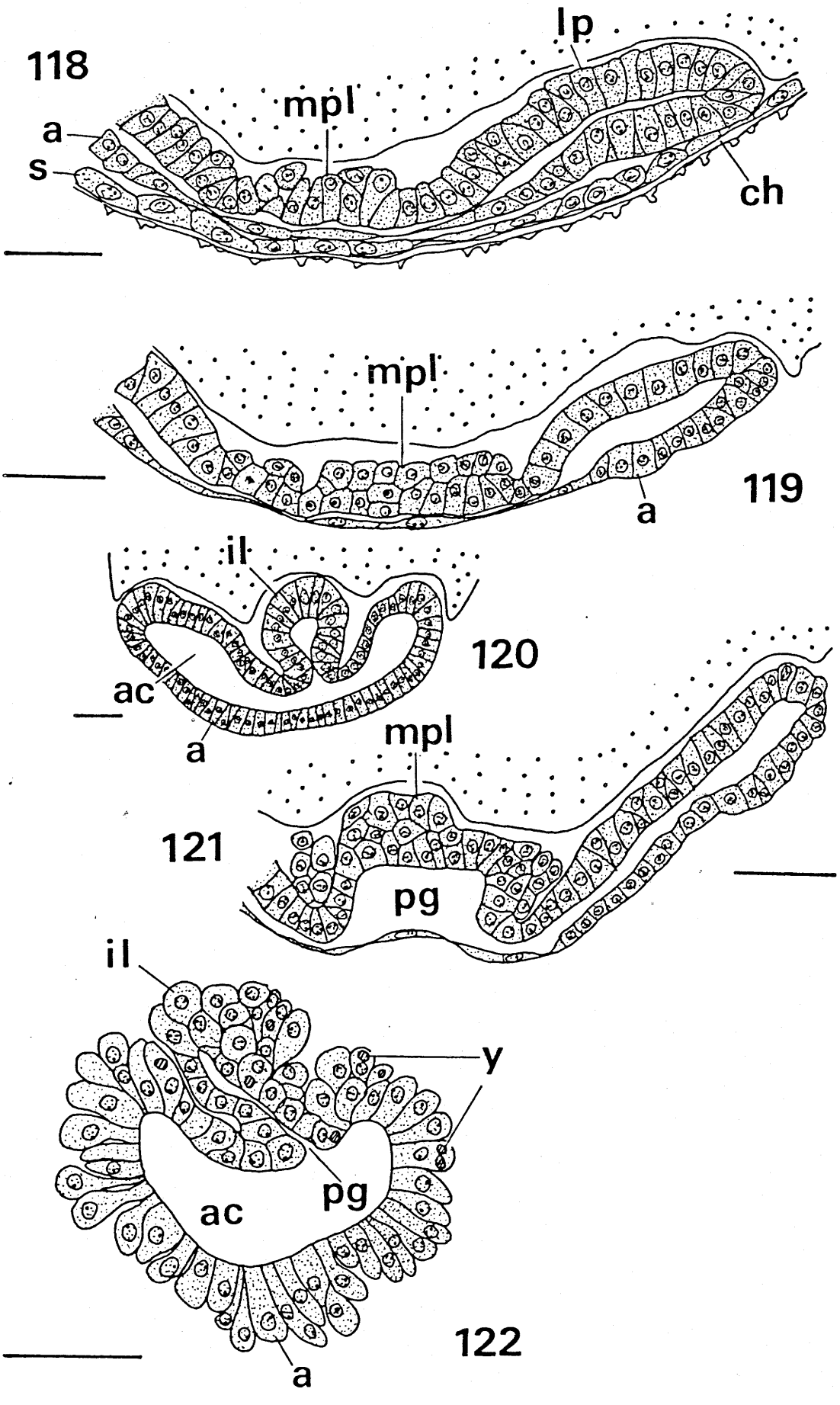
118
lp
mpl
a
s
ch
mpl
a
119
il
120
ac
a
mpl
121
pg
il
y
pg
ac
a
122

EXPLANATION OF FIGURES

123. Serosal cells of Pd. paradoxa late in Stage 3.

124. Transverse section through protocephalon of germ band of Pd. paradoxa late in Stage 3.

125. Transverse section through middle part of germ band of B. laevipes early in Stage 3.

126. Sagittal section of germ band of B. laevipes in Stage 3.

127. Transverse section through anterior part of germ band of Bo. westwoodi late in Stage 3.

Scales = 50μm.

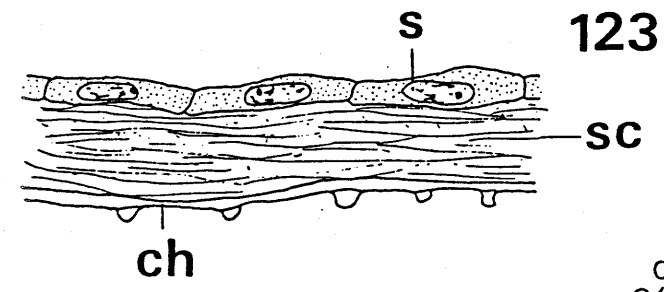

123

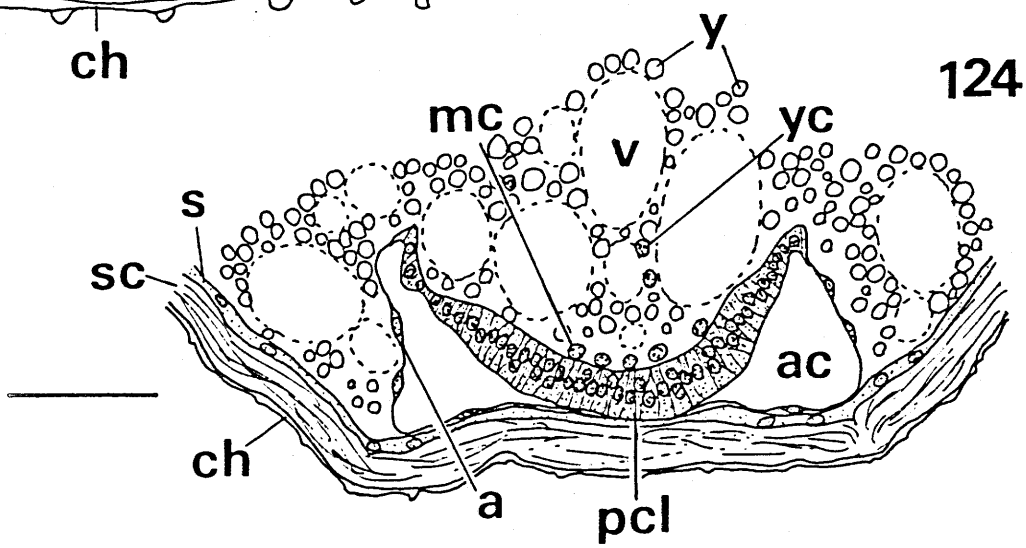

124

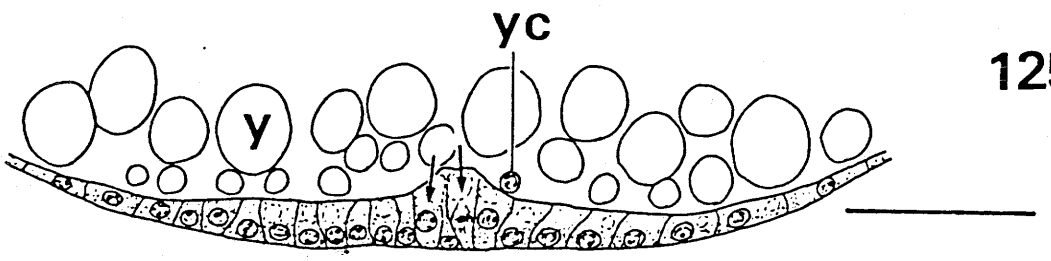

125

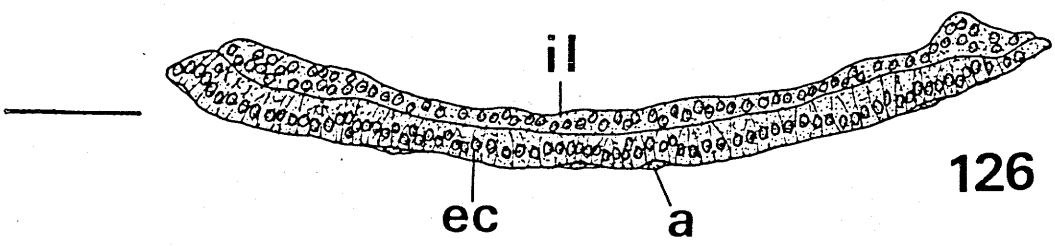

126

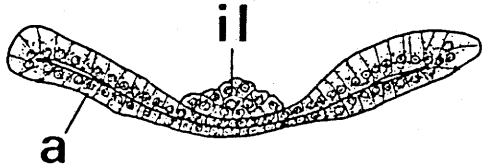

127

EXPLANATION OF FIGURES

128. Diagram showing the position of ectodermal invaginations of embryo. Dotted circles indicate transverse sections of bases of gnathal appendages.

129. Parasagittal section through cephalognathal region of embryo of P. pryeri late in Stage 5.

130. Slightly oblique parasagittal section through cephalognathal region of embryo of P. pryeri in Stage 6.

131. Parasagittal section through cephalognathal region of embryo of P. pryeri in Stage 6.

Scale = 100μm.

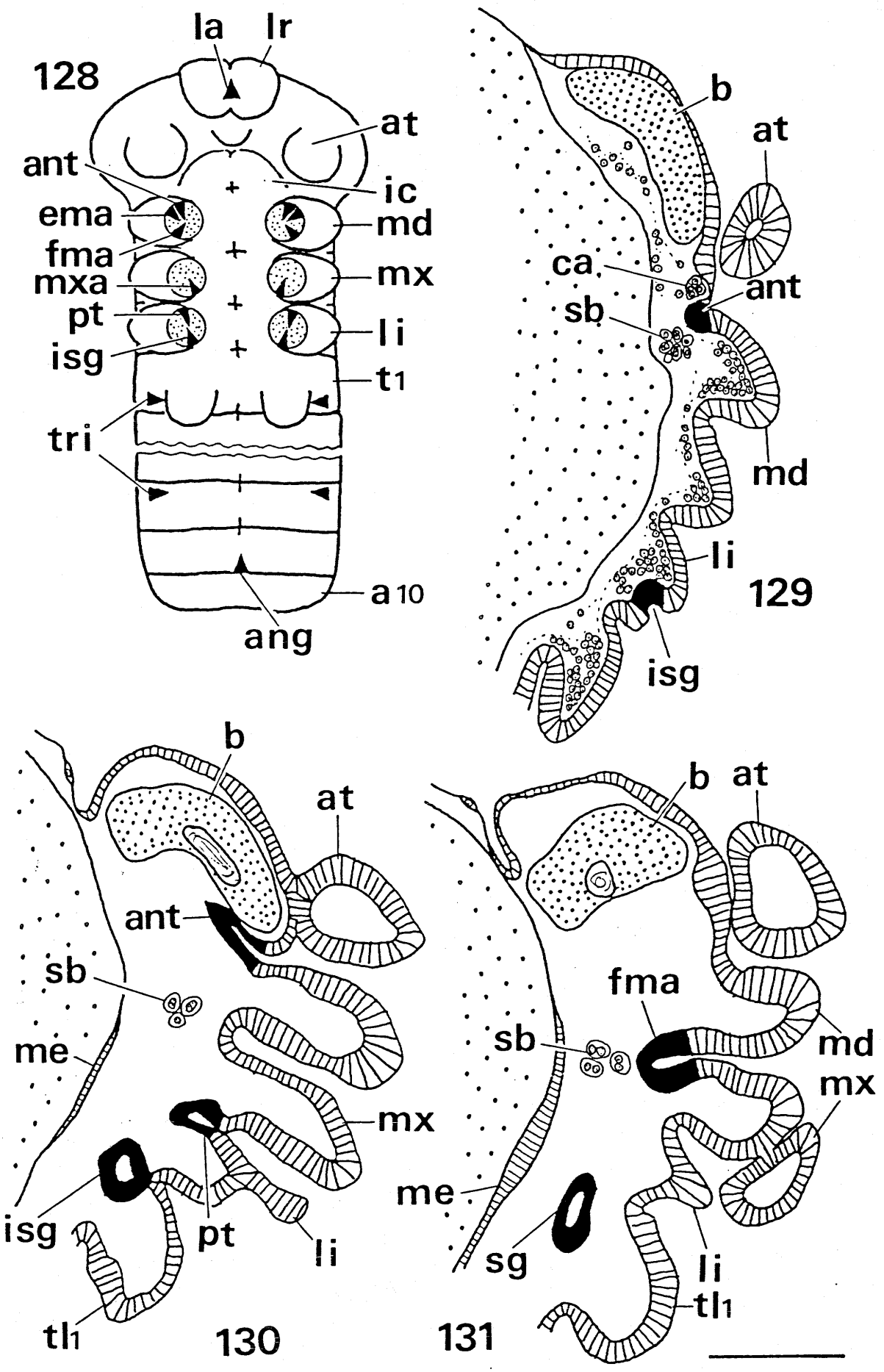
128
la
lr
at
ant
ic
ema
md
fma
mx
mxa
pt
li
isg
t1
tri
a10
ang
129
b
at
ca
ant
sb
md
li
isg
130
b
at
ant
sb
me
mx
isg
pt
li
tl1
131
b
at
fma
sb
md
mx
me
sg
li
tl1

EXPLANATION OF FIGURES

132. Transverse section through head of embryo of P. pryeri in Stage 7.

133. Sagittal section through head of embryo of P. pryeri in Stage 7.

134. Diagram showing endoskeletons of head of first instar larva of P. pryeri.

135. Part of longitudinal section of tentorium of first instar larva of P. pryeri.

136. Part of parasagittal section through head of first instar larva of P. pryeri, showing the proximal part of extensor mandibular apodeme.

137. Sagittal section through anal gland of first instar larva of P. pryeri.

Scales = 50μm (Figs. 132, 133) and 10μm (Figs. 135-137).

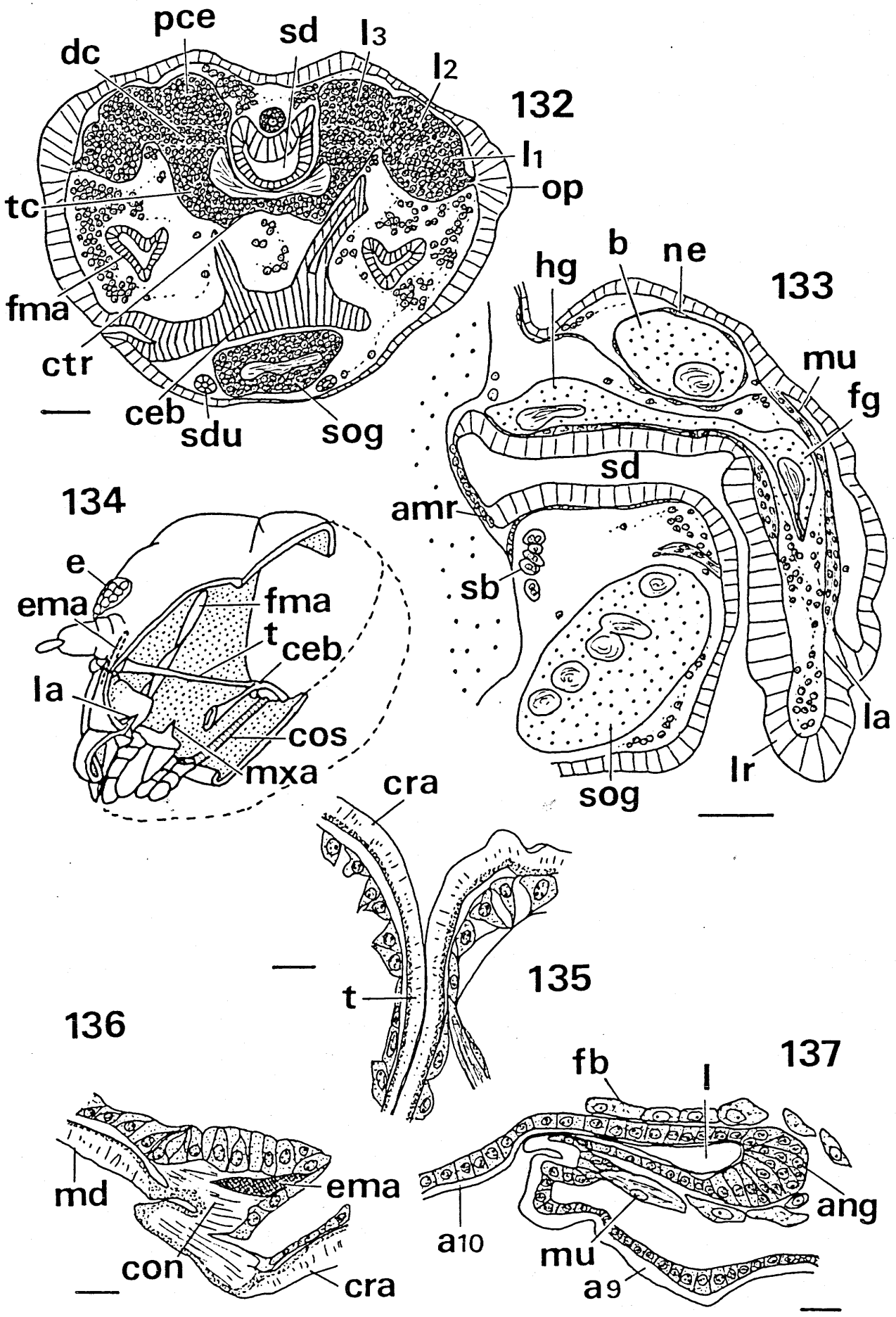
pce
sd
dc
l_3
l_2
132
l_1
op
tc
fma
ctr
ceb
sdu
sog
b
ne
hg
133
mu
fg
sd
amr
sb
la
lr
sog
134
e
ema
fma
t
ceb
la
cos
mxa
cra
t
135
136
fb
l
137
md
ema
ang
con
cra
a_{10}
mu
a_9

EXPLANATION OF FIGURES

138. Part of parasagittal section through cephalognathal region of embryo of B. laevipes in Stage 7.

139. Part of horizontal section through head of embryo of B. laevipes late in Stage 7.

140. Part of horizontal section through posterior region of stomodaeum of embryo of B. laevipes in Stage 8.

141. Part of transverse section through intersegmental region between the labial and first thoracic segments of embryo of B. laevipes late in Stage 7.

142. Anterior part of harizontal section through the first thoracic ganglion of first instar larva of B. laevipes.

Scales = 50μm.

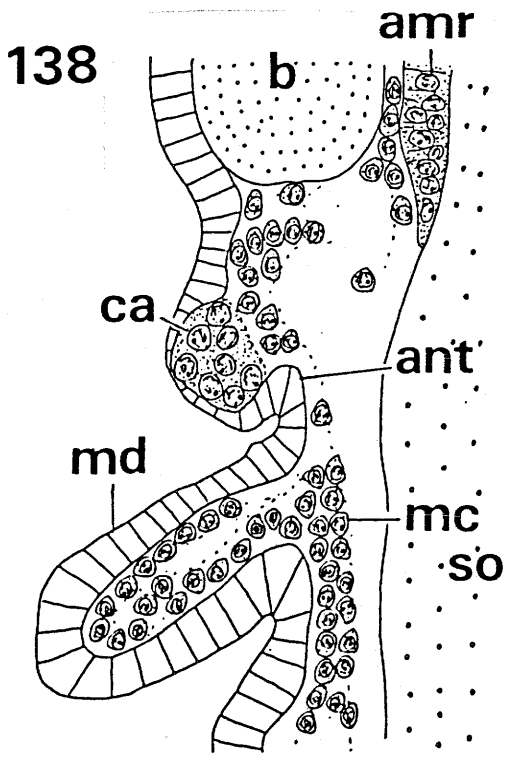
138
amr
b
ca
ant
md
mc

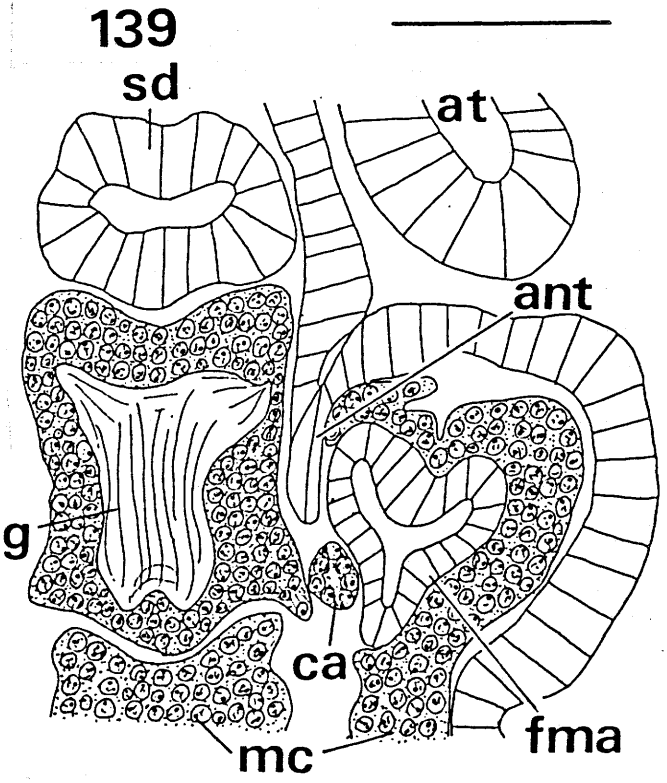
139
sd
at
ant
sog
ca
fma
mc

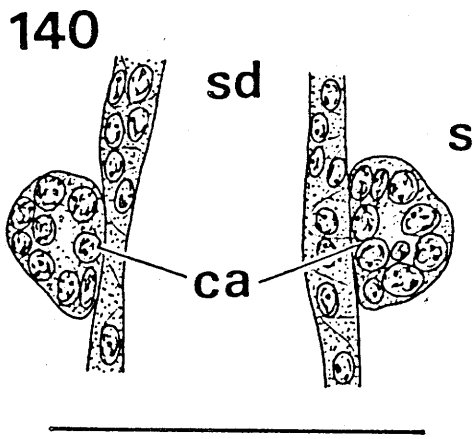
140
sd
ca

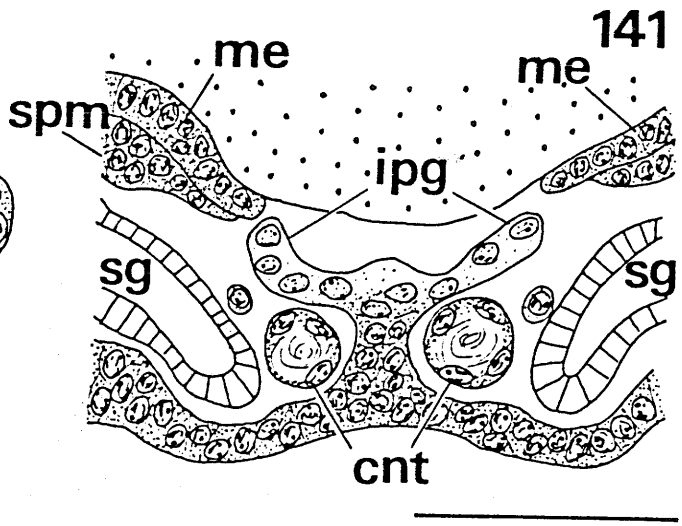
141
me
me
spm
ipg
sg
sg
cnt

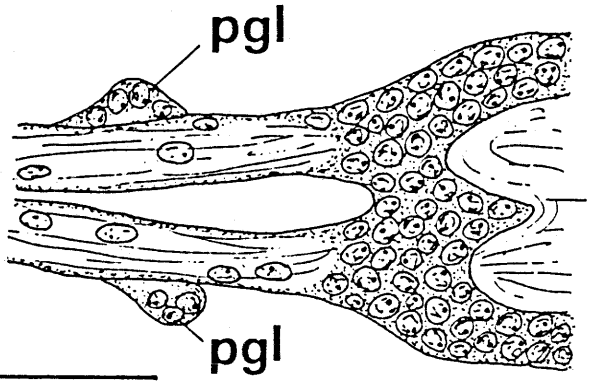
pgl
tg1
pgl

142

EXPLANATION OF FIGURES

143. Parasagittal section through thorax of embryo of P. pryeri late in Stage 5.

144. Parasagittal section through head and thoracic region of embryo of P. pryeri in Stage 6.

145. Part of transverse section through metathorax of embryo of P. pryeri late in Stage 8.

146. Atrium of first abdominal spiracle of embryo of P. pryeri late in Stage 9.

147. Part of transverse section through first abdomen of embryo of P. pryeri in Stage 7.

Scales = 50μm.

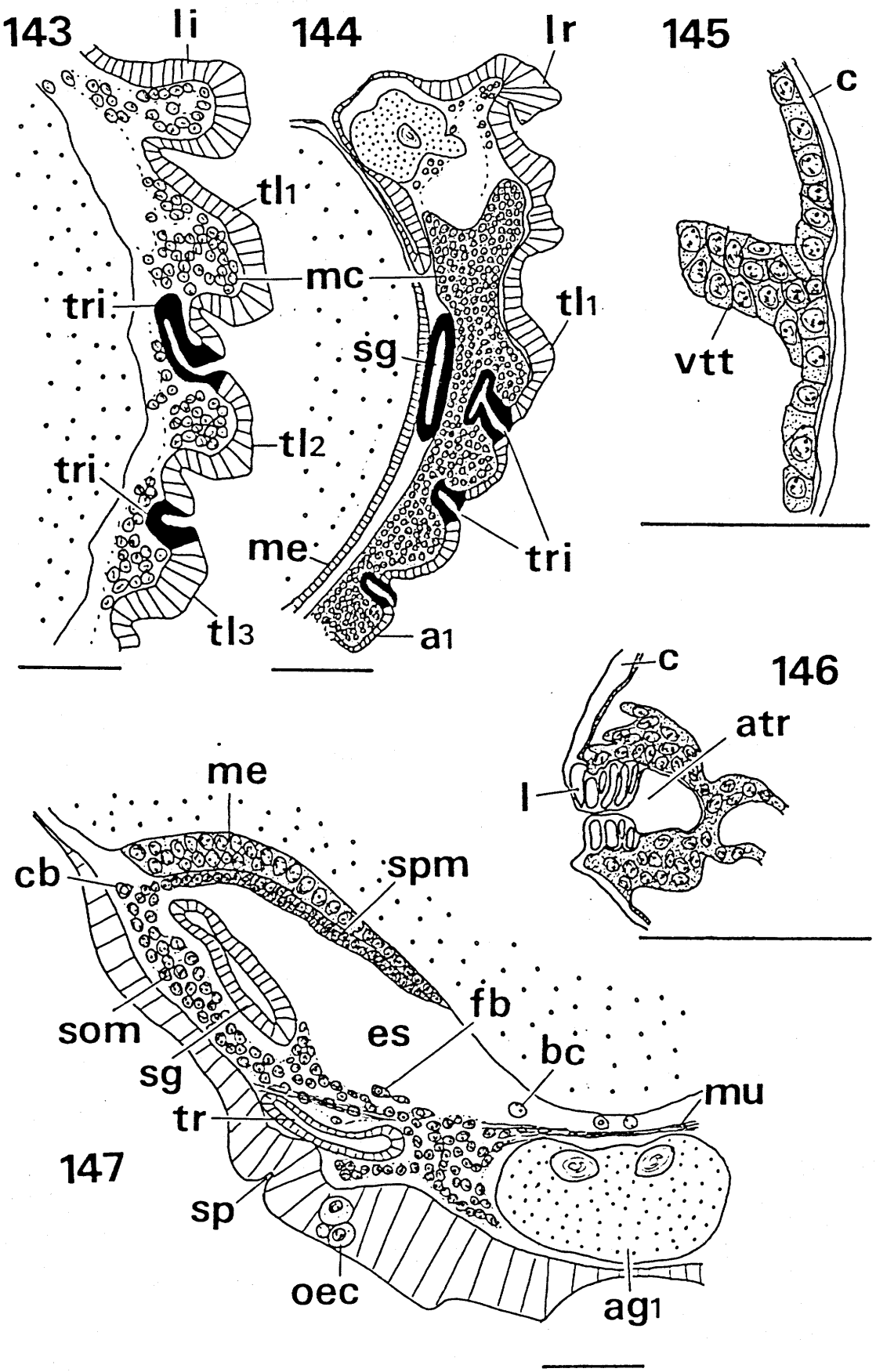
143
li
tl1
mc
tri
tl2
tri
tl3
144
lr
tl1
sg
tri
me
a1
145
c
vtt
146
c
atr
l
me
cb
spm
fb
som
es
bc
sg
mu
tr
147
sp
oec
ag1

EXPLANATION OF FIGURES

148. Part of transverse section through second abdominal segment of embryo of P. pryeri in Stage 7.

149. Part of transverse section through second abdominal segment of embryo of Pd. paradoxa in Stage 5.

150. Part of transverse section through prothorax of embryo of P. pryeri late in Stage 4.

151. Part of transverse section through prothorax of embryo of P. pryeri in Stage 6.

Scales = 50μm.

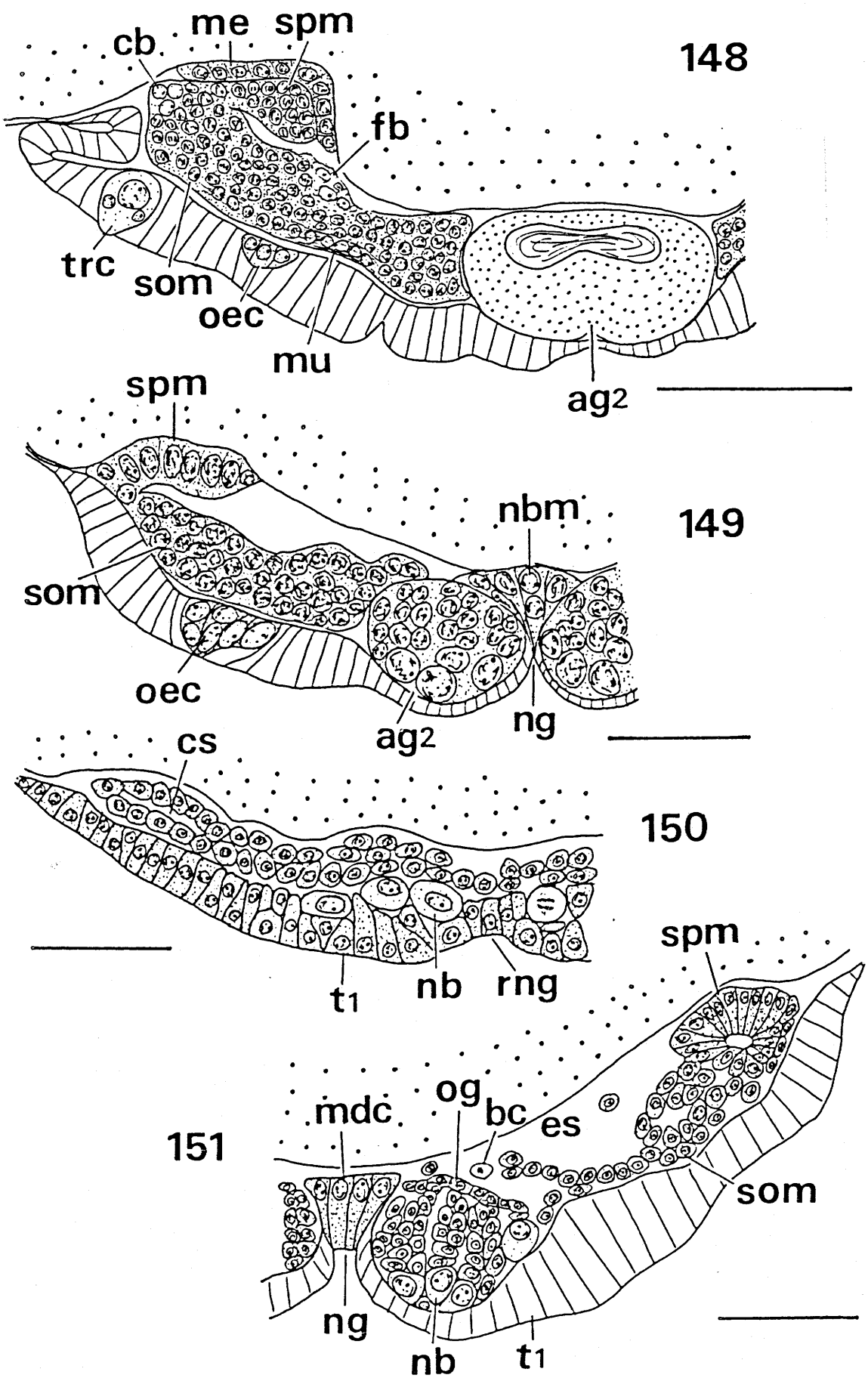
cb
me
spm
148
fb
trc
som
oec
mu
ag2
spm
nbm
149
som
oec
ag2
ng
cs
150
t1
nb
rng
spm
og
mdc
bc
es
151
som
ng
nb
t1

EXPLANATION OF FIGURES

152. Part of transverse section through metathorax of embryo of P. pryeri early in Stage 6.

153. Part of transverse section throufg second abdominal segment of embryo of P. pryeri in Stage 6.

154. Parasagittal section through posterior part of abdomen of embryo of Pd. paradoxa late in Stage 4.

155. Part of parasagittal section through thorax of embryo of Bo. westwoodi late in Stage 4.

Scales = 50μm.

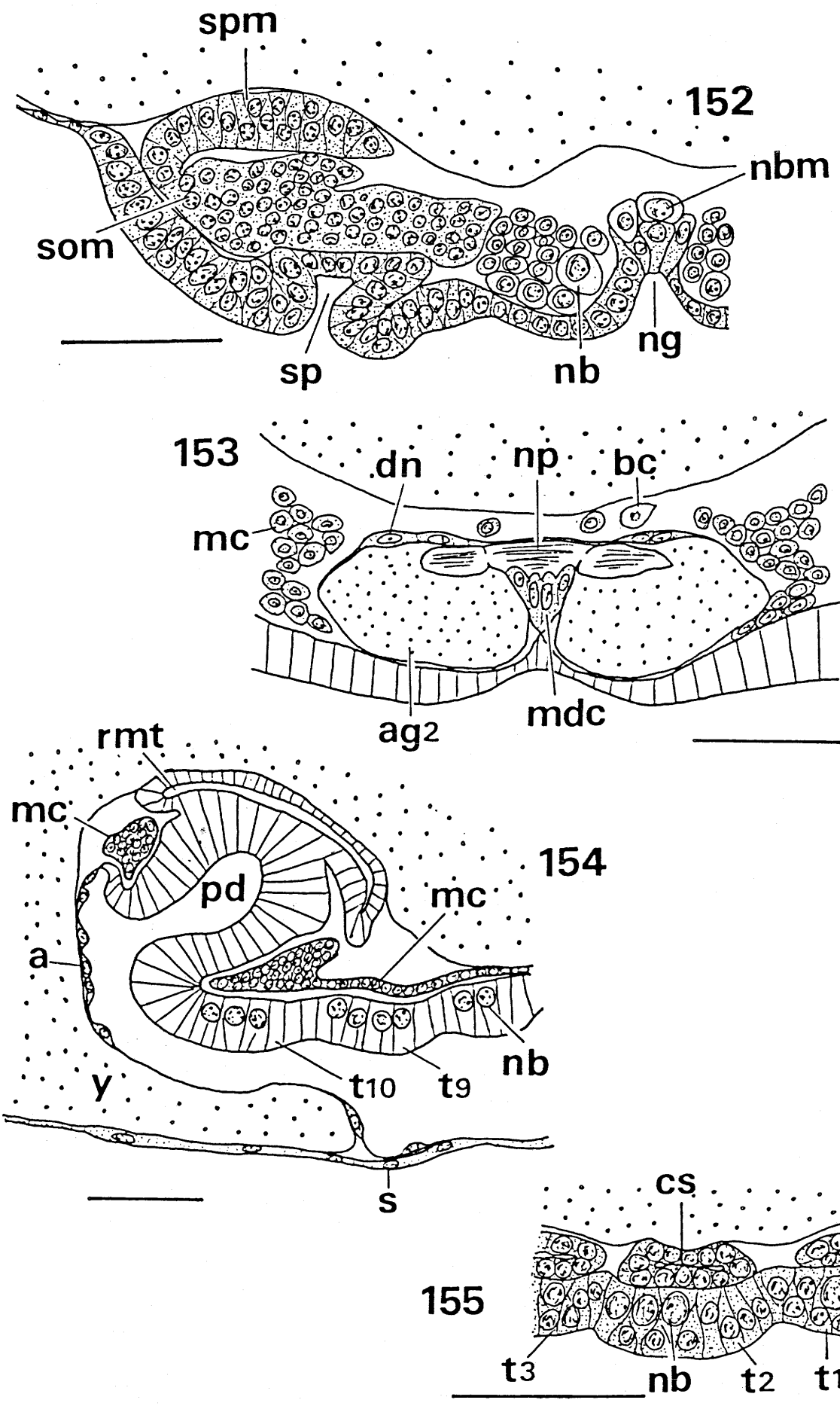
spm
152
nbm
som
sp
nb
ng
153
dn
np
bc
mc
ag2
mdc
rmt
mc
154
pd
mc
a
nb
y
t10
t9
s
cs
155
t3
nb
t2
t1

EXPLANATION OF FIGURES

156. Horizontal section through head of embryo of P. pryeri late in Stage 4.

157. Part of horizontal section through head of embryo of P. pryeri in Stage 5.

158. Diagrams showing the distribution of ganglia (A) and mesodermal cells (B) in the cephalognathal region of embryo of P. pryeri in Stage 5.

159. Horizontal section through head of embryo of P. pryeri in Stage 6.

Scales = 10μm (Fig. 156) and 50μm (Figs. 157, 159).

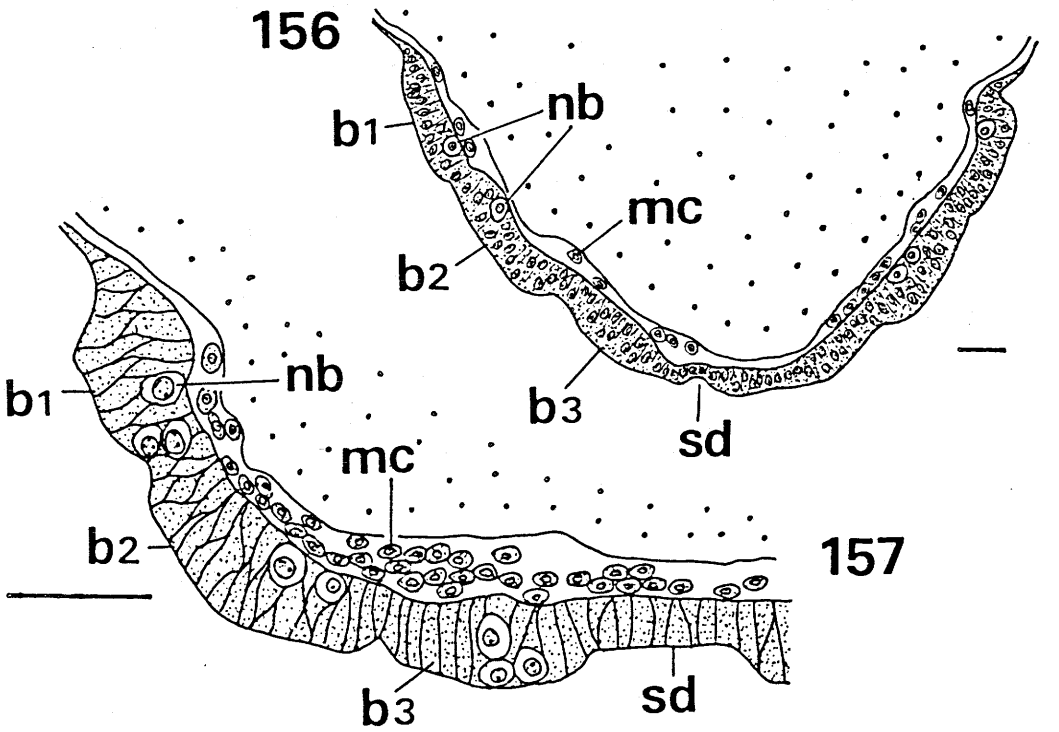
156
b1
nb
mc
b2
b3
sd
157
b1
nb
mc
b2
b3
sd

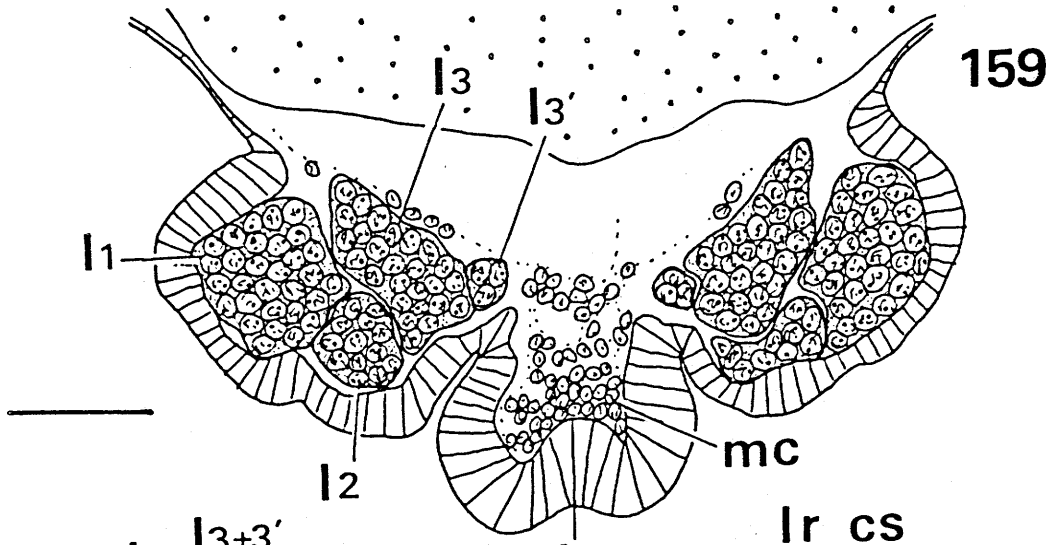
159
l3
l3'
l1
l2
mc
lr

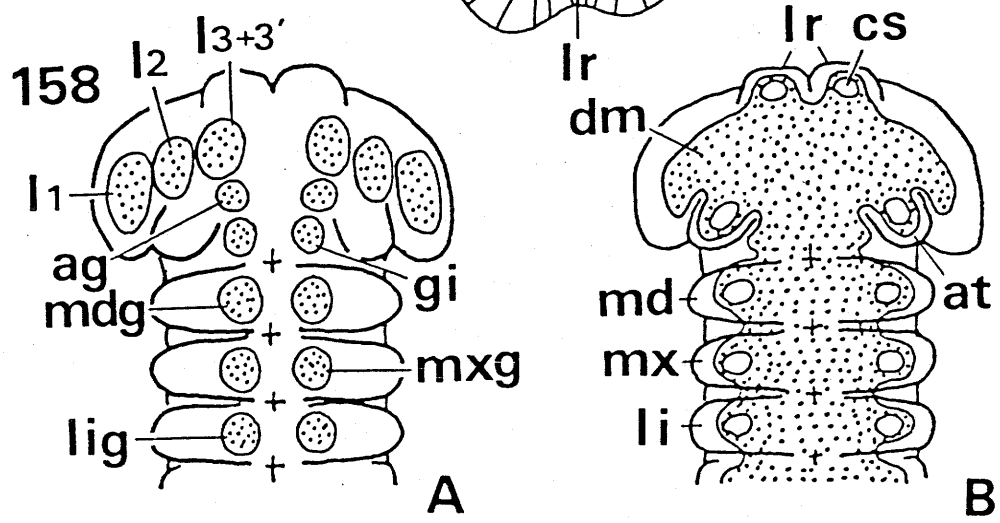
158
l2
l3+3'
l1
ag
mdg
gi
mxg
lig
A
lr
cs
dm
md
at
mx
li
B

EXPLANATION OF FIGURES

160. Part of transverse section through head of embryo of *P. pryeri* in Stage 6.

161. Part of transverse section through head of embryo of *P. pryeri* in Stage 7.

162. Part of transverse section through brain of embryo of *P. pryeri* in Stage 9.

163. Diagram showing the brain of first instar larva of *P. pryeri*.

164. Sagittal section through oral region of embryo of *P. pryeri* in Stage 5.

Scales = 50μm.

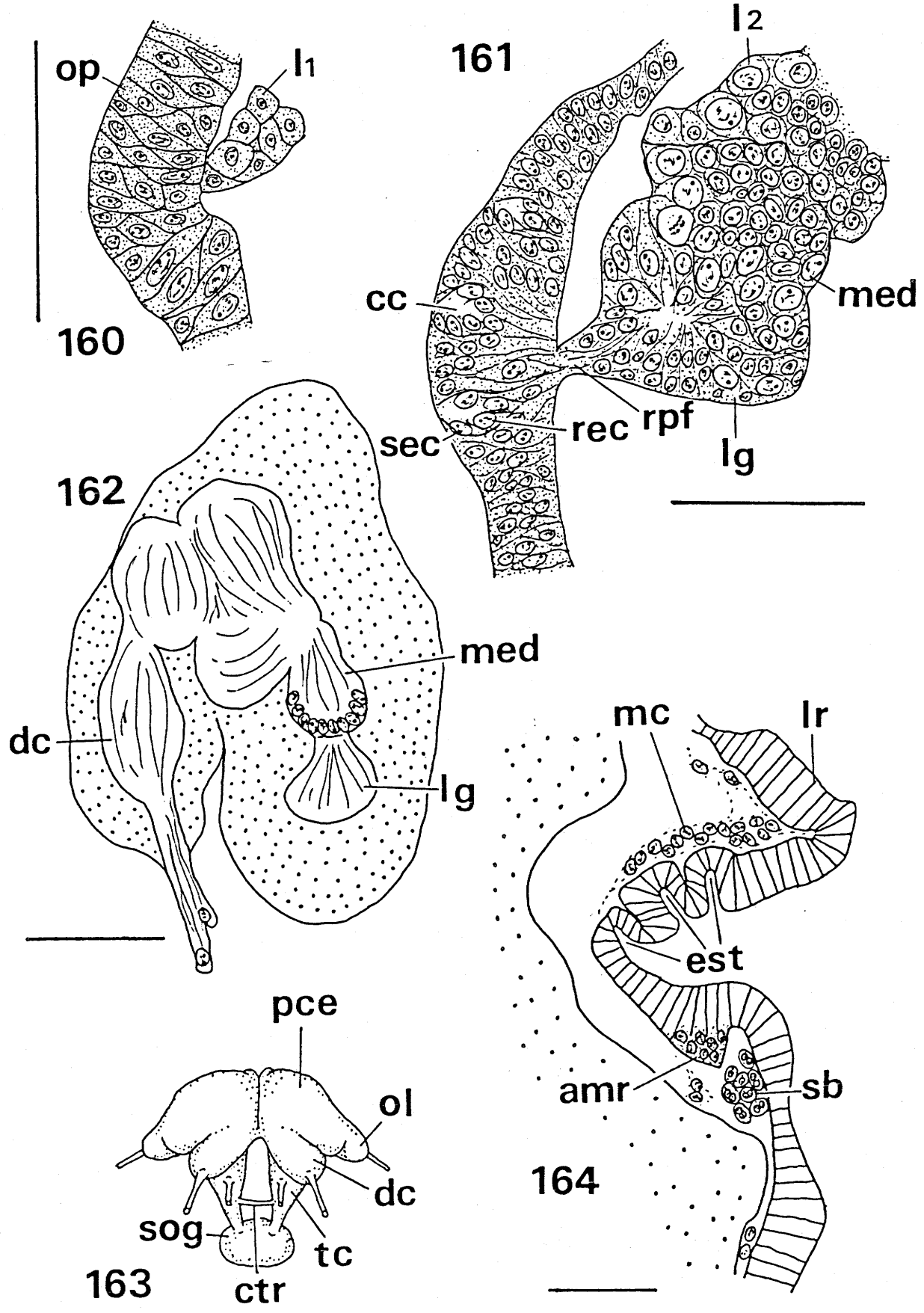
op
l1
160
161
l2
cc
med
sec
rec
rpf
lg
162
med
dc
lg
mc
lr
est
amr
sb
164
pce
ol
dc
sog
tc
ctr
163

EXPLANATION OF FIGURES

165. Sagittal section through head of embryo of P. pryeri in Stage 6.

166. Part of transverse section through head of embryo of P. pryeri in Stage 7.

167. Transverse section through posterior part of stomodaeum of embryo of P. pryeri in Stage 8.

168. Diagram showing the stomotogastric nervous system of first instar larva of P. pryeri.

169. Transverse section through middle part of stomodaeum of first instar larva of P. pryeri.

Scales = 50μm.

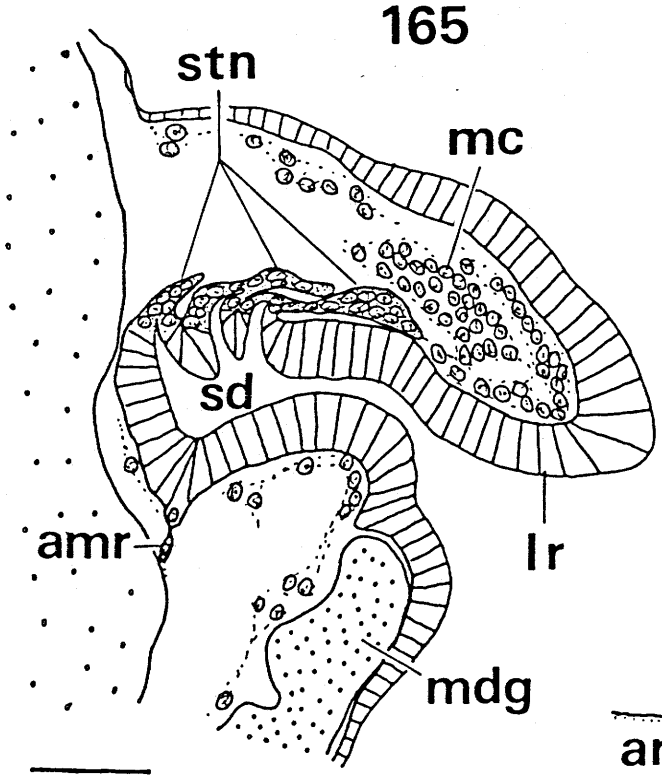
165
stn
mc
sd
amr
lr
mdg

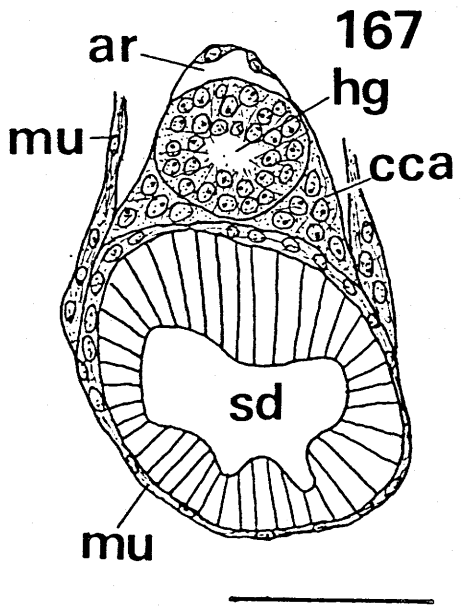
167
ar
hg
mu
cca
sd
mu

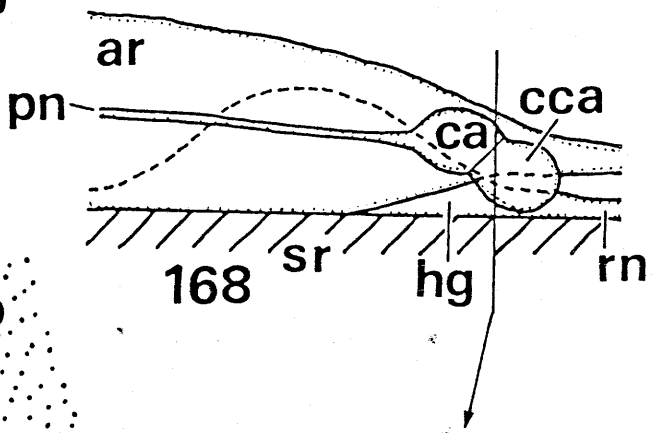
ar
pn
cca
ca
168
sr
hg
rn

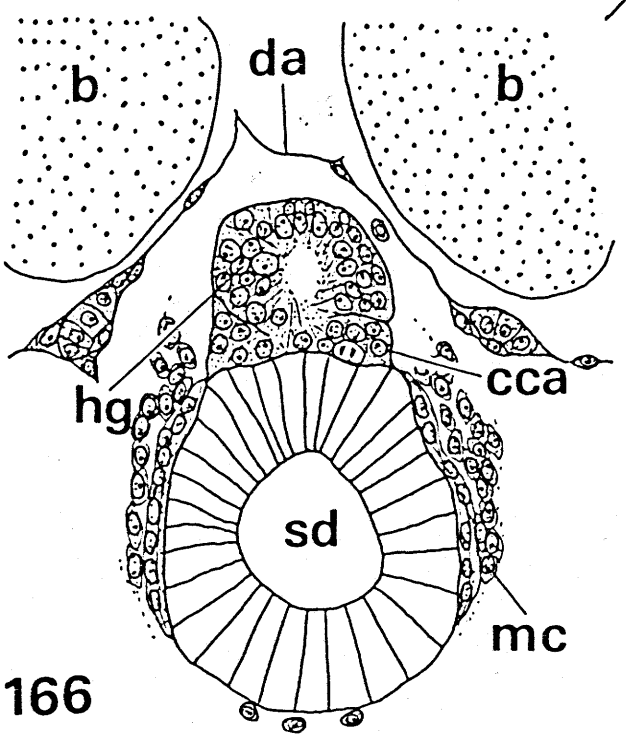
b
da
b
hg
cca
sd
mc
166

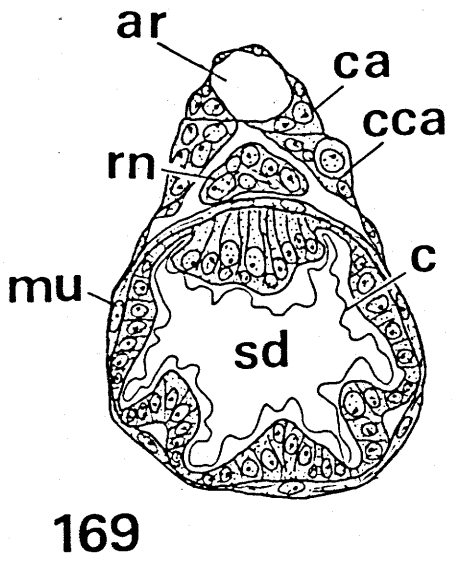
ar
ca
cca
rn
c
mu
sd
169

EXPLANATION OF FIGURES

170. Slightly oblique sagittal section through cephalognathal region of embryo of Pd. paradoxa in Stage 5.

171. Longitudinal section through compound eye of embryo of P. pryeri in Stage 9.

172. Longitudinal section through compound eye of first instar larva of P. pryeri.

173. Longitudinal section of ommatidium (A), and transversesection of crystallin cone (B) of first instar larva of B. laevipes.

Scales = 50µm (Figs. 170-172) and 10µm (Fig. 173).

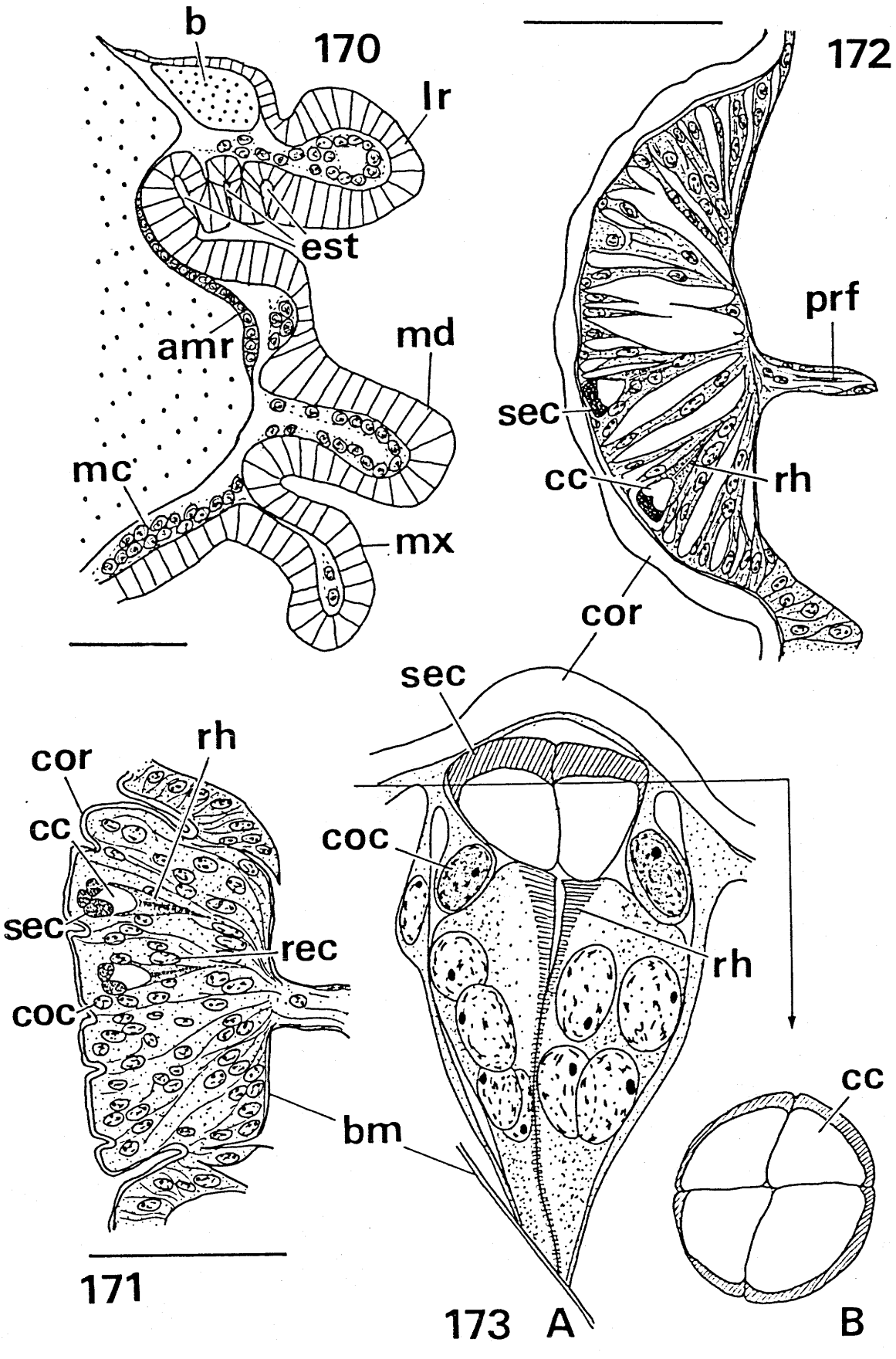
b
170
lr
est
amr
md
mc
mx
172
prf
sec
cc
rh
cor
sec
cor
rh
cc
sec
rec
coc
bm
171
coc
rh
cc
173 A
B

EXPLANATION OF FIGURES

174. Part of transverse section through head of embryo of Pd. paradoxa in Stage 5.

175. Part of transverse section through head of embryo of Pd. paradoxa in Stage 6.

176. Transverse section through maxillary segment of embryo of P. pryeri in Stage 4.

177. Sagittal section of egg of Pd. paradoxa in Stage 3.

178. Parasagittal section through posterior part of abdomen of embryo of Pd. paradoxa in Stage 4.

Scales = 50µm (Figs. 174-176, 178) and 100µm (Fig. 177).

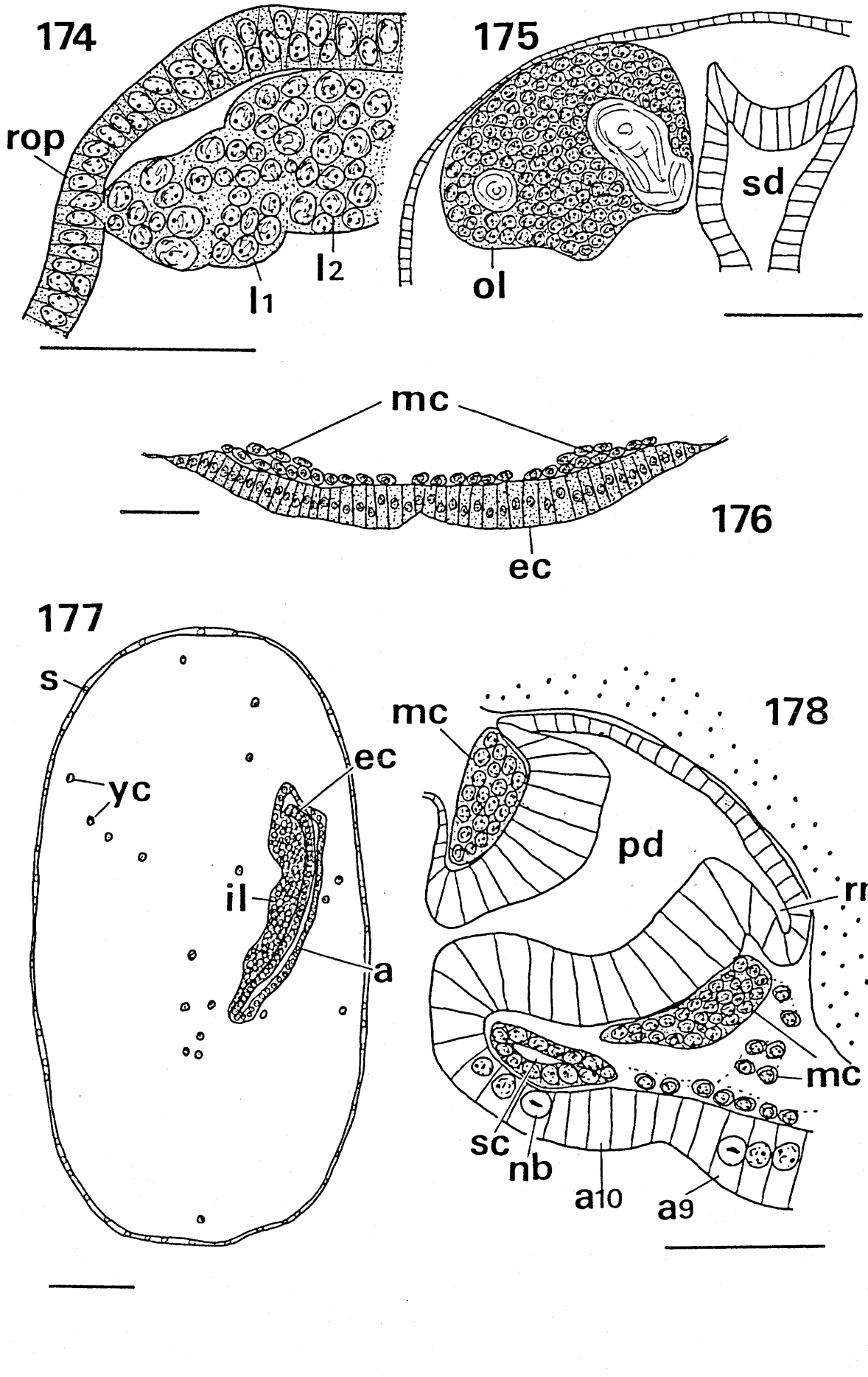
174
rop
l1
l2
175
ol
sd
mc
ec
176
177
s
yc
ec
il
a
178
mc
pd
rmt
mc
sc
nb
a10
a9

EXPLANATION OF FIGURES

179. Parasagittal section through head of embryo of P. pryeri in Stage 6.

180. Cardioblasts of P. pryeri in Stage 7.

181. Part of transverse section through first abdominal segment of embryo of P. pryeri in Stage 8.

182. Part of transverse section through third abdominal segment of embryo of P. pryeri in Stage 9.

183. Part of transverse section through intersegmental region between second and third abdominal segments of first instar larva of P. pryeri.

Scales = 50μm (Figs. 179, 183) and 10μm (Figs. 180-182).

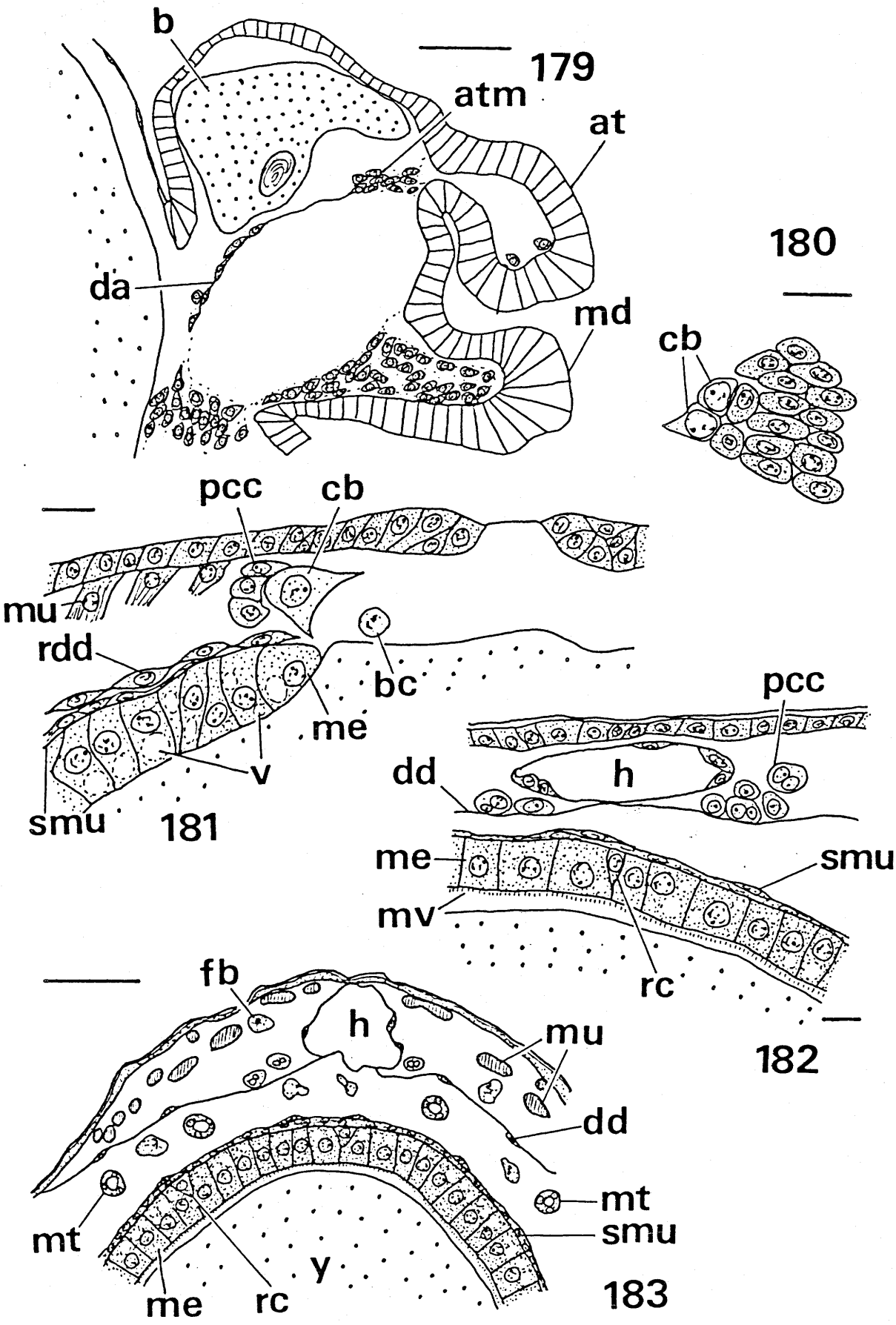
b
179
atm
at
da
md
180
cb
pcc
cb
mu
rdd
bc
me
v
smu
181
pcc
dd
h
me
smu
mv
rc
182
fb
h
mu
dd
mt
smu
mt
y
me
rc
183

EXPLANATION OF FIGURES

184. Transverse section of heart through seventh abdominal segment of first instar larva of P. pryeri.

185. Part of transverse section through mesothorax of embryo of Pd. paradoxa in Stage 5.

186. Sagittal section through posterior end of embryo of P. pryeri in Stage 3.

187. Sagittal section through posterior end of abdomen of embryo of P. pryeri in Stage 4.

188. Sagittal section through posterior end of abdomen of embryo of P. pryeri in Stage 5.

Scales = 50μm.

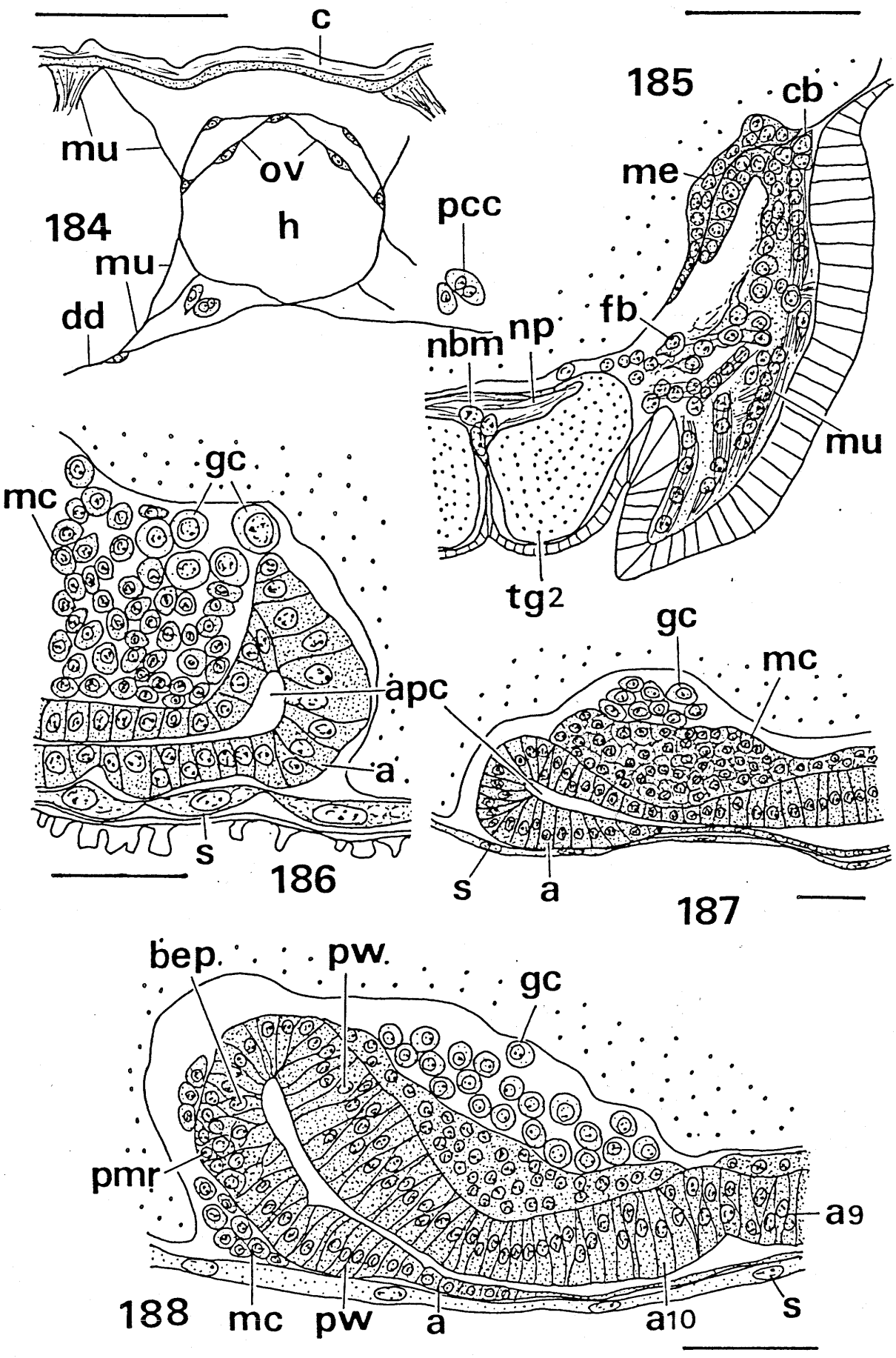
c
mu
ov
h
184
mu
dd
pcc
185
cb
me
fb
np
nbm
mu
tg2
gc
mc
apc
a
s
186
gc
mc
s
a
187
bep
pw
gc
pmr
a9
188
mc
pw
a
a10
s

EXPLANATION OF FIGURES

189. Part of parasagittal section through posterior region of abdomen of embryo of P. pryeri in Stage 6.

190. Part of transverse section through seventh abdominal segment of embryo of P. pryeri in Stage 6.

191. Part of parasagittal section through posterior region of abdomen of embryo of P. pryeri in Stage 8.

192. Sagittal section through posterior end of abdomen of embryo of B. laevipes in Stage 5.

Scales = 50μm.

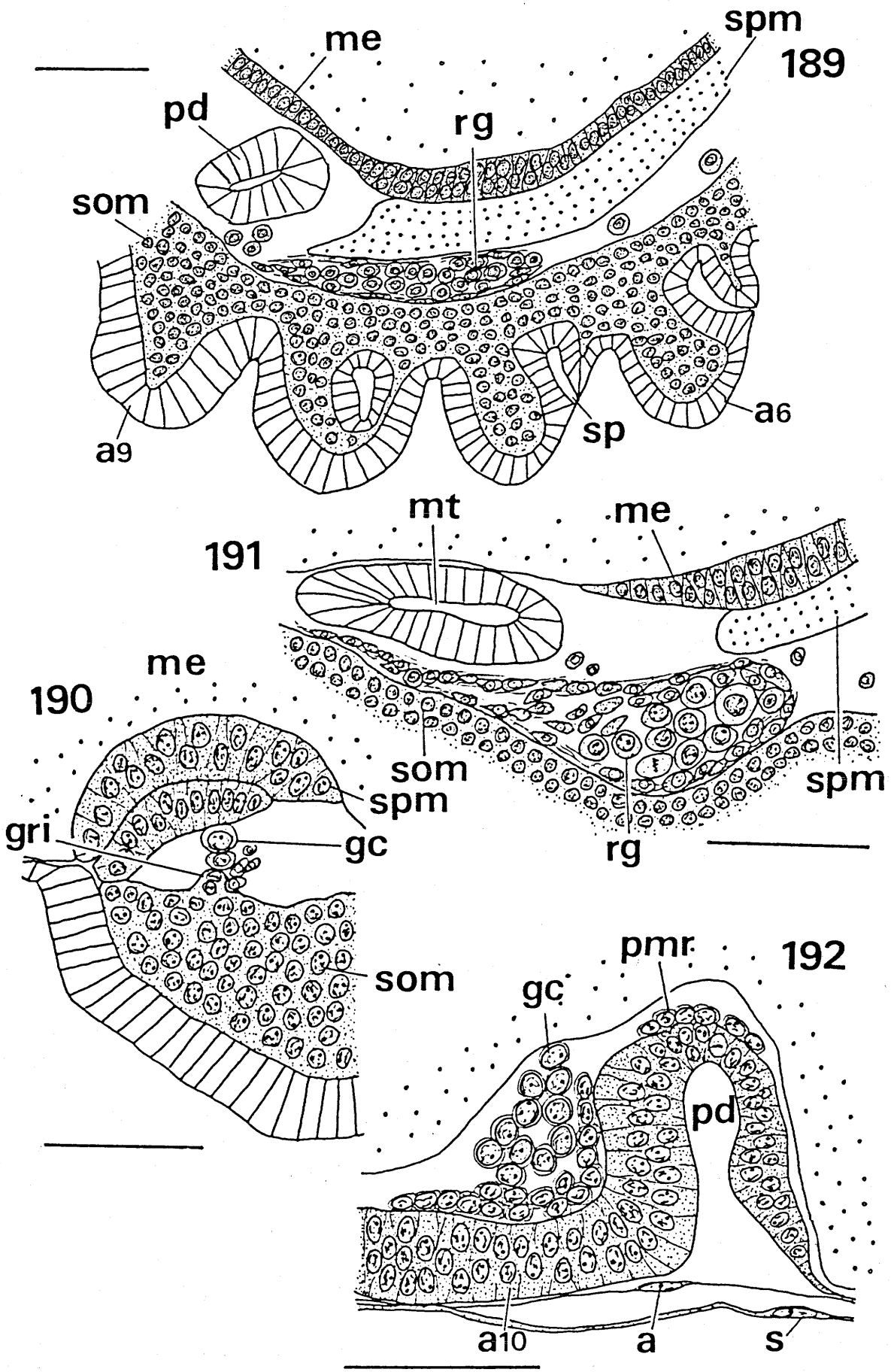
me
spm
189
pd
rg
som
a9
sp
a6
mt
me
191
190
me
som
spm
gri
gc
rg
spm
pmr
192
gc
som
pd
a10
a
s

EXPLANATION OF FIGURES

193. Diagram showing main musculature of metathorax and first abdominal segments of first instar larva of P. pryeri. Arrows = see text (p.85).

194. Diagrams showing posterior view of caudal end of abdomen (A) and parasagittal (B, C) and sagittal (D) sections through posterior part of abdomen of first instar larva of P. pryeri.

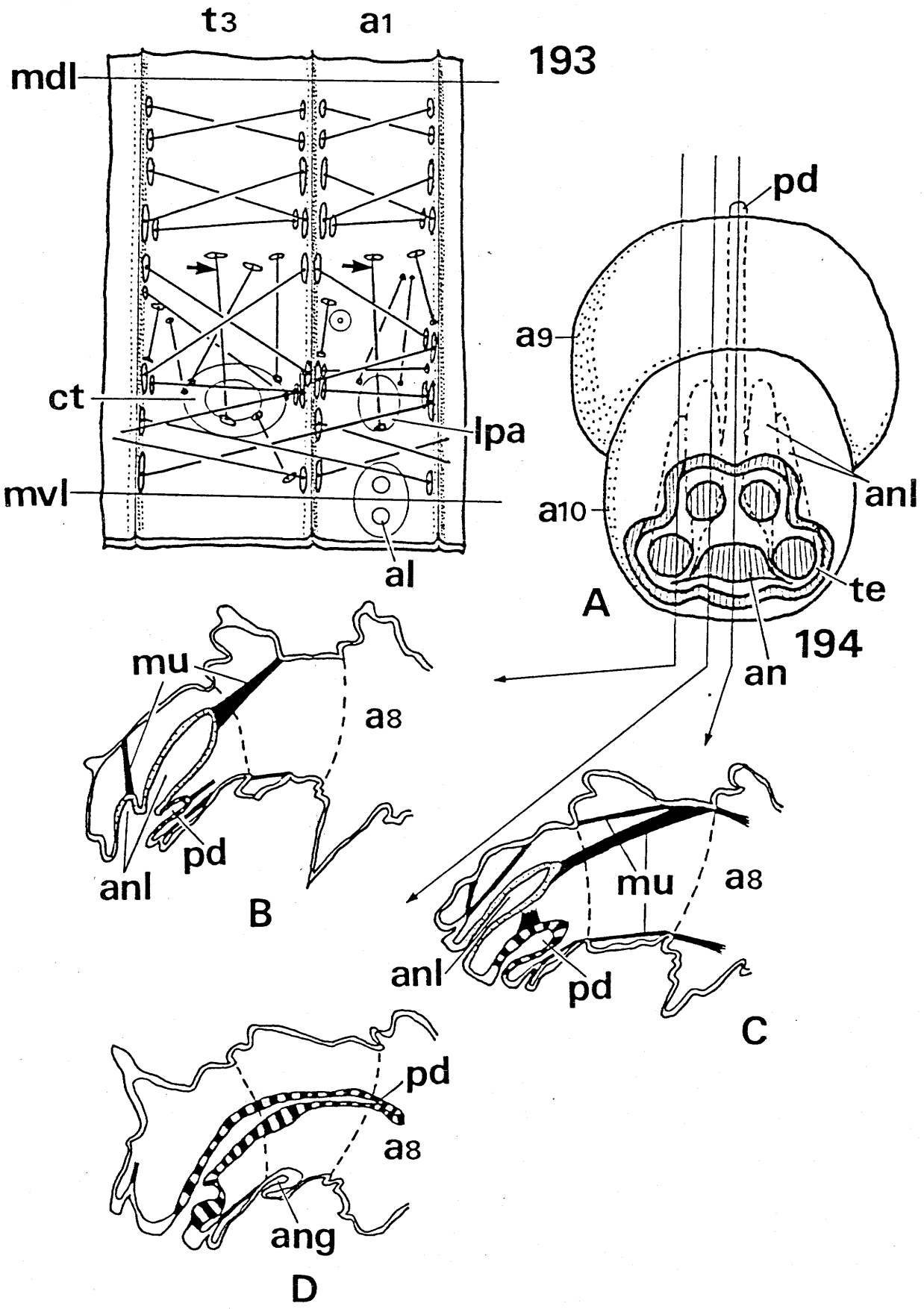
t3
a1
193
mdl
ct
lpa
mvl
al
pd
a9
anl
a10
te
A
194
an
mu
a8
pd
anl
B
mu
a8
anl
pd
C
pd
a8
ang
D

EXPLANATION OF FIGURES

195. Sagittal section through anterior part of midgut of embryo of P. pryeri in Stage 9.

196. Parasagittal section through posterior part of abdomen of embryo of P. pryeri in Stage 5.

197. Diagram showing alimentary canal of first instar larva of P. pryeri.

198. Sagittal section through stomodaeal region of embryo of P. pryeri in Stage 4.

Scales = 50μm.

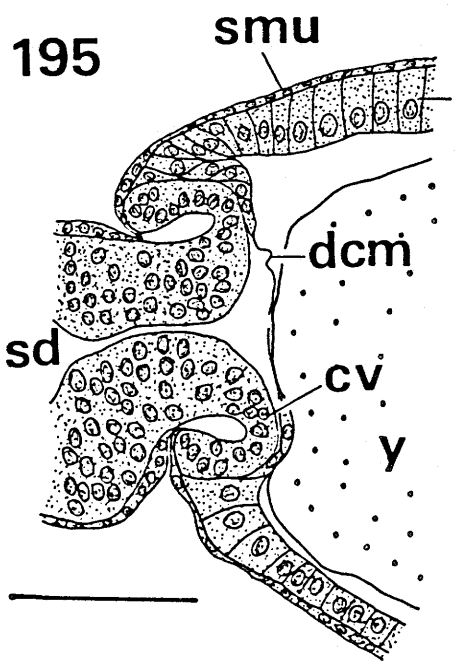
195
smu
me
dcm
sd
cv
y

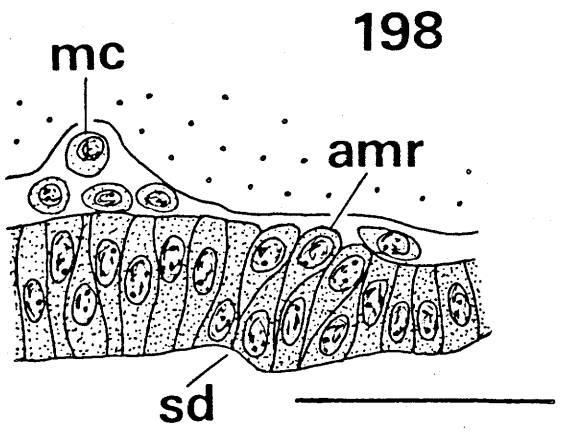
198
mc
amr
sd

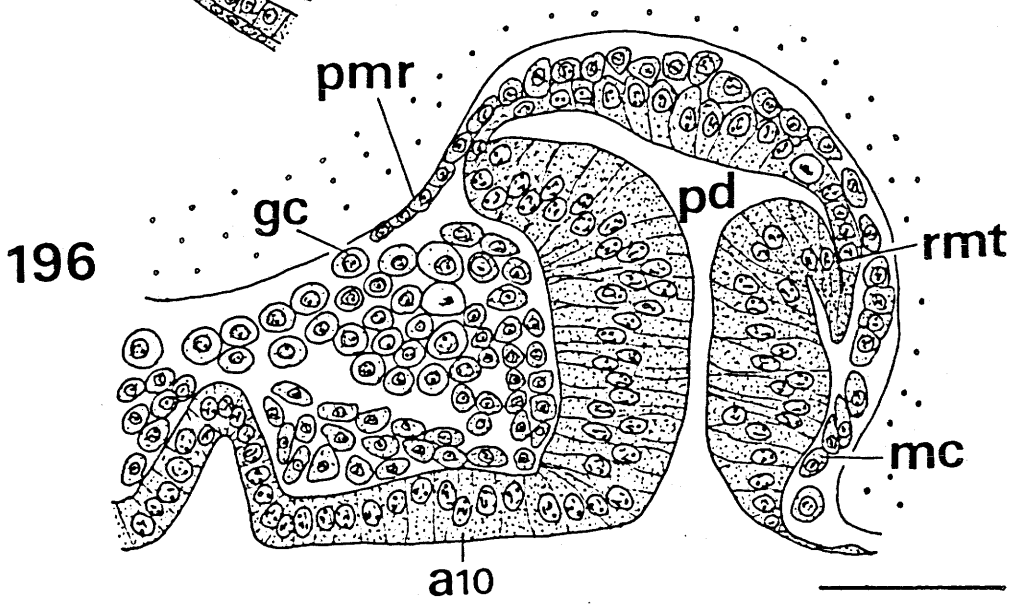
196
pmr
gc
pd
rmt
mc
a10

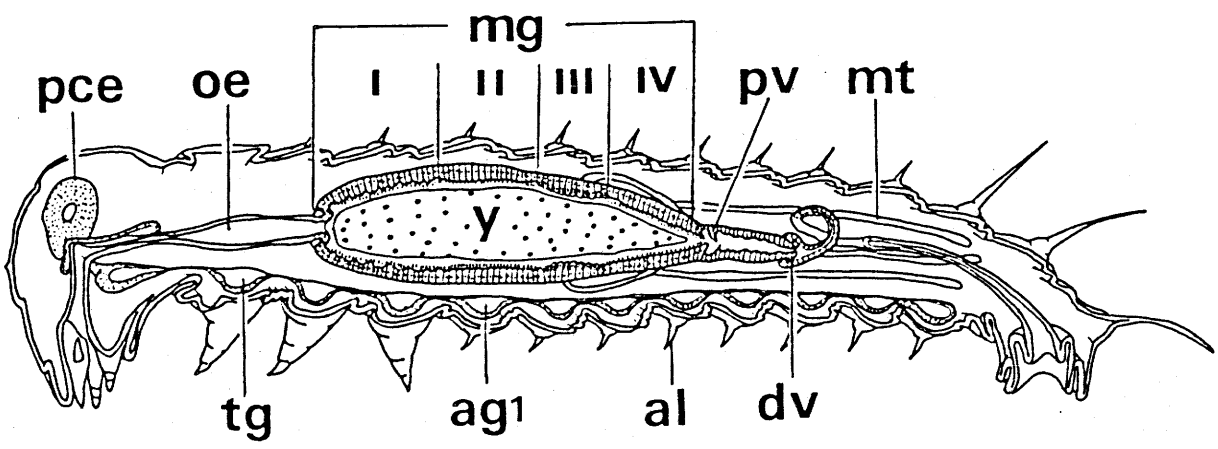
mg
pce
oe
I
II
III
IV
pv
mt
y
tg
ag1
al
dv

197

EXPLANATION OF FIGURES

199. Sagittal section through stomodaeal region of embryo of P. pryeri in Stage 5.

200. Part of transverse section through second abdominal segment of embryo of P. pryeri in Stage 8.

201. Midgut epithelium of Region I of first instar larva of P. pryeri.

202. Midgut epithelium of Region II of first instar larva of P. pryeri.

203. Midgut epithelium of Region III of first instar larva of P. pryeri.

204. Sagittal section through stumodaeal region of embryo of B. laevipes in Stage 4.

205. Sagittal section through stomodaeal region of embryo of Bo. westwoodi in Stage 4.

Scales = 10µm (Figs. 199, 201-205) and 50µm (Fig. 200).

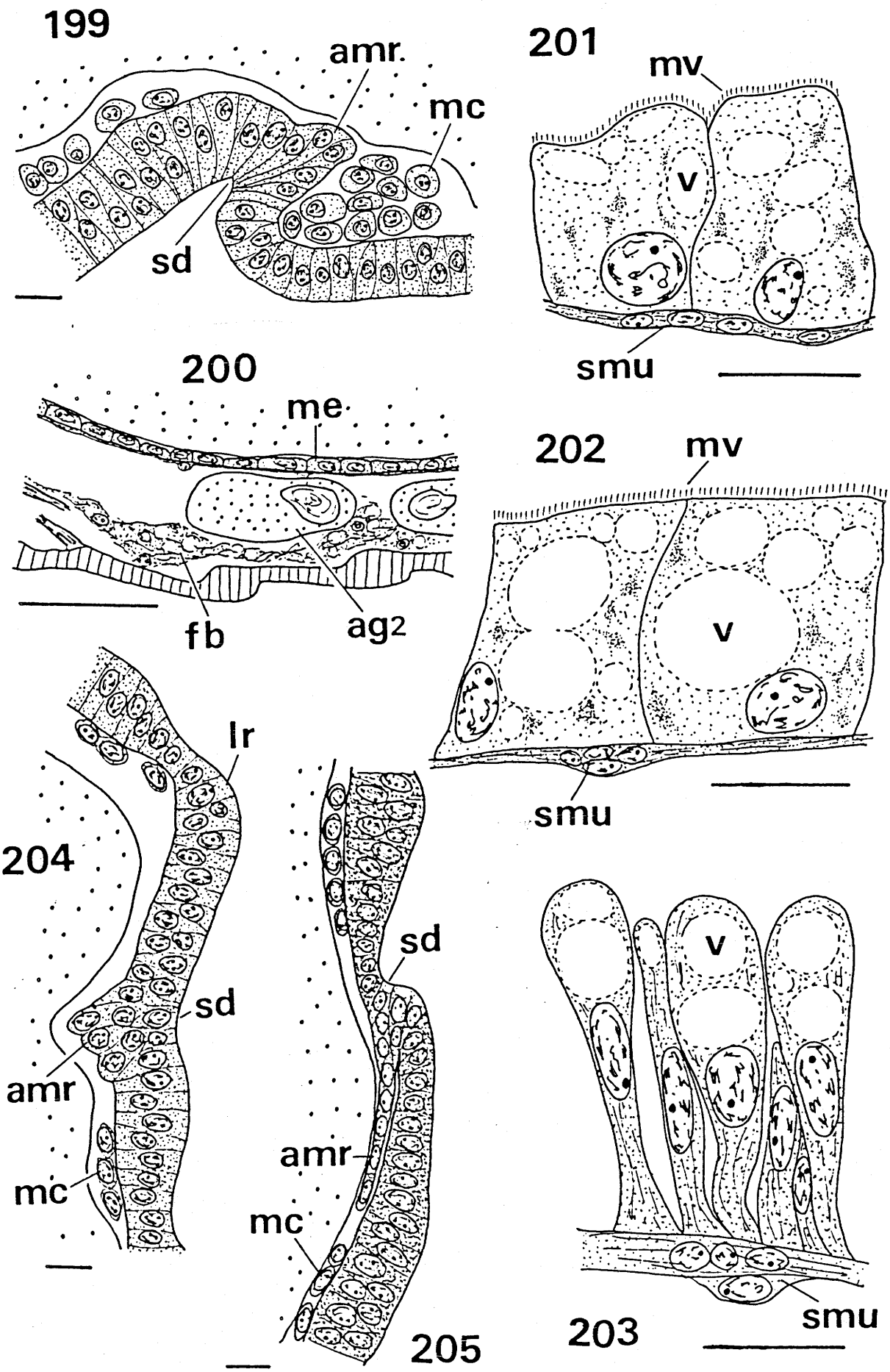
199
amr
mc
sd
201
mv
v
smu
200
me
fb
ag2
202
mv
v
smu
lr
204
sd
amr
mc
sd
amr
mc
205
v
smu
203

EXPLANATION OF FIGURES

206. Diagram showing lateral spread of amnion (A), and part of transverse section through head of embryo (B) of P. pryeri in Stage 4.

207. Diagram showing lateral spread of amnion (A), and part of transverse section through head of embryo (B) of P. pryeri in Stage 5.

208. Diagram showing lateral spread of amnion of embryo of P. pryeri in Stage 5.

209. Part of sagittal section through embryo of P. pryeri in Stage 5.

Scales = 50µm.

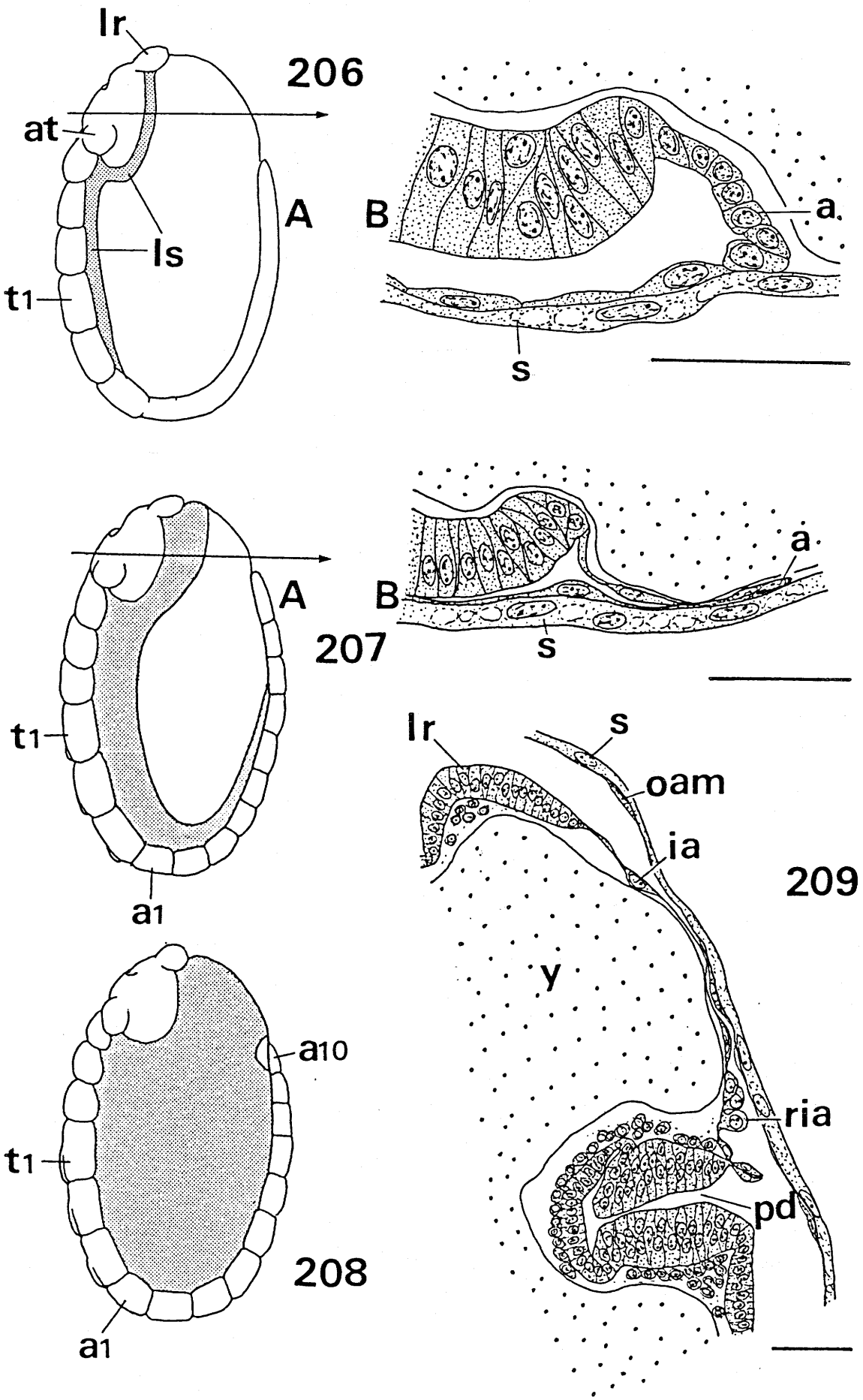
lr
206
at
A
ls
t1
B
a
s
207
a1
208
a10
209
oam
ia
y
ria
pd

EXPLANATION OF FIGURES

210. Sagittal section through thickened inner amnion of embryo of P. pryeri in Stage 7.

211. Sagittal section through anterior part of embryo of Bo. westwoodi in Stage 4.

212. Rudimental abdominal leg of second abdominal segment of embryo of P. pryeri in Stage 7.

213. Abdominal leg of second abdominal segment of embryo of P. pryeri in Stage 8.

214. Abdominal leg of second abdominal segment of embryo of P. pryeri in Stage 9.

215. Abdominal leg of second abdominal segment of first instar larva.

216. Small abdominal process of third abdominal segment of embryo of Pd. paradoxa in Stage 7.

217. Small abdominal process of third abdominal segment of first instar larva of Pd. paradoxa.

Scales = 10μm (Figs. 210, 212-217) and 50μm (Fig. 211).

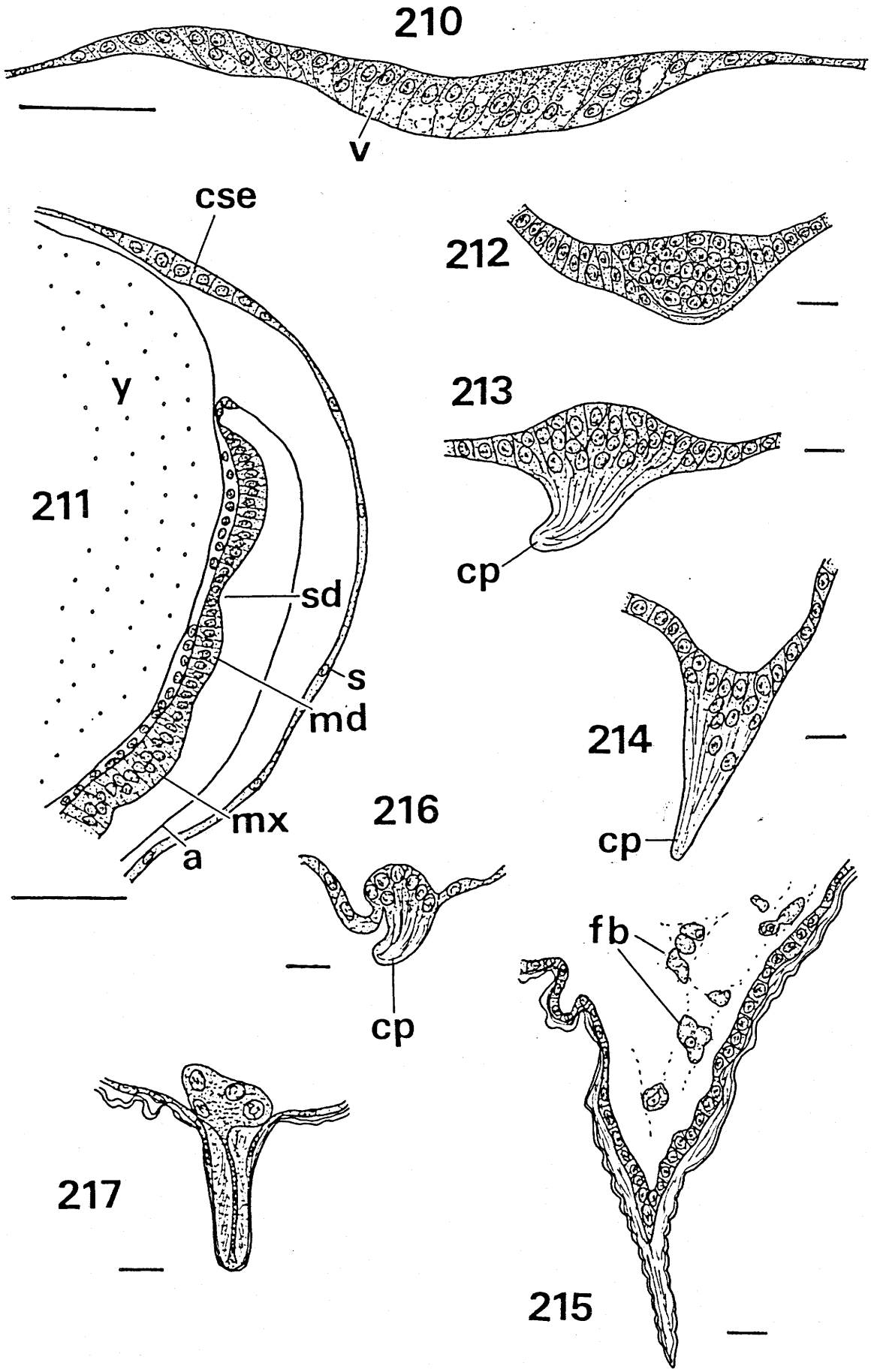
210
v
cse
y
211
sd
s
md
mx
a
212
213
cp
214
cp
216
cp
fb
215
217

EXPLANATION OF FIGURES

218. Part of transverse section through prothorax of embryo of P. pryeri in Stage 4.

219. Part of transverse section through prothorax of embryo of P. pryeri in Stage 5.

220. Part of transverse section through prothorax of embryo of P. pryeri in Stage 7.

221. Parasagittal section through posterior part of abdomen of embryo of P. pryeri early in Stage 7.

222. Parasagittal section through posterior part of abdomen of embryo of P. pryeri in Stage 7.

223. Parasagittal section through posterior part of abdomen of embryo of P. pryeri late in Stage 7.

Scales = 50μm.

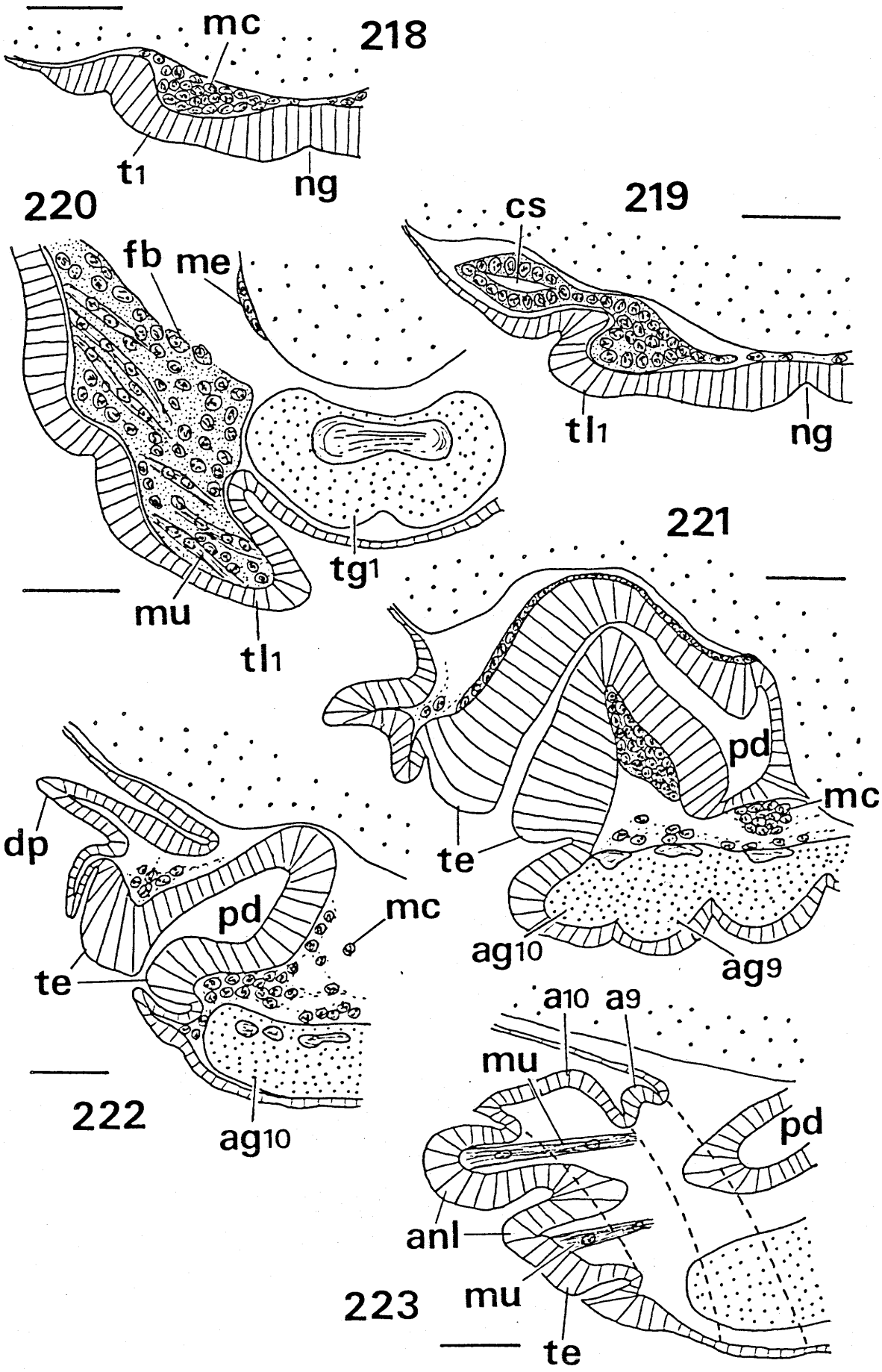
mc
218
t1
ng
220
fb
me
cs
219
tl1
ng
tg1
221
mu
tl1
pd
mc
dp
te
pd
mc
ag10
ag9
te
222
ag10
a10
a9
mu
pd
anl
223
mu
te

EXPLANATION OF FIGURES

224. Serosa and serosal cuticle of P. pryeri early in Stage 5.

225. Serosa and serosal cuticle of P. pryeri in Stage 5.

226. Parasagittal section through posterior part of abdomen of embryo of B. laevipes in Stage 7.

227. Diagram showing main caetotaxy of eighth to tenth abdominal segments of first instar larva of Pd. paradoxa. Arrows = see text (p.112).

Scales = 10μm (Figs. 224, 225) and 50μm (Fig. 226).

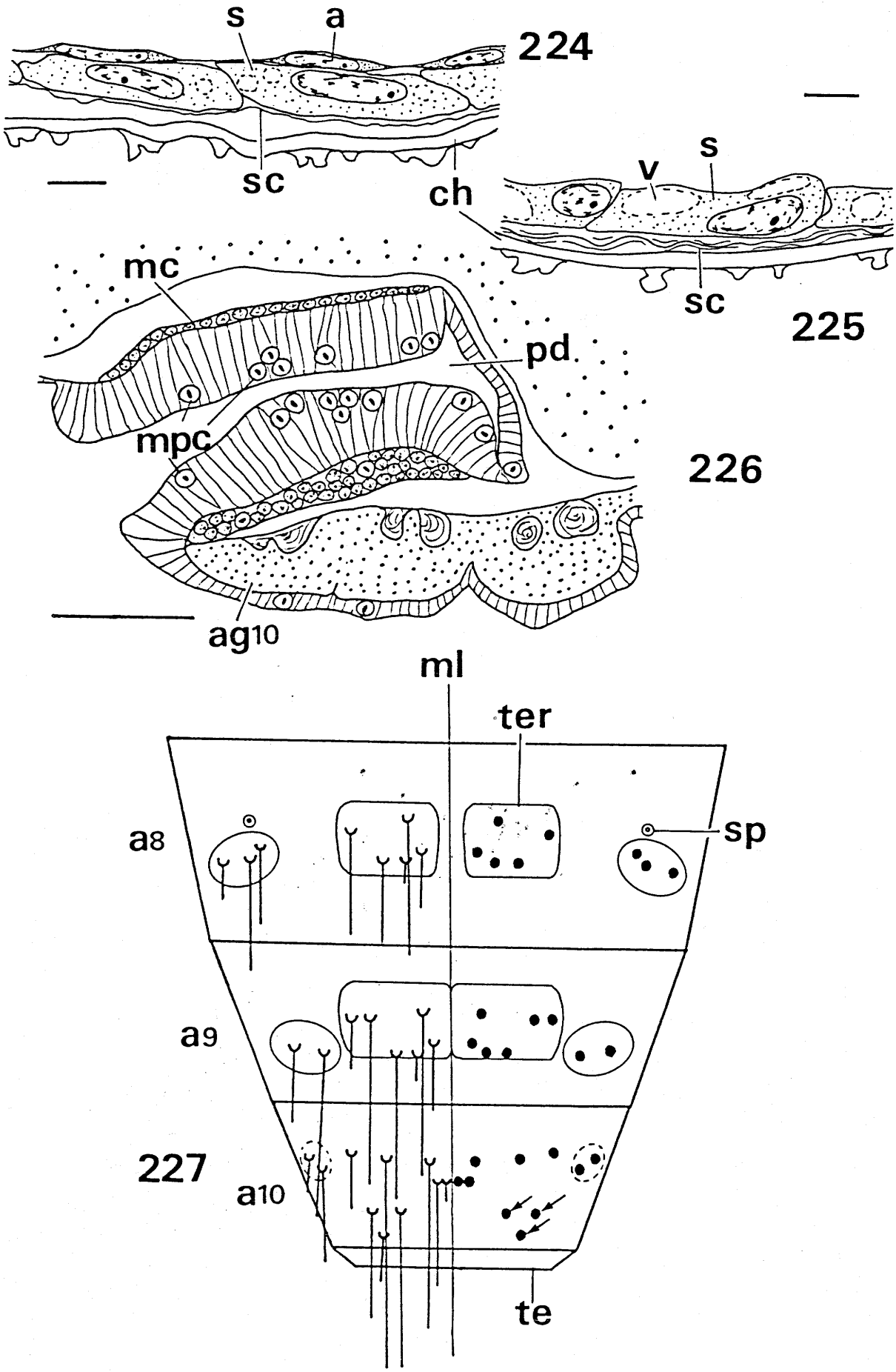
s
a
224
sc
ch
v
s
sc
225
mc
pd
mpc
226
ag10
ml
ter
a8
sp
a9
227
a10
te

EXPLANATION OF FIGURE

228. Diagrams showing types of germ band. A, B. laevipes; B, Bo. westwoodi; C, Pd. paradoxa; D, P. pryeri.

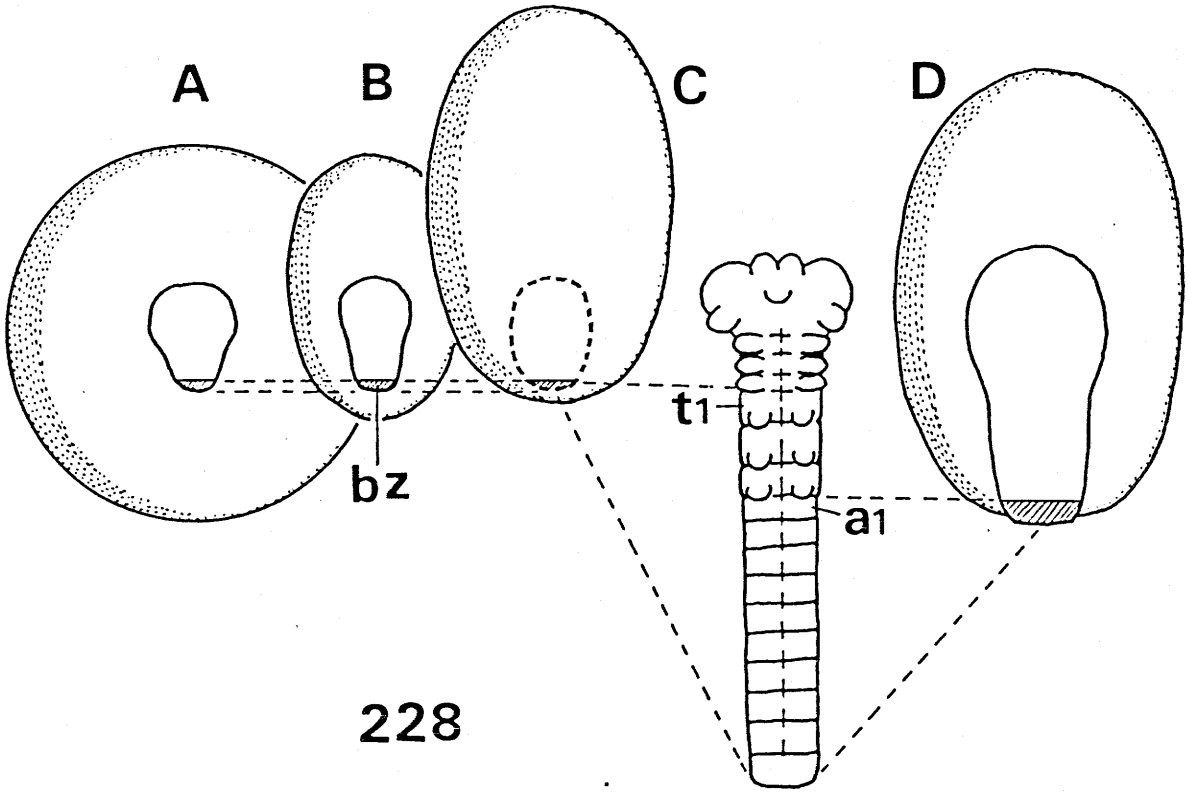

228